Production Readiness Review of Slats of Stations 3,4 and 5

9th November 2001

Abstract

The design of the Stations 3, 4 and 5 of the Dimuon Forward Spectrometer is presented. An important part is devoted to the slat mechanical structure, printed circuit boards (PCB) and to the test beam results. The related electronics, the supporting structure, the cooling and the integration issues are also discussed. The planning, the task sharing and the cost of the project are also reviewed.

Contents

1 Introduction

The present PRR is scheduled since a long time. In fact, a lot of items of Stations 3, 4 and 5 are not ready for production, but the planning shows that if collaboration wants to be in time for installation in experimental area in 2005, some components of the slats chambers have to be ordered as soon as possible, early in 2002., because they may be on the critical path.

1.1 Preliminary

The system of five trajectography stations for the Alice Dimuon Arm Spectrometer is made with Cathode Strip Chambers (CSC). Stations 3,4,5 will be made following slat design. Main parameters of the system are summarized below :

- Acceptance from 2^o up to 9^o
- Average thickness < 3%
- Maximum occupancy 5%
- bending plane, spatial resolution < 0.100 mm,
- non bending plane, spatial resolution < 2.0 mm,
- 2.5 mm wires spacing, 2 x 2.5 mm gap, Φ 0.020 mm tungsten-rhenium wires,
- Operating high voltage 1650 - 1800 V with 80%Ar / 20%CO_2 mixture,
- Operating pressure : 0.2 - 0.5 mbar differential pressure, 5.0 mbar ultimate differential pressure

1.2 Modular design

Aim of the modular design is to achieve reliability of experimental equipment, good compliance to task sharing between labs, limited cost with a significant amount of common parts. The modular design was first proposed in 1996 by PNPI St Petersburg team, then by Subatech Nantes team in 1999.

The specificity of the Station 3 (allowed room, cooling, integration...) induced by its location inside the dipole magnet of the dimuon arm does not allow a direct extrapolation from Stations 4 and 5, and some PCBs are different from standard sizes in order to fit with dipole magnet sizes.

The standard slat module features a rectangular shape (400 mm wide active area, vertical wires, 800 up to 2400 mm long). There are 20 different sizes of slats for the 3 stations. Slats are mounted in horizontal rows of variable lengths in order to achieve pseudo circular shape.

Total sensitive area for one ST4&5 chamber is roughly 23 m^2.

Overall external size (mechanical support structure included) is roughly 5700 x 5200 x 600 mm^3 for one station with its two chambers.

Designation	Slat amount	Spare amount	Length(mm)	Location	PCBs amount
$122000SR_1$	2	1	1200	Ch. 5	2x3x3
$122000NR_1$	2	1	1200	Ch. 6	2x3x3
$112200SR_2$	4	1	1600	Ch. 5	2x4x5
$112200NR_2$	4	1	1600	Ch. 6	2x4x5
122200S	4	1	1600	Ch. 5	2x4x5
122200N	4	1	1600	Ch. 6	2x4x5
222000N	8	1	1200	Ch. 5, Ch. 6	2x3x9
220000N	8	1	800	Ch. 5, Ch. 6	2x2x9
122300N	4	1	1600	Ch. 7, Ch. 8	2x4x5
$112230NR_3$	8	1	2000	Ch. 7, Ch. 8	2x5x9
112230N	8	1	2000	Ch. 7, Ch. 8	2x5x9
222330N	8	1	2000	Ch. 7, Ch. 8	2x5x9
223300N	8	1	1600	Ch. 7, Ch. 8	2x4x9
333000N	16	1	1200	Ch. 7, Ch 8, .Ch. 9, Ch. 10	2x3x17
122330N	4	1	2000	ch. 9, ch. 10	2x5x5
$112233NR_3$	8	1	2400	ch. 9, ch. 10	2x6x9
112233N	8	1	2400	ch. 9, ch. 10	2x6x9
222333N	8	1	2400	ch. 9, ch. 10	2x6x9
223330N	8	1	2000	ch. 9, ch. 10	2x5x9
333300N	8	1	1600	ch. 9, ch. 10	2x4x9
Total	132	20			2x653

Table 1.1: Sharing of slat chambers -> see full document Slat Table_Stations 3,4,5 _ up date 05.11.2001

2 Slat design

2.1 Main features

Instead of most of wire chambers which feature a stiff frame with thin windows, slat chambers are made from stiff and thick windows (which are also cathode planes) with lightweight spacers located between windows and setting both pitch and gap for wires.

Requirement of transparency leads the use of lightweight materials, this may be possible if active width of a module remains below 600 mm, taking into account that longer wires means larger loading on the mechanical structure. Another reason to limit the length of wires is to avoid wire spacers which are manpower and time consuming and lead to some inefficiency zones in the sensitive area.

Studies lead to choose 400 mm long wires. In fact, length of wires is rather given by mapping of PCBs and necessity to avoid too long and too thin read out strips.

With 400 mm long wires, TRIPPE and RICE-EVANS formulas give minimum stretching load 25g @ 1.8 kV, 19g @ 1.6 kV, 17g @ 1.5 kV, 15g @ 1.4 kV.

Experimental tests show that HV working range is 1700-1800 V, so their stretching load can be set within 30-40 g without electrostatic instabilities.

This relative low mechanical loading allows the use of lightweight structure. Despite "windows" are stiff and thick, thanks to sandwich design they perform a low X/Xo.

A slat module is made from 2 up to 6 "square unit", mechanically it is a single component, electronically it is an assembly of, 2 up to 6, 400 x 400 mm^2 useful area PCBs.

A quarter of ST5 chamber features, from the beam plane to the top, 7 rows of rectangular modules (slats) with respectively 5, 6, 6, 6, 5, 4, 3 "square units", plus a 5 units central slat.

Drawings Q083DDM107, Q084DDM115 refer to final design of slat, and sizes of all kind of slats.

Main components of slat design are:

1. Sandwich panel : aim to give mechanical stability to slat
2. PCBs : aim to contain read out devices and front end electronics
3. Spacers : aim to set pitch and gap for wires
4. Frames : aim to transform slats into chamber

Main features of slat design are:

1. Cathode planes made from sandwich structure.
2. 400 mm segmentation of readout structure
3. 400 mm segmentation of H.V. supply for degraded-survival operation if wires failed.
4. Readout pads and Front End Electronics on the same PCB.
5. Use of high modulus carbon fibers for stiffness.
6. Wires glued instead of soldered.
7. No metallic parts in mechanical structure

8. Sealing with RTV Silicon resin (soft glue), without screws but re-openable.

9. Optimized guard wires

The 2400 mm long slat prototype integrated during spring 2001 shows that handling is easy : 2 persons are required to handle longest slats while small ones can be integrated and handled by only 1 person.

One feature of the design is its robustness : if a wire fails, there is normally only a 0.16 m^2 lost area for a near 23 m^2 chamber.

Critical points of the design are the ability to achieve the required accuracy ($\pm$ 50 μm) for the PCB width (399.800 mm) and the PCB flatness, H.V. supply connections, constraints for L.V. supply distribution to MANU345 boards, cooling of FEE, accessibility of slats in experimental area.

- Amount of matter

Slats are designed as transparent as possible in order to be overlapped and avoid dead areas : no horizontal frames in active area, vertical inefficient zone within 30-40 mm wide.

Rough evaluation of radiation length for one standard module electronics included :

Value over non overlapped areas (45% of area) : 1.0% X/Xo

Value at outer parts of PCBs (8% of area) :1.6% X/Xo

Value at overlapped zones (5% of area):2.0% X/Xo

Value at MCM boards location (40% of area) :2.1% X/Xo

Peak value at spacers location (3% of area) : 2.4% X/Xo

Mean value (with electronics, without cables) :1.6% X/Xo

The "transparency" of slat modules allows overlapped areas without dead areas.

- Geometric thickness, weight

A standard module with FEE electronics, is 31 mm thick.

- overall thickness of one ST4, ST5 chamber : 265 mm

- overall thickness of one ST3 chamber : 215 mm

Weight of a ST5 chamber is estimated roughly at 100 kg, with support structure, with electronics, without cables, 230 kg with cables

Slats are mounted on a mechanical structure which aims to insure accurate and stable location in time and temperature of every slat with respect to the others. Raw material expected for this mechanical support structure is carbon / epoxy composite selected, not only for its high stiffness/mass ratio, but also for its good thermal stability (1.2 $10^{-6}K^{-1}$) which minimizes problems linked to monitoring, and the composites process which allows good flatness.

The structure will be designed and engineered by CEA Saclay.

2.1.1 Cathode Sandwich Panels

Documents :

"Programme fonctionnel" (CCTP) + "Règlement de consultation pour appel d'offres sur performances" (file : programme_fonctionnel_panneaux_sandwich.doc)

Drawings : Q083DDM126, Q083DDM127, Q083DDM128, Q083DDM129, Q083DDM130, Q083DDM141, Q083DDM142, Q083DDM143, Q083DDM144, Q083DDM145, Q083DDM146, Q083DDM147

Cathode panels use sandwich structure in order to achieve both stiffness and lightweight.

- Core is made from Nomex honeycomb 24 kg/m^2 (1347 g/m^2 for the whole sandwich panel) 8 mm thick.

- Skins are made from 2 x 0.1 mm thick high modulus carbon/epoxy prepeg. The carbon fiber from Mitsubishi company is impregnated with 28% of resin epoxy, cured at 80-120^{o}C, and performs 314 Gpa tensile modulus for the composite cured material (210 Gpa for steel alloys, 76 Gpa for aluminum alloys).

The limited width of a module (400 mm) allows a small flexure deformation under gas differential pressure loading. Simulations with Finite Elements Application show a maximum deflection of 12

μm/mbar and a 5 mm thick foam core, and 8 μm/mbar maximum deflection with a 0.2 mm thick carbon/epoxy skin and a 6 mm thick core. Experimental validation performs a deflection within 10% of Finite Elements simulation.

Initial flatness of sandwich panels is specified within 150 μm/m ($\pm$0.075 mm/m <->$\pm$ 0.050 mm/0.4 m)

Last development panels meet easily flatness specifications (better than $\pm$ 100 μm), but this result was performed only after 6 months of unsuccessful trials. Process of fabrication have to be quite different from current process used by companies, especially cold process is required in order to avoid strain induced by thermal stress.

Production of sandwich panels will be made by a composites producer company. 304 sandwich panels to produce, including spares, featuring a total area of 250 m^2.

Total production time estimated to 225 working days, roughly 1 sandwich panel/day.

The sandwich panels will be provided by Subatech Nantes to other labs.

2.1.2 Rigidity & Gap Fluctuations

Assuming a 0.5 mbar differential pressure, a 6 mm thick core, a 0.2 mm thick skin of high modulus carbon fiber, the deflection is 4 μm.

Experience from wire chambers with same parameters show that a $\pm$15% ΔG/G relative variation of gain is OK.

Formulas show that with present parameters, a ΔG/G of 15% is induced by a Δg/g of 4% (110 μm) relative variation of gap.

Conclusion : the design allows, to stay within $\pm$ 15% variation of gain, including a $\pm$ 30 μm tolerance for location of wires, and a 50 μm safety margin (for initial flatness of sandwich panel, ...).

2.1.3 Status and planning of production

- More than 20 different sandwich panels of different sizes produced since October 1999.
- 4 development prototypes which meet requirements produced by 2 companies on spring 2001
- Market survey launched in May 2001,
- Market survey closed on July 2001, 4 companies selected for next step.
- Technical specifications written and corrected
- Specifications to be sent to companies by end of November 2001
- Choice of contractor expected by end of January 2002
- Order expected in March 2002
- Head of production expected in May 2002
- Start of production expected in June 2002
- End of production expected in May 2003

2.2 Design of anode-cathode spacers

Aim of spacers is to set both pitch and gap.

The compression load induced by stretched wires is sustained by sandwich panels not by the wire support itself (spacers) which just transmit the load.

The wire support is rather a spacer and an electrical insulator than a mechanical (structural) component.

Raw material

This spacer is made from Noryl raw material which is chosen for its low water absorption both at room and at elevated temperature, and for its excellent electrical properties which remain stable aver a wide range of temperature, humidity and frequency variation. These properties allow to reduce problems

linked to leakage currents. Noryl spacers were widely used in ALEPH Electromagnetic Calorimeter for the same reason.

The SE100 variety of Noryl is selected (PPO, Noryl SE100, flame retarded, easy flow, 115 ^{o}C, 2300 Mpa, (= 1.11 g/cm^{o}). Safety documents from CERN allow the use of flame retarded Noryl.

Alternative material is PPO Noryl foam FN 150 which is lighter than standard Noryl (105 ^{o}C, 2000 Mpa, (= 0.90). Unfortunately there is not enough time before production to qualify this raw material.

In order to insure a good gluing, Noryl requires to be chemically treated with a sulfa-chromic solution : 45g dichromate Na + 885 g H2SO4 + 70 g H2O, process temperature 20 ^{o}C, process time 20'.

Shape (see drawings)

Final design features spacers with V grooves in order to glue the tungsten wires at the right location in pitch and in order to perform the right value of gap.

Status and planning of production for spacers

Prototypes machined in December 2000

3 companies have produced samples to prove feasibility.

Survey market launched in May 2001.

CCTP done.

Contract : on the way

Documents :

"Cahier des Clauses Techniques Particulières (CCTP), Expression des besoins pour spacers, trajectographie dimuon Alice"

Drawings : Q083DDM106, Q083DDM111

Figure 2.1: The two regions in the Cathode Plane Circuit.

2.3 The Cathode Printed Circuit Board (PCB)

2.3.1 Introduction

The SLAT chamber cathode planes are made by double sided Printed Circuit Boards (PCB). Owing to the required detector performances, the circuit design, production and assembly is a challenging task which requires after production accurate quality checks on the electrical properties and mechanical tolerances.

Since the beginning of 1999 more than 60 circuit samples have been produced. Extensive tests have been made on their properties. Some of them have been assembled to make SLAT prototypes, tested at CERN PS with pion beams or in the labs with sources.

In this section we present the requirements for these circuits, their mechanical and electrical characteristics, the quality controls during their production, the compatibility with the other detector parts, their assembly procedure and the foreseen costs and time schedule for production.

2.3.2 Circuit Characteristics

Each cathode plane element is a rectangular circuit, with an area of 580 x 400 mm^2, which can be divided into three regions (see fig.2.1) : the active area, 400 x 400 mm^2 wide, where the pad matrix is etched, and the electronics region made of two rectangular stripes 400 x 90 mm^2, to host the readout cards, plugged on 100 pin connectors. Each active pad is linked to the corresponding connector pin through a connecting line which is etched on the circuit backplane.

The SLAT modules have a constant width of 1 circuit (580 *mm*). Precise dimensions are indicated in drawing N. Q083DDM107. To guarantee the required stiffness and flatness PCBs will be glued on sandwich carbon fiber - honeycomb panels one next to the other.

2.3.2.1 Requirements

Here is a list of the main requirements for PCBs:

- Etching precision. The geometrical regularity of the pad matrix is an important issue to be able to locate each pad on the SLAT with an accuracy of not worse than 70 μm.
- Overall dimensions. The circuit nominal 400 *mm* size is to be carefully respected to be able to mount adjacent circuits without superpositions. This implies a precise etching and a strict tolerance on the border cutting, especially in the x direction.
- Positioning. Precision holes should guarantee the correct positioning of the circuits on the granite tooling during the assembly.
- Inter pad distance. The regularity of this distance is important to avoid dead areas or cross talk effects.
- Width of the connecting lines. Due to the limited space in the high pad density configuration, the connecting lines should be as thin as possible, to leave enough space between each other to reduce crosstalk effects.
- Thickness. The circuit should be as thin as possible compatibly with its stiffness, the impedance coupling with the readout cards and crosstalk effect between pads and underlying connecting lines.
- Gas tightness. This requires to close the circuit vias.
- Long life. Circuit performances should be kept for 15 years operation.

From the study of many circuit prototypes and discussion with PCB and raw material producers, and with CERN TIS, we have developed and improved the circuit project to satisfy the above requests in view of standard production.

2.3.2.2 Circuit Description

In the following we discuss the main characteristics of the PCB we intend to produce.

Dimensions The standard PCB size is 400 x 580 mm^2. This is a good compromise between the SLAT segmentation and the largest circuit size that most of the industries are able produce at an affordable price. A further increase in the dimensions would have led to a decrease in the etching precision and a sensible cost increase. The active area is 400 x 400 mm^2. For the Slats with rounded circuit of type R_3 we are obliged to extend the width of one PCB from 400 *mm* to a higher value. Figs 2.2 and 2.3 show the schematics for density 1 circuits of Bending and Non bending plane respectively.

Thickness In the choice of the PCB thickness the following factors have been considered:

1. reduce as much as possible the radiation length;
2. keep a minimal stiffness, mainly required in the regions where the readout electronics is located;
3. couple the impedance between the cathode circuit and the readout electronics;

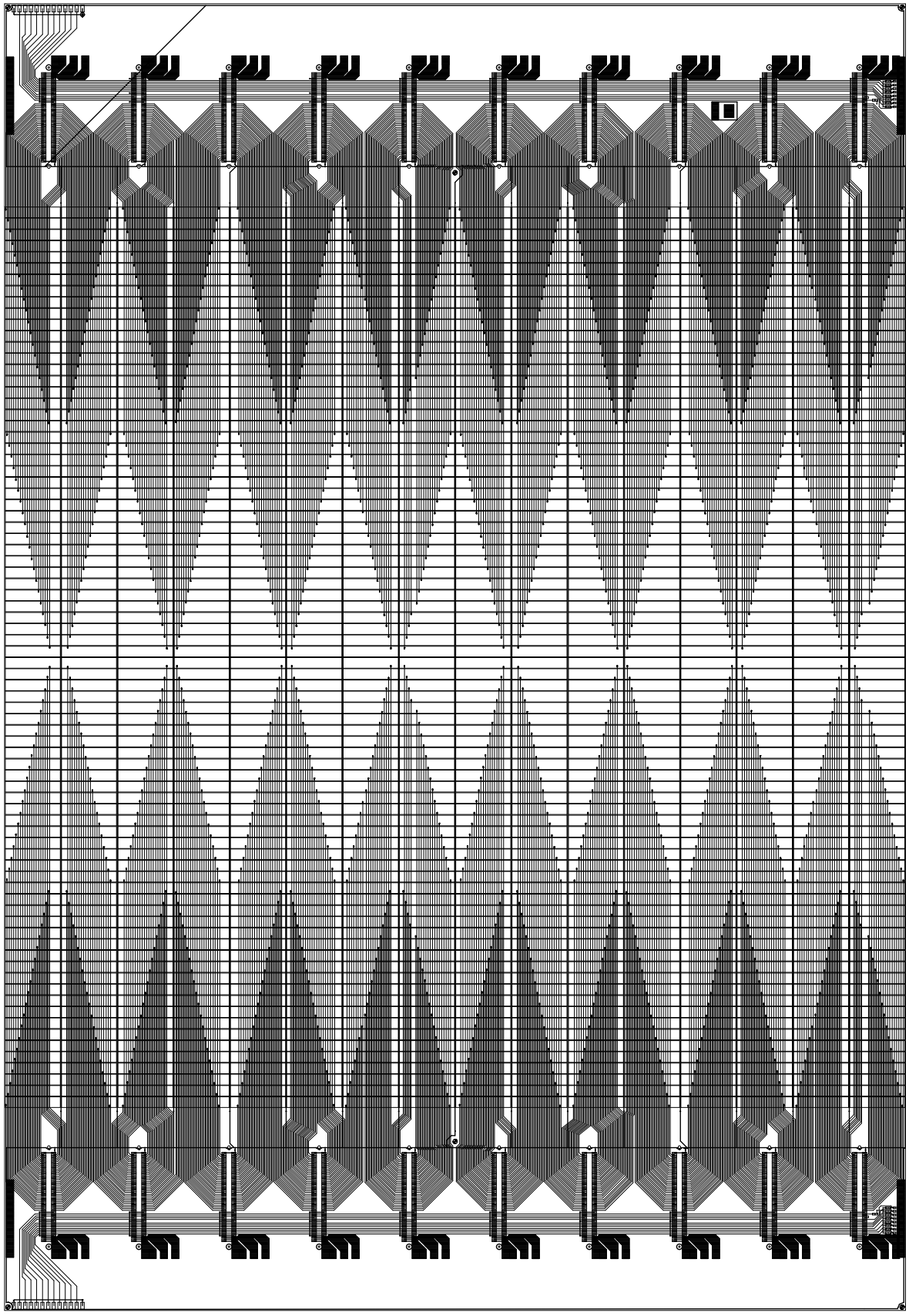

Figure 2.2: Schematics of Bending plane PCB for highest density pads.

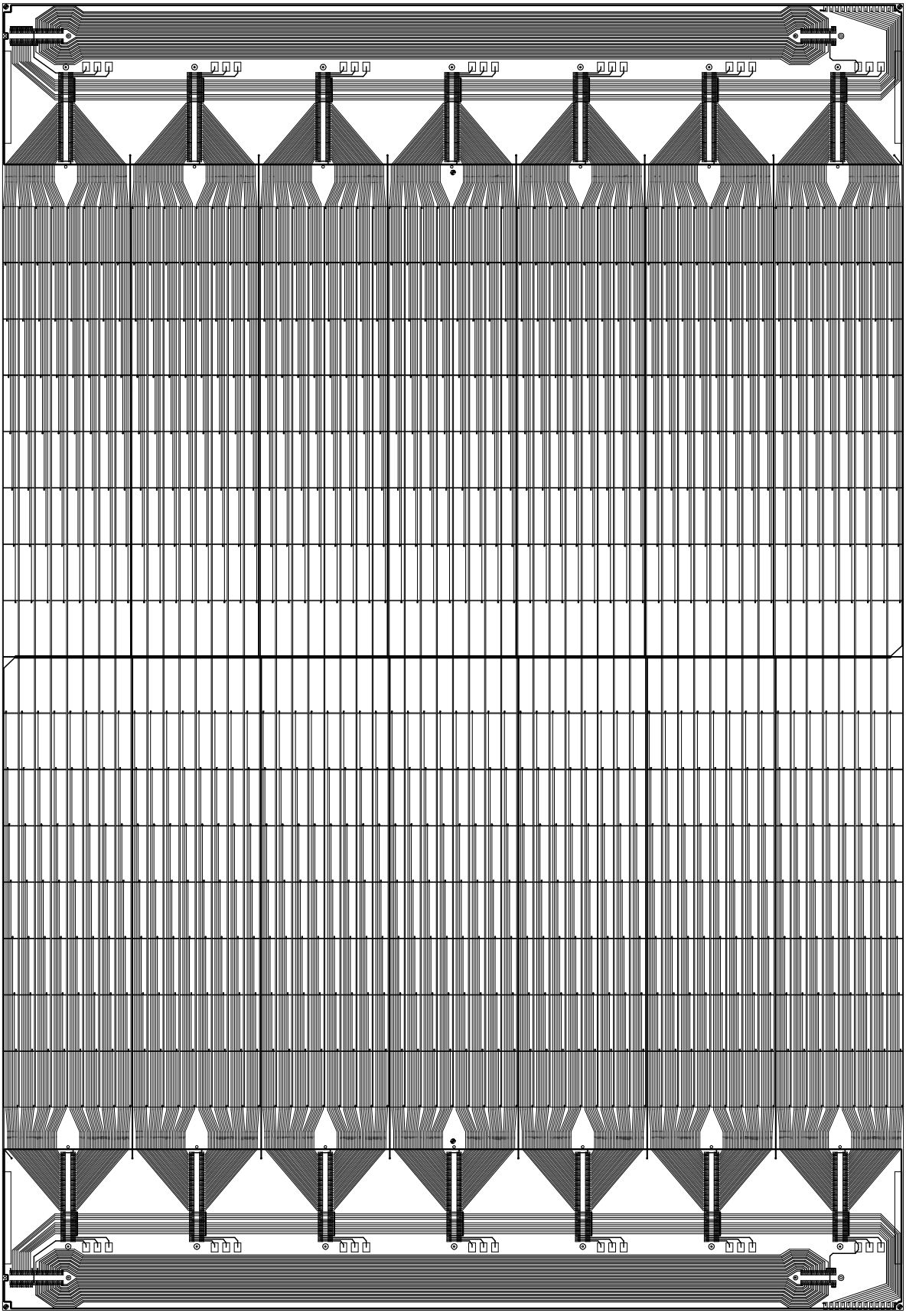

Figure 2.3: Schematics of Non Bending plane PCB for highest density pads.

	Bending Plane (mm^2)	Non bending Plane (mm^2)
Density 1	5 x 25	7.143 x 25
Density 2	5 x 75	7.143 x 75
Density 3	5 x 100	7.143 x 100

Table 2.1: Pad Size for Bending and Non Bending planes.

Originally some prototypes were assembled with 0.2 *mm* thick circuits. This value doesn't well satisfy the second and mostly third point. In fact to keep the value of 0.2 *mm* and guarantee the impedance coupling, we should have reduced the connecting strip width down to a critical value for mechanical resistance and production cost. We have decided to increase the laminate thickness to 0.4 *mm*. This value has been used for the last prototypes assembled in a 2400 *mm* slat.

For what concerns first point, namely the radiation length, of course the most important role is played by the metal layer. So far we have used many values for the Cu layer depending on the availability on the market, and from our experience 9 μm of base material seems a good value. We will come back on this point in paragraph 2.3.3.2

Pad Size Rectangular active pads are etched on one side of the circuit. The size of pads has been chosen as a compromise between the chamber occupancy (5%) and the total number of channels. They are shown in tab.2.1. In the Non bending plane the pad width, 7.143 *mm* is chosen to have exactly 56 pads per row to optimize the number of connectors per PCB. A smaller size like 5 *mm* would have increased too much the number of channels, while a larger one like 8.333 *mm* (48 pads per row) has been shown to reduce the possibility to identify the hit wire.

2.3.2.3 Distance between Pads

The distance between pads is chosen to minimize crosstalk effects with a negligible lost in active area. Along the y axis the chosen distance is 250 μm. Along the x axis, perpendicular to wires, PCBs are glued one next to the other. The circuit positioning is obtained from the reference pins inserted into the assembly tooling. The distance between pads along this direction is 500 μm. It has been chosen taking into account the following points:

- The superposition between adjacent circuits must be avoided,
- The tolerance on circuit etching is 150 $\mu m (\pm 75 \mu m)$,
- The error on PCB border cutting is another 170 $\mu m (\pm 85 \mu m)$,

2.3.2.4 Connecting Lines

Each strip is connected to the readout electronics by means of a line on the circuit backplane. The chosen line width is 180 μm. This value allows to keep a minimum distance between lines of 250 μm in the highest density region, in order to reduce crosstalk effects without changing the circuit class. In some rounded PCBs we will decrease the strip width down to 150 μm, so the class will be N.5 (more expensive) instead of N.4.

2.3.2.5 Circuit Design

The circuit design will be made with CADENCE-ALLEGRO package. Up to now all the samples have been designed either at INFN Cagliari or SUBATECH Nantes. Given the relevant amount of different designs to be produced, a task sharing between these two labs is foreseen for the standard production.

Before production circuit designs have been crosschecked and validated by the Orsay and Saclay group involved in the design of the readout cards and busbars production.

Circuit Number and Types Each chamber has been subdivided into three regions for what concerns the pad size, as shown in fig. 2.4. To reduce the number of PCB types to be produced, each circuit will have pads of only one size. In this way there will be three "standard PCB" types per plane.

Moreover in the region around the beam pipe, slats with rounded PCB have been foreseen to reduce event losses. These PCBs are of pad density 1 with special shape and dimensions. There will be two types of rounded PCBs in station 3, and one type in stations 4 and 5. Their drawings are shown in fig.2.5,2.6,2.7. In chamber 5, due to the constrains imposed by its position inside the magnet and to its location in z, another type of special PCB is required. This circuit will be 350 x 580 mm, namely 50 mm shorter than the standard one.

In the "slat table" the total number of circuits required is shown. The first column identifies the slat type according to the following convention: the number of digits not zero represents how many PCBs there are in the slat, while their value corresponds to the pad density (1,2 or 3). A following "N" or "S" indicates if all the PCBs are standard or if one is shorter. Finally a letter "R" is added when a rounded PCB is present.

Column 2 indicates how many SLATS of each type are to be assembled, plus spares indicated in column 3. We have then reported the slat active length in column 4, its location in column 5 and finally the PCB total number in column 6. We obtain in the end a total of 653 + 653 circuits to be produced subdivided into 14 different typologies.

2.3.3 Raw Material

The circuit etching is made starting from a double sided laminate made of a glass fiber support and two layers of copper. We have contacted two laminates producers (DITRON and ISOLA-MAS) to have information about the characteristics of the product available on the market which can satisfy our requirements.

2.3.3.1 Insulator

The main requirement for the insulator is the dimensional stability during the etching process, the storage before assembly and the many years of chamber operation.

In table 2.2 and 2.3 column 3, we report the main physical and electrical characteristics of a "standard FR4", EP-84, produced by DITRON, which could be employed for our circuits.

Ordinary glass transition temperature (TG) is 130°. From our discussion with laminate producers, since the PCB will not operate at high temperatures a higher TG should not be needed.

A dimensional dilatation within 100 μm during the fabrication process has been indicated by circuit producers (CERN lab, Cistelaier). It implies an uncertainty in the pads etching. We can confirm this value from our experience on the samples we measured and we have taken into account this uncertainty when considering the clearance to be left between pads in the x direction and the border cutting distance.

Another possible source of dimensional variation is humidity. We have measured a dilatation of 60 μm over 400mm in the x dimension of a circuit, not assembled, stocked for months at a non stabilized temperature and humidity. This effect can be recovered by reconditioning the circuit for few hours at 120° and is anyway within tolerances. Nevertheless PCBs will be stocked after production in a room already existing at INFN Cagliari at a stabilized temperature and humidity. After gluing on the sandwich panels, PCBs will not show any appreciable dimensional change.

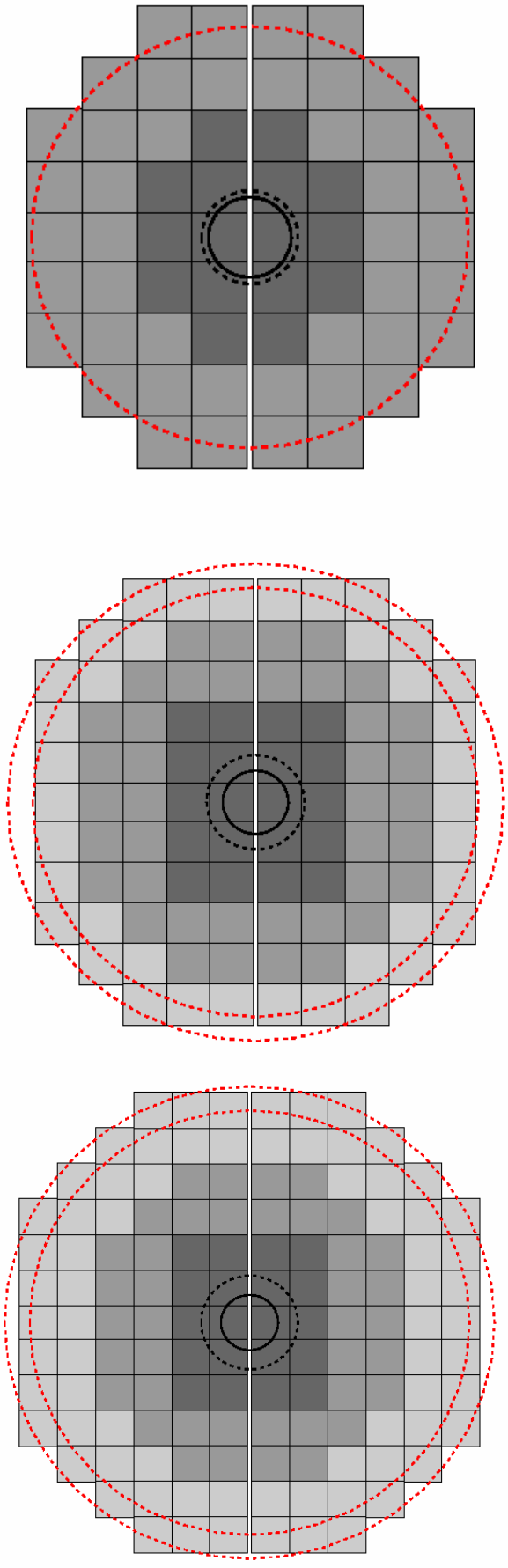

Figure 2.4: Schematic view of a chamber of station 3, 4, and 5 respectively with the different pad densities.

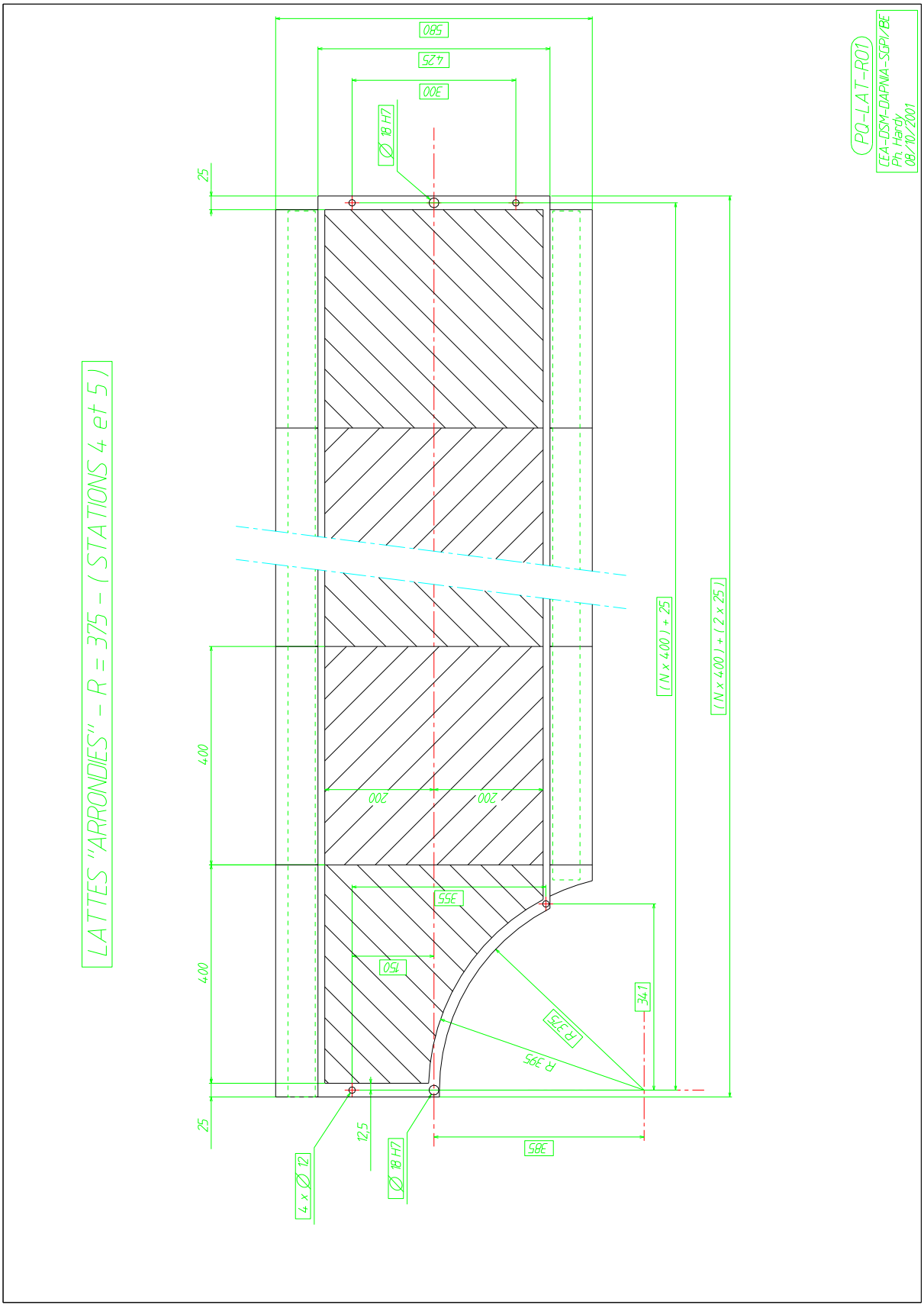

Figure 2.5: Slat with rounded PCB R1.

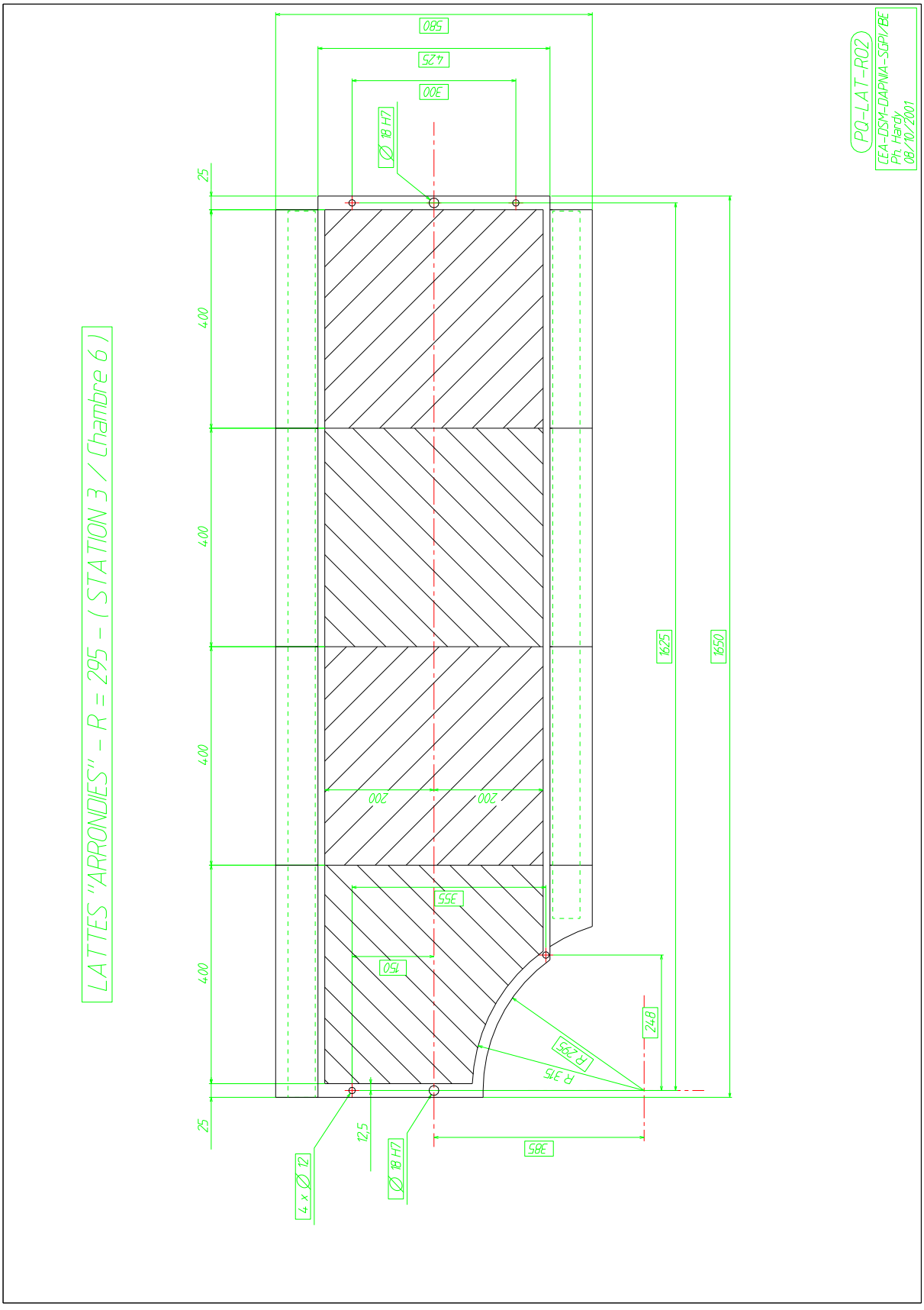

Figure 2.6: Slat with rounded PCB R2 (station 3 chamber 6).

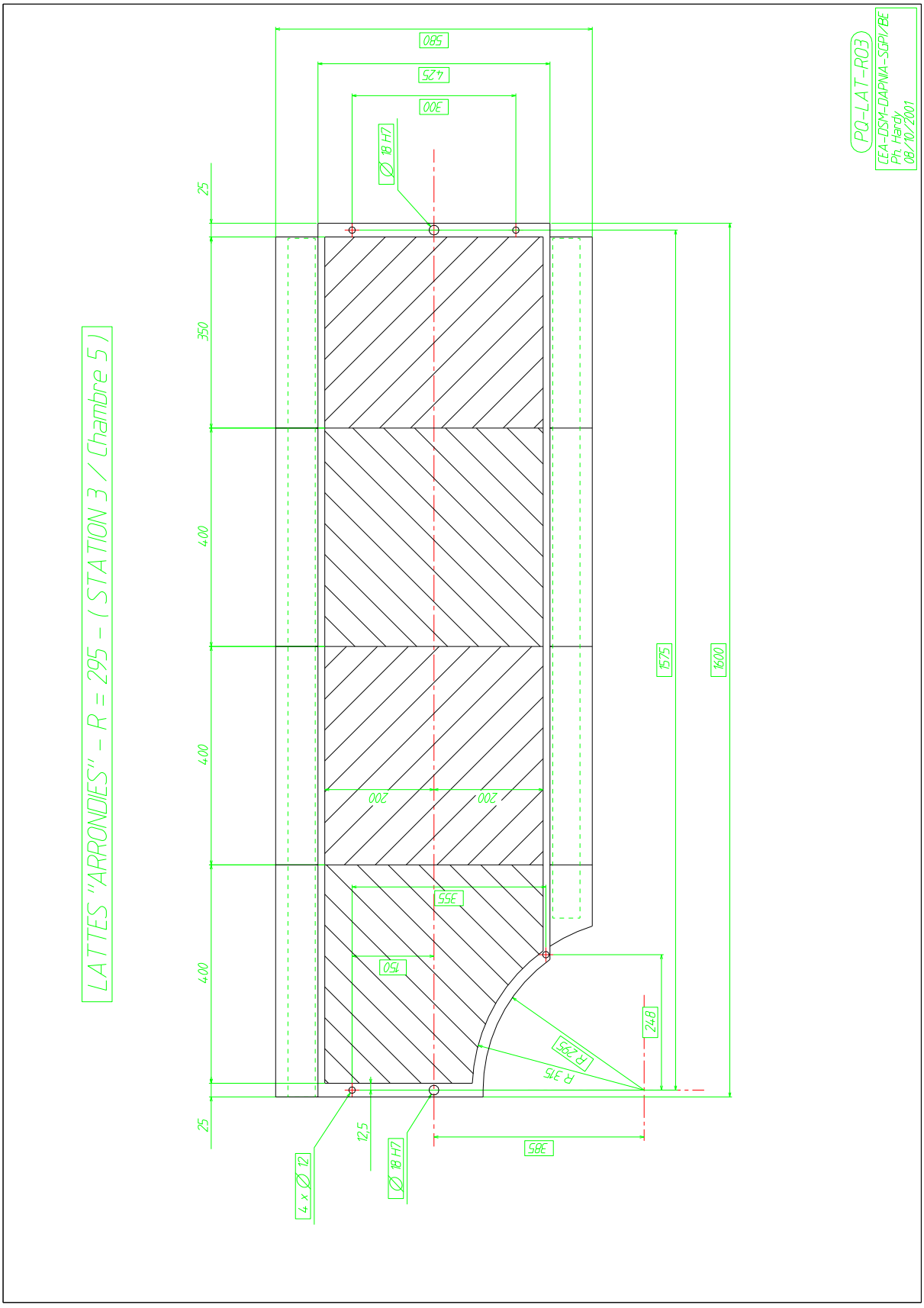

Figure 2.7: Slat with rounded PCB R3 (station 3 chamber 5).

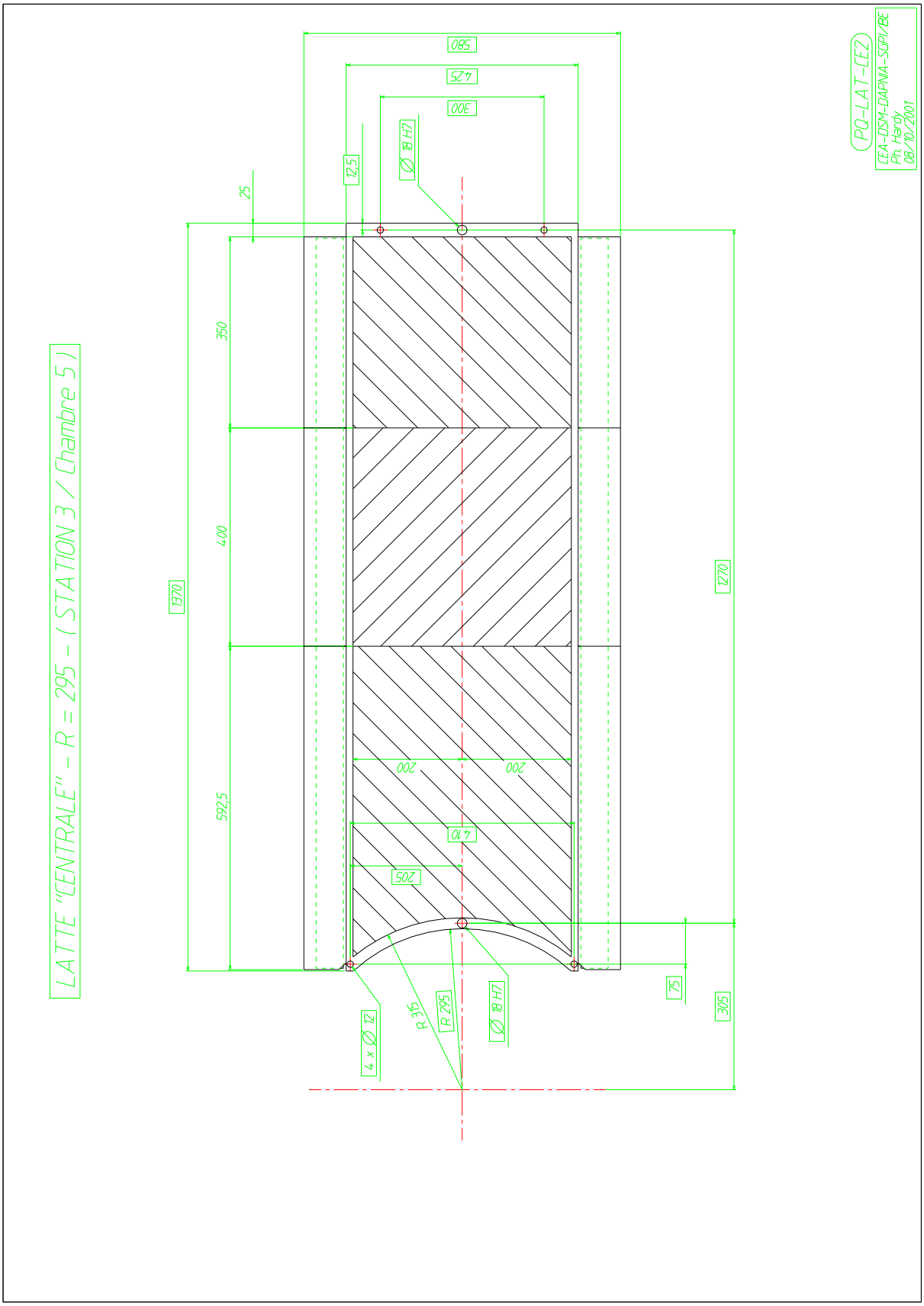

Figure 2.8: Slat with rounded half-moon PCB, chamber 5.

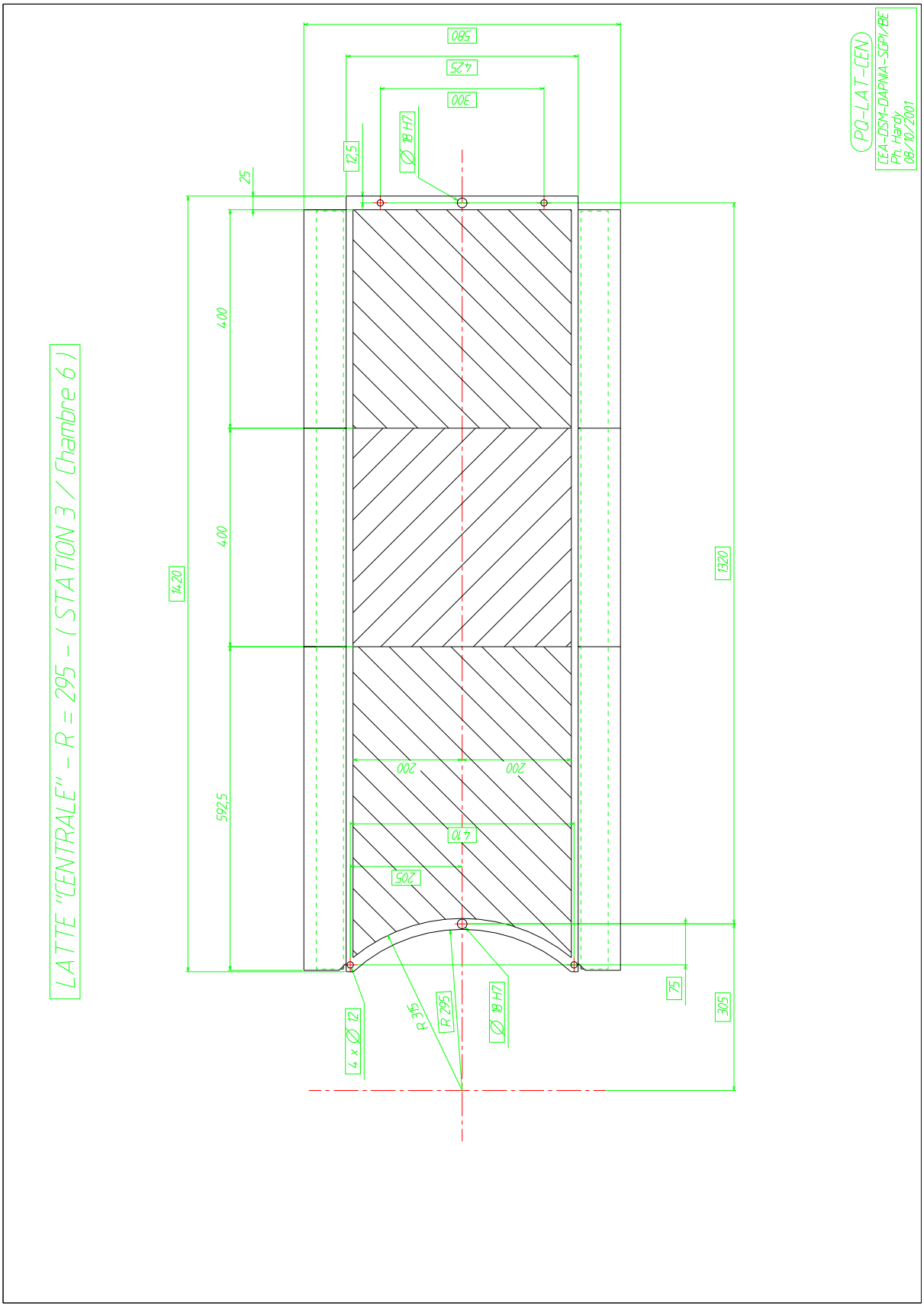

Figure 2.9: Slat with rounded half-moon PCB, chamber 6.

PHYSICAL PROPERTIES	Unit of measure	DITRON EP-84	DURAVER E-Cu 156
FLAMMABILITY	sec. (max)	4	3
		7	5
WATER ABSORPTION	% (max)	0.15	-
PEEL STRENGHT			
-As received		180	-
-After thermal stress	kg/m	160	185
-At temperature 125° C	(minimum)	140	175
-After exp. to processing solutions		160	175
FLEXURAL STRENGHT			
-Lengthwise	kg/m^2	5.5×10^7	6.6×10^7
-Crosswise	(minimum)	4.5×10^7	5.8×10^7
GLASS TRANSITION TEMPERATURE	°C	> 130	> 120
COEFFICIENT OF LINEAR EXPANSION	$^\circ C^{-1}$		
-X, Y direction		1.4×10^{-5}	1.3×10^{-5}
-Z direction		7×10^{-5}	14×10^{-5}

Table 2.2: Physical properties for standard FR4 and Duraver E-Cu 156 halogen free.

ELECTRICAL PROPERTIES	Unit of measure	DITRON EP-84	DURAVER E-Cu 156
DIELETRIC BREAKDOWN -step by step	kV (minimum)	85	75
LOSS TANGENT -at 1 MHz	tgδ (max)	0.020	0.020
PERMITTIVITY -at 1 MHz	ε (max)	4.5	4.5-4.9
ARC RESISTANCE	sec. (minimum)	120	90
VOLUME RESISTIVITY	MΩ/cm		
-After moisture resistance	(minimum)	1×10^8	8×10^8
-At high temperature		1×10^9	8×10^6
SURFACE RESISTIVITY	MΩ/cm		
-After moisture resistance	minimum	7×10^7	4×10^6
-At high temperature		7×10^8	7×10^6
Q (RESONANCE)			
-at 1 MHz	minimum	90	90
-at 50 MHz		120	120

Table 2.3: Electrical properties for standard FR4 and Duraver E-Cu 156 halogen free.

Halogen Free material At CERN, TIS is discussing in these months the possibility, for safety reasons, to allow in the LHC experimental halls only PCBs made of halogen free material.[1]

Although the decision will be probably taken at the end of this year, we have investigated this possibility for our circuits. In particular we wanted to know if there are possible variations in the mechanical and electrical properties of the halogen free material, and what could be the price increase.

Since up to now halogen free laminates have been scarcely used, PCB producers normally don't have such material on stock. Thus it is not easy to obtain few samples to test. Fortunately at CERN PCB laboratory, since some test is going on, we found the possibility to produce 6 samples which are now being etched. Anyway according CERN group (R.De Oliveira) this material should be compatible with the standard one, but its production much slower, for market reasons. The same opinion was given by a laminate producer, MAS-ISOLA, from which we are waiting in these days for a cost and a fabrication delay estimate. In tab 2.2 and 2.3 column 4 we report the properties of an halogen free material, Duraver E-Cu 156, produced by ISOLA-MAS.

In conclusion we intend to complete the tests on the halogen free circuits already ordered and to compare costs before the final decision on the raw material.

Insulator Thickness The chosen thickness is 0.4 *mm*. The normal tolerance guaranteed by producer on this value is $\pm 10\%$ going from one roll to another. Local variations which could introduce gap changes should be normally much less. Random measurements on the produced circuits confirm this fact and will be made on the standard production. On the other hand the requirement of FR4 with a more stable thickness would sensibly increase the price.

2.3.3.2 Metal

Owing to its radiation length of 14.3 mm, the Copper layer must be chosen as thin as possible. Most of the PCB on the market are made starting with a base Cu layer of 17 μm. After vias metallization a refilling is performed generally of 20 μm. The final chemical gold plating introduces only 1 or 2 μm. To have a thinner Cu layer, it is necessary to start from a non standard laminate and to control the refilling. We have produced several samples with Cu base layers of $9\mu m$ and even 5 μm, reaching a final thickness of 15-20 μm. Even though we have observed good electrical properties in both of them, the value of 9 μm seems a good compromise.

2.3.4 Circuit Fabrication

Here is a list of the fabrication procedures and of the items to be checked.

2.3.4.1 Etching

A tolerance of not more than ± 40 μm will be allowed on the pad etching. This value will be randomly checked along each circuit. From our experience this point is not critical since the normal error we measured on the pad size is less than ± 30 μm. A tolerance of $150\mu m = \pm 75\mu m$ on the distance from the first to the last pad column along the x direction will be considered.

[1] From the minutes of the 77th Safety Co-ordination Meeting for LHC Experiments (21/9/2001):

- "Replacement materials for printed circuit boards containing halogens - status (feasibility of electrical tests at CERN) - Instruments for test is now ready; person has been selected to perform tests but has not yet accepted."
- "Replacement materials for printed circuit boards containing halogens - status (Alternative PCB materials (prototype testing) - R.Schmidt thought that H.J.Hilke should be invited to present their current findings."

2.3.4.2 Vias

Each strip has a via for the connection to the backplane. Its diameter is 0.2mm, the minimal value which doesn't require a laser technique for its drilling. To avoid gas leakage vias are finally closed by the solder mask varnish. Up to now we have observed a good gas tightness.

2.3.4.3 Gold Plating

The gold plating after recharge prevents from Cu oxidation and should guarantee good functioning of the circuits for 15 years. From the discussion with producer, a chemical gold plating seems the best procedure. A visual check on each circuit will be made to detect the presence of non uniform golden areas or other impurities on the surface.

2.3.4.4 Solder Mask

The two requirements for the solder mask are a good compatibility with the ARALDITE glue and the closure of vias hole. We have verified both this features on several samples by using a varnish solder mask.

2.3.4.5 Border Cutting

The precision in the border cutting is critical along the x direction to avoid superpositions between circuits or cuts of the last pad column. For this reason the inter pad distance was increased in this direction to 500 μm.

The nominal value of the active area along the x axis s 399.500 mm. Taking into account the etching tolerance and the error on the position of the reference pins on the assembly tooling we estimate that the border should be cut with an error of not more than $\pm 85 \mu m$ with respect to the nominal value of 399.795 mm. To reduce the error the cutting should be made using the center PCB axis as a reference, instead of the reference marks which, since etched, suffer this uncertainty.

The value generally guaranteed by PCB companies is between 100 and 150 μm, since the cutting is performed with a numeric controlled milling machine, using as a reference the marks etched on the design. Moreover there is an uncertainty coming from the tooling degradation during the milling procedure. Nevertheless we measured a milling precision on our samples as machined by the producers of 100 μm at worst. We have verified then that it is possible to specify to the producer a tolerance on the border cutting of $+0\mu m - 100\mu m$. The samples employed for the 2400mm prototype were cut with this technique to $400mm + 0\mu m - 100\mu m$, a value which allowed their assembly without problems.

To better control the cutting precision another alternative was proposed. A customized machine was designed and built at PNPI, to cut and punch PCBs. It is based on a flat stainless steel table where the PCB can be fixed after micrometric positioning with the help of three microscopes. In this way the axes of the machine are perpendicular to the circuit axes. The PCB is then fixed and the cut is performed with two blades that can move along two rails.

The machine was installed at INFN Cagliari in October and tested up to now on three circuits with very satisfactory results. The border cutting is quite uniform with a 20 μm dispersion with respect to the nominal value. The cut time is around 20 minutes per circuit, which means a total of 6 months of work including the circuit measurement. More circuit samples are now under production to make further extensive tests also on the blade duration, which should be around 50 cuts.

Anyway whatever will be the final choice, we feel confident to obtain the required uniformity and precision on cuts. On the other side this decision doesn't slow the call for tender, since anyway the circuit is milled by the producer and we can ask a border of 2 mm to be successively cut with the customized machine.

2.3.4.6 Positioning Holes

The PCB positioning on the slat panels is achieved through two precision holes (H7) drilled on the middle axis of each PCB. The circuit is positioned on the assembly tool through reference pins (g6) inserted in these holes.

In case the custom cutting machine will be used, the holes will be punched instead of drilled. To allow the cutting and assembly process one of them will be rectangular 3x4 mm^2. Measurements performed on these punched holes gave satisfactory results on their precision (8 μm in the diameter) and positioning (10 μm).

2.3.4.7 Connectors

Each PCB has a variable number of 100 pin SMD connectors ranging from 4 to 20, to plug the readout electronics. The chosen connectors are: BERG STAK series surface mount header, 0.80 mm centerline, produced by Framatome Connectors International [2]. In the Non bending plane other two 60[3] and two 40[4] pin connectors are present to place the Bridge Board and the Translator Board.

2.3.4.8 Connectors Soldering

SMD connectors will be soldered on PCBs after their optical and geometrical check. As explained a further electrical check of short circuits and interruptions also at the soldering level is foreseen.

2.3.4.9 Circuit Assembly

The assembly technique involves the PCB positioning and gluing. It has been refined during two years in the labs involved in the project.

2.3.4.10 Positioning

Circuit positioning is performed through the reference pins inserted in the assembly tooling. The required tolerance for these pins is $\pm 10 \mu m$ on their nominal position. This value was already achieved on the assembly tooling installed at SUBATECH, and used for the large Slat Prototype mounting.

As already mentioned the two holes on the PCB will be rounded if drilled or one rounded and one rectangular if punched. Anyway they will be used for the positioning of the circuit with respect to the table and sandwich panel.

2.3.4.11 Gluing

PCBs are glued on the NOMEX insulator sheet which is glued on the sandwich panel. ARALDITE 2011 epoxy glue is used for this purpose. It is a multifunction adhesive bi-component of high resistance and toughness, which polymerizes at room temperature. We have crosschecked a complete compatibility between the PCB solder mask and the ARALDITE.

2.3.4.12 Cathode Flatness

To achieve the required cathode plane planarity, the circuit and panel are assembled onto a granite assembly tool with a planarity of less than 100 μm over 1m. During the glue polymerization a uniform load is exerted on the cathode through vacuum pumping between the granite and a nylon foil that envelope the sandwich.

[2] code 61083-102-002
[3] code 61083-062-002
[4] code 61083-042-002

2.3.5 Quality Check

Before their assembly, PCBs must be electrically and mechanically checked. This operation will be made at INFN Cagliari before sending the circuits to all the laboratories involved in SLAT production. After delivery to Cagliari and during the quality control, circuits will be stocked in a room in which humidity will be controlled and temperature kept at $20^0 \pm 2^0$. Humidity will be also controlled durin transportation to other labs for assembly, with a special packaging.

2.3.5.1 Electrical check

Each circuit will be electrically tested by the producer with an optical device. This test guarantees the correspondence between the design and the circuit, but cannot detect some electrical defects like for example interruptions inside vias. To do so an electrical test is required with an "ad hoc" device. Moreover this test is needed after the connector soldering. We have enquired several companies about the possibility to perform it. Some of them are simply not able do develop such a device for so large circuits, others could make it but the cost is sensibly high. We have then decided to develop an electrical testing device at INFN Cagliari. A short functional description is given in the following section.

Electrical test device A system to perform electrical test on the PCBs has been designed and it is currently under development. In order to be able to test all the different PCB layouts, on different stage of mounting (i.e. with or without connectors) and on both the analog (pads to MANU) and digital (LVTTL and LVDS BUS) connections, a full modular system has been designed. The schematic diagram of the control unit is shown in fig. 2.10. The unit can operate stand-alone or connected to a PC. When in stand-alone mode the configuration to test a specific PCB must be loaded (just once, from the PC) in the EEPROM memory. The operator can then control the unit and check the results of the test through the front panel display and keys. When connected to a PC the unit will be controlled by the application which runs on it.

The Unit is connected to the PCB with two flat cables, through adapter pods and contact plates specific for the PCB and the type of test (see fig. 2.11).

Principle of operation.

The out matrix has 64 outputs that are normally on a high-impedance state. They are pulled to ground one by one during the test. The 64 inputs of the input matrix are then selected in sequence and the state of each compared with the configuration in memory to verify the connection quality or any short circuit between adjacent lines. A pull-up resistor network on the inputs assures a valid state when there is no connection to ground through the output matrix lines. While 64 I/O lines are enough to test the digital buses, the pads in the PCB are up to 640, so one line of the output matrix will drive several pads. A special care is taken on the design of the contact plates to assure that the pads driven simultaneously can not be shorted due to a defect on the PCB.

An estimated time for fully test a PCB is between 10 to 15 minutes, thus if a total number of 1300 PCB must be tested the amount of time needed will be around 300 hours.

2.3.5.2 Dimensional check

The geometrical check will be performed on each circuit with the help of a measuring device, installed since two years at INFN Cagliari, and full time available for the ALICE experiment. This device, a CMM (Coordinate Measuring Machine) with a CCD camera, can measure distances with an accuracy of 7 μm over 1 m range.

All the circuit up to now produced have been measured with this machine. The foreseen checks are intended to verify the following parameters:

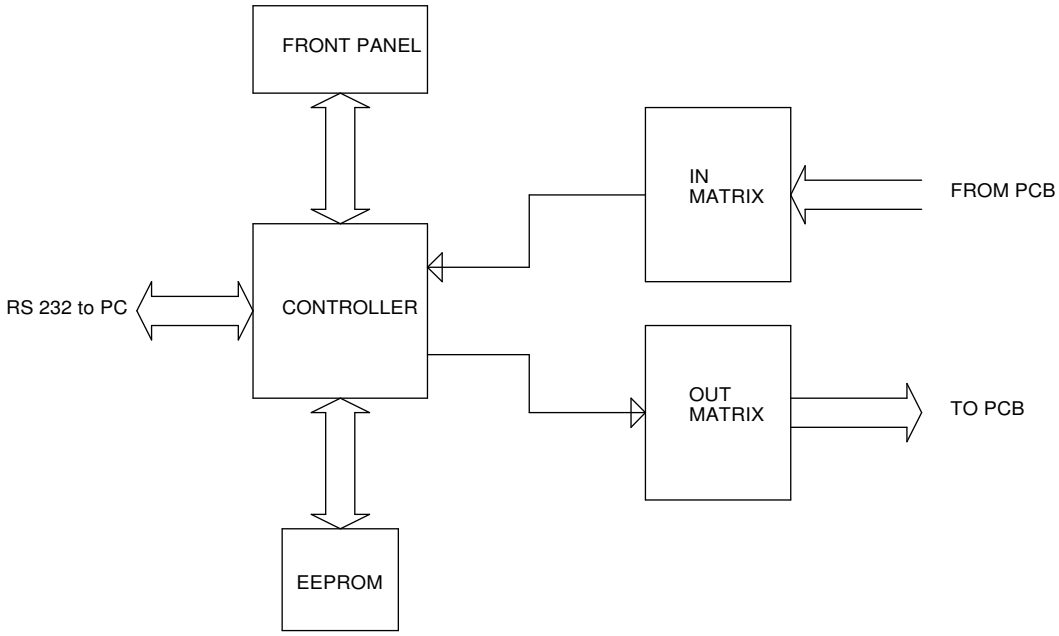

Figure 2.10: The schematic diagram of the control unit.

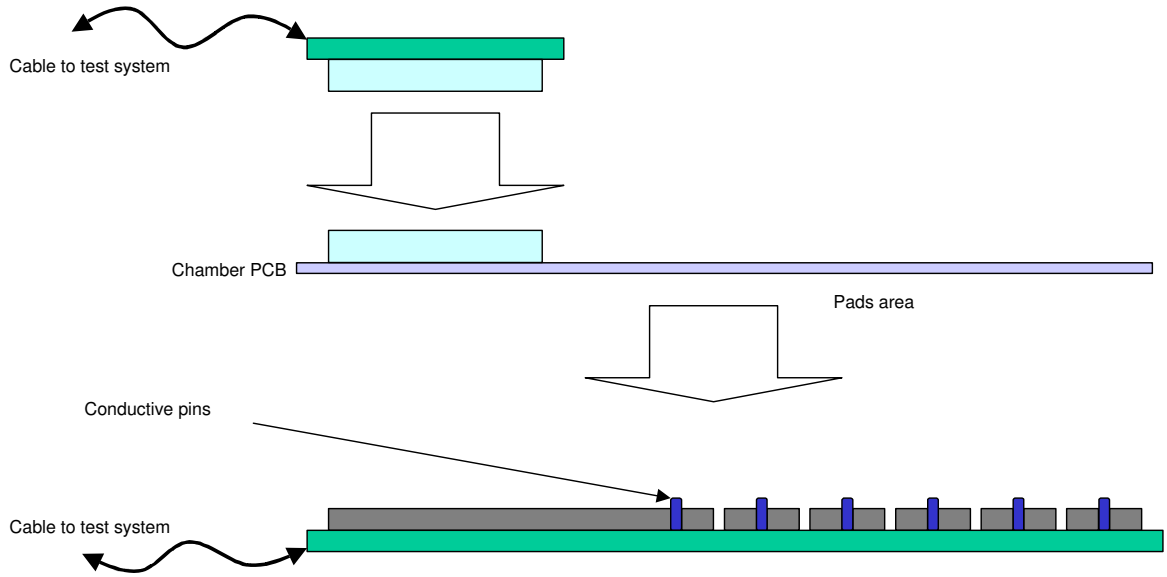

Figure 2.11: Connection of the unit to the PCB through two flat cables.

- Overall circuit size in y and x. It is important particularly to check the border cutting, namely that the x dimension is not greater than the nominal value of 399.800mm (theoretical value of 399.795 *mm*) and the etching precision.
- Distance between the positioning holes. The nominal value is 430 $\pm$0.010 mm. This distance is crucial to have a correct PCB positioning. The holes axis must be aligned with the PCB y axis within 10 μm.
- Distance between pads. This value is 250 μm along the y axis and 500 μm along the x axis The tolerance on these values are $\pm$ 70μm. This measures will be randomly crosschecked along the circuit.

2.3.6 Costs

According to the ALICE Memorandum Of Understanding, Slat cathode plane PCBs production is in charge to INFN.

A cost of 500CHF per circuit was foreseen (ALICE CORE) for the circuit production, connectors purchase and connector soldering. From our recent and preliminary estimations we can confirm this costs.

We can subdivide the production into three items:

1. Standard PCB production;
2. Rounded PCB production;
3. Connectors Purchase;

4. Connector soldering.

The sum for all the project has been financed in two tranches by INFN in years 2001 and 2002. Since the call for tender will take several months, and the first amount has already been allocated for 2001, the financial procedure at least for point 1 and 3 should start by the end of the this year. This means that the committee which rules the purchasing procedure should be nominated in order to allocate the correct amount of money for each item, but does not imply that the final design must be freezed by this date.

2.3.7 Time Schedule for design, production and test

The start of the first standard slat assembly is foreseen for December 2002. The time schedule is done to allow design, production, quality check and delivery of the first circuits by November 2002. The production and test procedure should be ended by October 2004.

2.3.7.1 Design

The last 2400 mm slat prototype cathode planes were compatible with the new version of the readout electronics. Although not final, it is very close to the final one. Thus the bending and non bending plane circuit designs need only very small modifications. These circuits are the most difficult for what concerns the routing, since they have the highest pad density. We plan to complete the design for all the standard circuits by April 2002.

The rounded PCB design is more complicated, given its shape and asymmetry. A rounded slat prototype with the new version of the readout electronics will be tested in spring 2002. So we foresee to complete the deigns of this type of circuits by November 2002. Since the rounded slat will be assembled in a second phase, this point is less critical.

2.3.7.2 Production

According to our experience, the production delay is not easy to estimate and depends on many factors like the availability of raw material and the working schedule of the producer. We can roughly foresee a production time of six months for the standard circuits and three months for the rounded ones. Of course this time could be much longer if it will be decided to use a halogen free laminate. The connector soldering could be done in around one month for all our production. Thus we plan to start the circuit fabrication by October 2002.

2.3.7.3 Border Cutting

In case the border cutting will be made by the producer, PCB will be delivered already cut. If we decide to cut the circuits in our labs, we can estimate about 90 days full time working to complete the job.

2.3.7.4 Quality Check

The geometrical check of one PCB takes about 30 minutes plus 15 minutes for the electrical control. This means about 120 days to complete the job, which of course could run in parallel with the border cutting.

2.3.8 Appendix 1 : List of the contacted PCB Industries

Here is a list of the companies up to now contacted and wether they are able to produce our circuits or if they have already. These contacts and the samples produced were very useful to know what is available on the market and what are the limitations. Producers are indicated with a number. Complete list with names is available on request.

CERN PCB laboratory (Mr. A.Gandi). Samples produced. Good quality. Not able to produce on large scale.

1. Producer 1

   Produced circuits of good quality on $17\mu m$ Cu. Other samples now under production for mechanical and electrical tests.

2. Producer2

   Many samples produced of good quality. $5\mu m$ Cu raw material available on stock.

3. Producer 3

   Produced samples of good quality.

4. Producer 4

   Circuits presently under production (standard fr4).

5. Producer 5

   Produced circuits of good quality. No estimation for series production received since 1 year.

6. Producer 6

   Not able to produce at home.

7. Producer 7

   Produced circuits of poor quality.

8. Producer 8

   Not interested to produce small series (150 pieces).

9. Producer 9

   No quotation received.

10. Producer 10

    Not able to produce such large circuits.

11. Producer 11

    Unable to produce such large circuits.

12. Producer 12

    Not able to produce such large circuits

2.3.9 Appendix 2 : Contacted laminates Producers

1. ISOLA ag. MAS Italia S.p.a.,

   I-51032 Bottegone (PT),

   e-mail: Boldrini@isola-mas.com

   Standard raw material received and used for cutting tests. Estimation requested for halogen free laminate.

2. DITRON Address: Novara Telephone: 0321 771711 Fax 0321 771746. e-mail: ditron-srl@libero.it

   Standard raw material received for mechanical tests.

2.4 Slat integration process

2.4.1 Documents :

- Description of slat assembly (file : assemblagioNantesEng_V2.doc)
- Slat integration, Operator's Manual (file : slat_integration.doc)
- Drawing Q083DDM107
- Drawing Q084DDM115 : Slat Cross section
- Drawing Q080DDM109A : Assembly table (Marbre d'assemblage 2450)
- Drawing Q083DDM106 : V grooves spacer

2.4.2 Preliminary

Integration of slats requires dedicated room, temperature controlled (20 ^{o}C$\pm$ 2 ^{o}C), humidity controlled (< 60% RH), fairly clean (Grey room), minimum area of 40 m^2 + storage area @ RH<60%

2.4.3 Assembly table (drawing Q080DDM109A)

This tooling is the masterpiece of integration of slat table, it aims to :

1- define a reference of flatness : specified flatness is Class 2 (0.020 mm/m)

2- define absolute location of each PCB, define location of readout pads

3- support of vacuum system which produces mechanical load for different gluing process

The prototype of the assembly table was designed and engineered by Subatech Nantes in 2000.

Granite raw material is supplied by Maitre company, fine machining was achieved by EADS on a large jig-boring machine (one of the largest one in Europe) in a 20 ^{o}C temperature controlled room, tolerances of $\pm$0.010 mm were performed for location of Φ3H7 bores which aim to locate PCBs.

The assembly table was qualified in spring 2001 with 1600 and 2400 mm long prototypes.

2.4.4 Dielectric sheet assembly

A dielectric sheet is intercaled between the PCBs and the sandwich panel in order to reduce capacity and induced electronic noise.

0.250 mm thick Nomex (PolyImid material) is selected and validated as dielectric sheet.

Nomex sheet is glued on the carbon/epoxy skin of the sandwich panel with a film of araldite 2011 epoxy resin, 2 x 0.020 mm thick.

Total amount of Nomex 550 x 0.44 = 242 m^2,

Nomex will be supplied to each laboratory by Nantes group.

2.4.5 PCBs assembly

The PCBs are glued on the sandwich panel (Nomex side) in order to form the cathode planes. Accurate location of PCBs is given by assembly tooling ref. Q080DDM109A which is mainly a large flat granite table with locating bores Φ3H7.

Mounting of each PCBs uses the two Φ3mm H7h6 rods, located in the middle of each PCB, 430 mm $\pm$0.020 mm spaced, one rod is located at 215 mm $\pm$0.010 mm of the median centerline will be used as locating rods during gluing process on the sandwich panel. 2 Φ16 mm H7h6 rods locate sandwich slat versus PCBs.

A standard 2400 mm long slat uses 200 g of Araldite 2011 for gluing Nomex and PCBs sheets.

All gluings use 2 x 0.020 mm layers of Araldite 2011 used with a mix ratio 100/60 (1.67/1, ρ = 1.066 g/cm^3)

PCBs are supplied to each laboratory by Cagliari group with locating holes, sides machined and connectors soldered.

2.4.6 Spacers assembly

Spacers are supplied to each laboratory by Nantes group.

V grooves spacers (X spacers) are glued first on X PCBs (bending planes)

2.4.7 Wiring process

Φ 0.020 mm tungsten-rhenium wires are supplied to each laboratory by Cagliari group.

There are 3 winding machines located at Cagliari, Gatchina and Saclay.

Saclay group will supply Nantes group in wounded frames.

Wires are fixed by gluing not by soldering.

Glue is standard epoxy with modified mix ratio in order to insure better adhesivity properties

Gluing avoid chemical induced failure of wires. When soldering process is used there is an emission of a $ZnCl_2$ spray which chemically attacks wires and induces failure by decrease of the wire cross section. $ZnCl_2$ is one of the components of the soldering flux which aims to clean the metal surfaces.

Chemical attack can be avoid by washing planes just after soldering in a slightly basic solution and by washing in a demineralized water bath. But a few labs have the required washing equipment (generally ultrasonic baths). Moreover the washing process is probably to avoid with the slat chambers which contain a large amount of hygroscopic materials like epoxy resin and polyimids.

Tungsten wires gluing process was qualified on different prototypes, mainly on the 2400 mm long prototype which was tested at CERN in June and October 2001.

Long term tests are on the way in order to know if there is an ageing effect for adhesivity of wires. First results show that the Φ 0.020 mm tungsten wire brakes (at ultimate tensile strength) before to slide in glue.

2.4.8 Sealing of slats (soft gluing)

In order to limit amount of matter the design avoid mechanical parts like screws, bolts, seals, and so modules will be sealed with RTV160 (one component Room Temperature Vulcanizing silicon resin, with alcohol by-products (non corrosive), from General Electric).

Amount : 400 ml / 2400 mm long slat.

With the help of a zip nylon wire located at the bottom of the groove where is pasted the RTV , slats can be reopened, this operation requires about 2 hours, but cleaning may require 3-5 days for longest slats.

This concept was experimentally qualified in small prototypes at Cagliari, Nantes, since summer 2000, and then on the 2400 long slat prototype in summer 2001. Other qualification tests are expected on various prototypes in order to have more statistics.

In order to be able to replace quickly a disturbed slat during a shut down, each model of slat will have one spare.

2.5 Organization of slats production

Today, this point is not frozen.

Amount of slat to build :152

Involved labs :4

-> rough sharing : 38 slats / lab

Different types of slats :20

Maximum number of slats for a given type :16 (slat ref. 333000N)

->in order to save time, it is wishable that all slats of one type will be integrated in the same lab

The 38 slats/lab option leads to unequal sharing in work, and does not allow to build all slats of a same type in a given lab.

	Final Design	Validation	Survey Market	Contract	Realization
Sandwich Panels	Done	Done	Done	On the way	0%
PCBs	Done	33% Done	50% Done	0%	0%
Spacers	Done	Done	Done	On the way	0%
Wires gluing	/	Done	/	/	
RTV Sealing	/	Done	/	/	
Assembly tooling	Done	Done	Done	0%	0%
Assembly Process	Done	Done	/	/	
Frames	80% Done	0%	50% Done	0%	0%
Cooling	90% Done	0%	0%	0%	0%
Busbars	80% Done	50% Done	50% Done	0%	0%
Chamber Integration	80% Done	0%	50% Done	0%	0%
Cagliari Wiring Machine	Done		Done	Done	80%
Gatchina Wiring Machine	Done				80%
Saclay Wiring Machine	Done	50% Done	/	/	0%
MANU345	Done	80% Done			0%

Table 2.4: Status of engineering (November 2001)

Other options are foreseen which lead to unequal sharing in number but quasi-equal sharing in areas of mounted slats (more equal share in manpower).

2.6 Other toolings

2.6.1 High voltage test bench

The high voltage test is important quality control procedure to be performed before the final sealing of the slat. The goals of the operation are:

- Final cleaning of the slat
- Visualization of the slat defects
- Localization of the remaining impurities

The High Voltage Test Bench is specially designed to do this task.

2.6.1.1 Design

The views of the HVTB are presented in Figure 2.12. Actually, this is a box with transparent top. The size of the box is sufficient to accommodate the largest slat. The positioning holes of the slat are used for its right positioning with respect to the top of the box.

The box top is equipped with spacers and the metallic mesh. The spacers will guarantee the required position of the slat to be tested with respect to the mesh. The mesh will be used as the second cathode in the real chamber in order to reproduce the electrostatic field inside the chamber.

The pneumatic devices (rubber membranes distributed at the distance 40 cm over the box bottom) are used for the lifting of the slat. The slat position in horizontal plane is defined by the positioning rods which fit the positioning holes in the slat. One of the rods has round profile, the others are elliptical, thus allowing some degree of liberty along the slat. This design gurantees soft and homogen contact between the slat and top spacers thus reproducing the assembled slat geometry. The tests on the prototype prove the gomogenity of the lifting and that the slat do not stuck during this process.

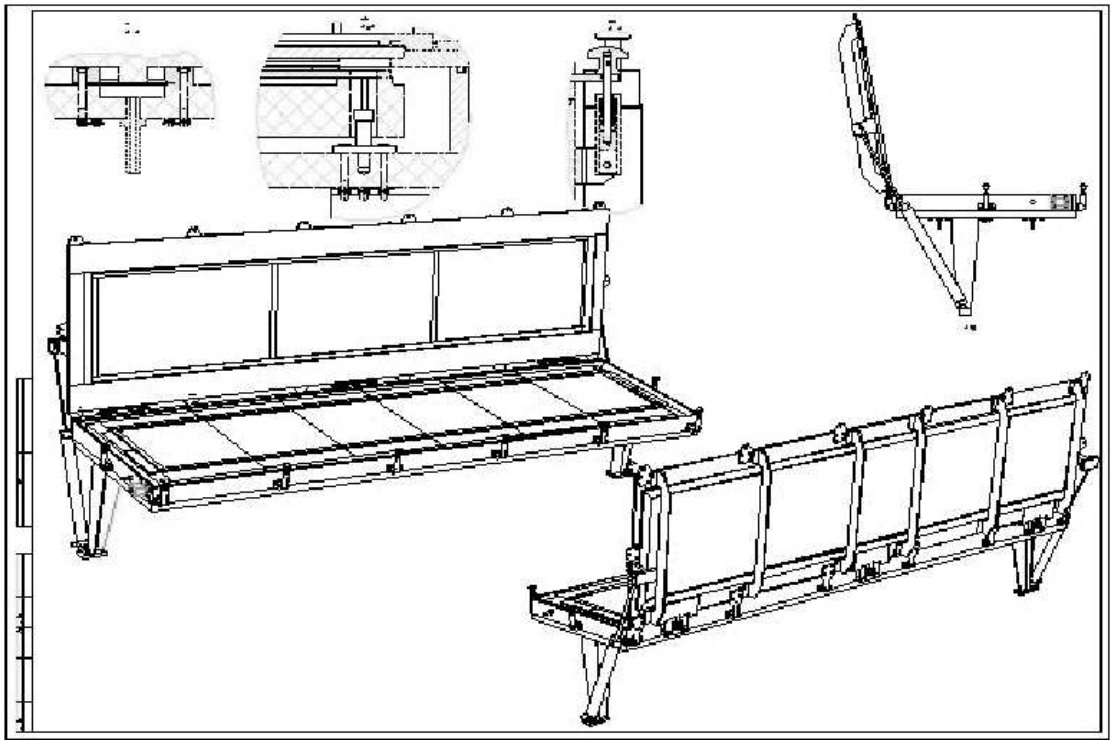

Figure 2.12: The overall view of the HV test bench. The inserts in the upper raw of the drawing illustrate the idea of (from left to right, correspondingly) the slat lifting device, slat positioning and the box sealing.

2.6.1.2 Main principles of the operation

The half-slat equipped with the anode wires should be positioned in the Test Box in such a way that the metallic mesh at the top of the box is parallel to the anode plane at he distance 2.5 ± 0.15 mm. In this case the voltage is applied between the anode wires and the two cathodes (pad and mesh), so the configuration of the electrostatic field would reproduce that of the assembled slat.

The volume of the box is filled with pure nitrogen. The nitrogen property to provoke the corona discharge instead of sparking is extensively used. The sparking is potentially dangerous for the chamber, namely for its anode wires. The corona could be seen in the darkness, thus one can localize the defects like still remaining dust or sharp tungsten peaks on the anode wires. The wires with insufficient tension could be also seen as they produce the glowing.

The procedure also cleans the chamber as when the corona is produced at some peak, it causes the ion bombardment, which would destroy the small dust pieces.

2.6.1.3 Operation

Before putting into the box all the pads of the slat cathode should be connected to the ground by means of the special connectors plugged in the MANU slots. Once the slat is put into the box, its anode wires are connected to the high voltage source, the box top is closed, the slat is properly positioned with respect of the top mesh, and the volume should be filled with pure nitrogen. Before turning the HV on, make sure that the gas in the box is stabilized (i.e. the volume of the nitrogen passed through the box is not less than ~10 volumes of the box).

Increase slowly the HV, checking simultaneously the current through the chamber. Look at the glowing of the wires, paying attention to the anomalies seen. The current (if it exists) should decrease to a reasonable level.

2.6.2 Winding machines

There will be 3 winding machines for the production of slats, in Cagliari, Gatchina and Saclay. Saclay will supply Nantes with wires frames.

2.6.2.1 Winding Machine at INFN Cagliari

The winding machine of INFN Cagliari has been designed to achieve a great accuracy in the distance between two wires, in the distance between the first and the last wire and in the value of the mechanical tension of wires.

The main features of the device are the following:

- Maximum frame dimension $1500 \times 900 mm^2$
- Thickness of anode wires from $10 to 200 \mu m$
- Mechanical tension from 1 to 300 g
- Winding step from 0 to $10 \pm 0.005 mm$
- Winding speed from 1 to 10 rpm

It will be so possible to achieve the following performances:

- Dimension of frames $1370 \times 750 mm^2$
- Wires mechanical tension $50 \pm 2g$
- Distance between two wires $2.5 \pm 0.005 mm$
- Total error between the first and the last wire $\pm 0.015 mm$
- Winding max speed 10 rpm

This machine is made by:

- the structure of HEB 140
- the motorized linear motion slide
- the rotation system for the frames
- the wire tension controller
- the drive controller

The linear motion slide is composed by a clearance-free precision ball screw and a integral ball rail system with integrated measuring system and AC servo motor.

A wire tension controller (Meteor MDR033A) allows to obtain a mechanical tension of wires from 1 up to 300 g which can be either setup by means of a computer or manually, directly on the device.

The rotating frame has been studied to use two or six wire frames to optimize the working time. In this case it is therefore possible to have more frames with one working cycle only. All movements are made with AC servo motors which have enclosed the readout system of the absolute position in order to arrange the position of wires if needed and its movement is synchronized with the wire carriage by the software control.

The system software controls the speed of motors in order to keep the precision of winding step.

2.6.2.2 Winding Machine at PNPI Gatchina

Purpose To wind the wire anodes to the frames (size of 500x700 mm^2). The acceptable wire thickness range: from 15 to 250 mm .

Tension range from 30 to 300 g.

Winding step is 2.5mm. It is defibed by the Combs - the dedicated screws of special profile. The screw profile and its step define the winding step and the precision of the wire positioning. In this particular device the *wire position tolerance* does not exceeds 30μm, the *accumulated error* along the total length of the frame is below 50μm.

The winding step could be changed by the replacing of the combs. No other modifications of the device are required.

The optimized rotation speed is ~10 rpm, so the winding time of a frame with length of 420 mm is about half an hour. The software step motor control allows the variations of the winding speed.

The Principle Parts

The Photos of the Machine principle parts are presented in the following pages. The parts are:

1. The rotating frame with the combs in appropriate holders. The two transfer frames are inserted inside the comb frame. After the winding is completed, the wires are glued to the transfer frames. These transfer frames are used for tha anode assembling in the slats.

2. The wire carriage with rollers is designed for the wire feeding at right position according to its rotation speed and the required winding step. The software controls the synchronization of the carriage movement with the frame rotation: once the number of pulses sent to the stepping motors is known, it is possible to synchronize the frame and carriage positions for good wire feeding.

3. Wire tension and feeding mechanism.

The tension is controlled by the device, consisting of the two fixed and one movable wheals. The movable wheal (roller) is hanged on the wire loop. The weight of this roller determines the wire tension. The tension tolerances are by

- **Friction** in the wheel system (quite unstable parameter) and
- **Acceleration** of the movable roller: it runs up and down. This acceleration has two contributions:

  Derivative from the wire consuming by the rotating frame.
  Acceleration caused by the wire supply motor.

These two components are subtracted, thus partly compensate the effect. The motor with gear has been chosen for wire supply in order to minimize the acceleration. The motor is controlled by optical sensor: as soon as movable roller height exceeds the predefined one, the sensor turns on the motor for 3 - 4 seconds. As the wire is fed, the roller goes down. When the motor stops, the roller goes up due to the wire consumption, and the cycle repeats.

The step motors are used for the frame rotation, they are controlled by the PC using CAMAC interface and step motor control module. There are no special requirements for the PC.

The transfer frame is required for transportation of the winded part of the anode to the assembling table and for anode wire positioning and assembling.

Figure 2.13: Rotating frame

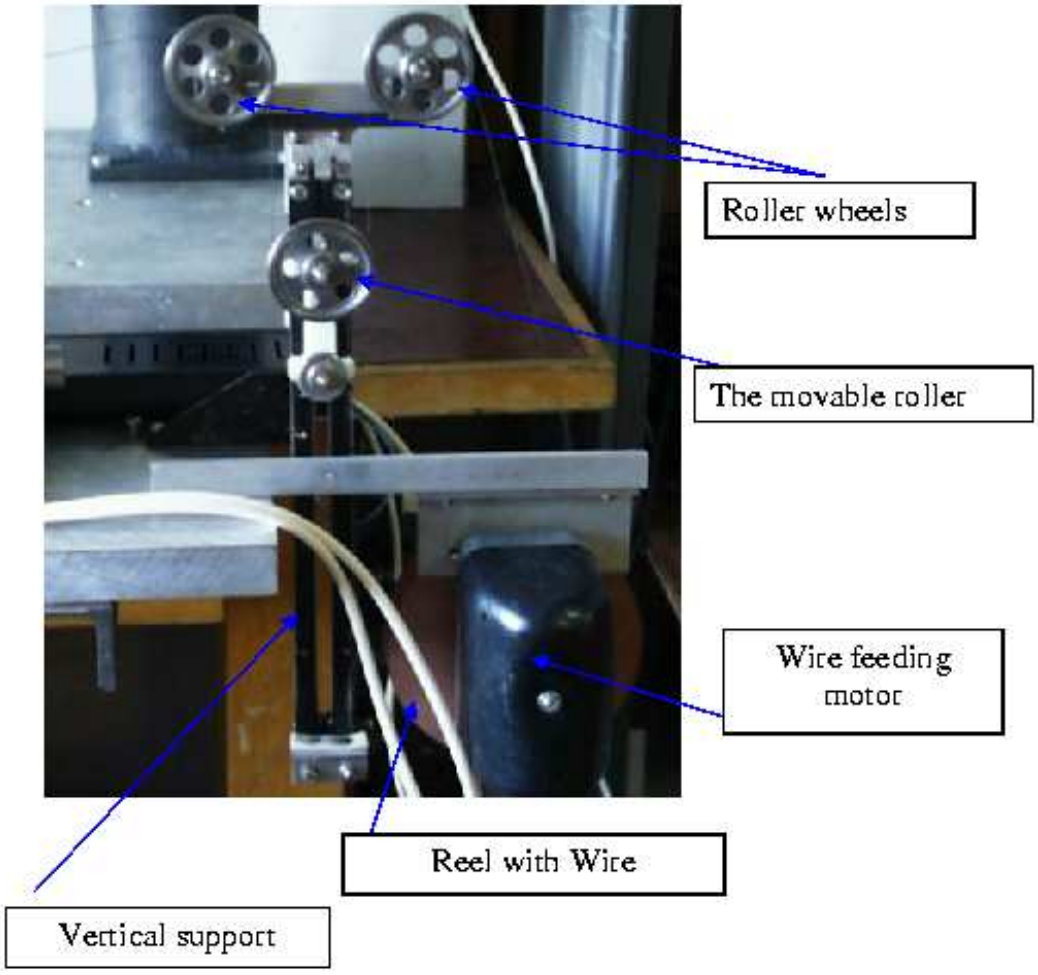

Figure 2.14: Wire feeding and tension control

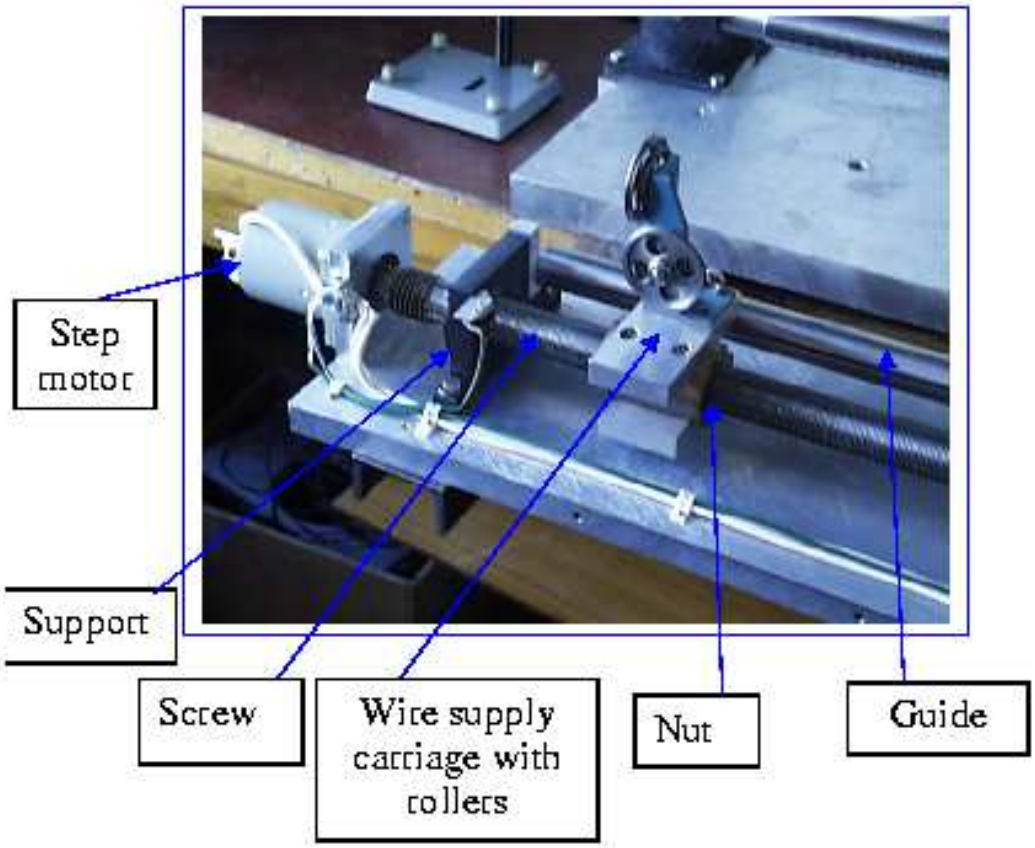

Figure 2.15: Carriage

Figure 2.16: Transfer Frame

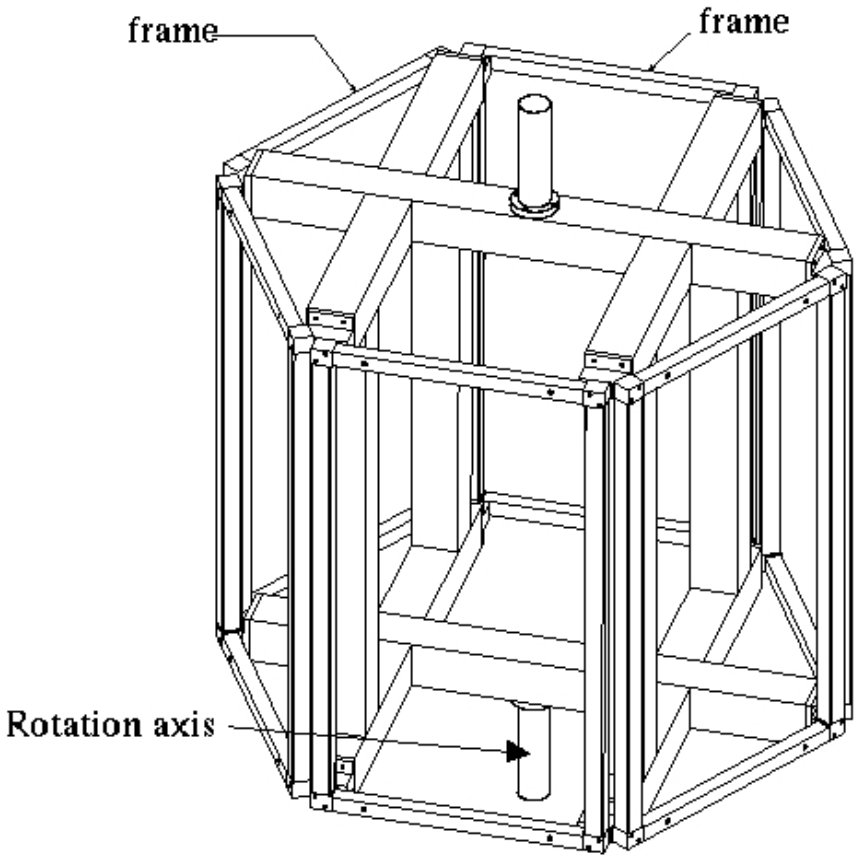

Figure 2.17: Squirrel cage with the 6 frames

2.6.2.3 Winding Machine at CEA Saclay

The Saclay winding machine has already been used by several experiments in the past. Several slats have been wounded with this machine including the 2.4 m long prototype succesfully tested last October. We only remind few characteristics :

- Rotation speed : 0 - 10 rpm
- wiring pitch : O - 20 mm, with a $\pm 5\mu$m accuracy
- Wire tension : 17 - 275 g

This machine will be upgraded with a new winding mechanism next year. In order to reduce the machine occupancy, up to 6 transfer frames will be wounded at the same time using a squirrel cage (fig. 2.17).

3 Frames and integration

3.1 Status report on slats supports

3.1.1 Introduction

The mechanical supports must hold slats in precise location in time, with loads associated to electronics, busbars, cables and the incoming gas supplies. The total weight supported by the slats support structure, including all, is estimated to 150 kg, 195 kg and 230 kg for Stations 3, 4 and 5 respectively. Each half chamber of Stations 3-4-5 have its own support. The 12 half chambers of Stations 3-4-5 have the same design, while the dimensions of supports depends on the number of slats for each stations. In total, there are 3 sizes of supports. These parameters are detailled in Table 3.1.

Table 3.1: Dimensions, with tolerances, and total weight of the sandwich panels for the chambers of Stations 3-4-5.

Chambers number	Height (mm)	Width (mm)	Total Weight (kg)
CH 5	$3780^{\pm 1}$	$1620^{\pm 1}$	<150
CH 6	$3780^{\pm 1}$	$1670^{\pm 1}$	150
CH 7-8	$4900^{\pm 1}$	$2200^{\pm 1}$	195
CH 9-10	$5700^{\pm 1}$	$2600^{\pm 1}$	230

These supports were presented with frame design (hollow structure) in the Addendum of the TDR (December 2000) in paragraph 2.4.4 [1]. For mechanical, physical and financial reasons, Saclay decided to study a more suitable design, in every respect. The actual design consists of sandwich panels (full structure), which is a much more rigid structure and has been already presented in the Dimuon Cagliari Meeting this year [2]. A mixed design with a sandwich panel featuring frames at edge side may be also foreseen.

This status report presents first the different constraints due to physics, mechanics and environment. All this contraints lead to the proposition of sandwich panels structure, studied in details in order to answer all the requirements. Saclay prepares the order procedure for this market and some plans are exposed below. During the year 2001, some investigations have been made in several compagnies, in order to check the feasability of our design, to modify some technical points if necessary and to get an idea of the global cost. The main results of investigations are presented too in this report. Finally, the estimated planning of tender and fabrication is given.

3.1.2 Physical, mechanical and interfaces constraints

3.1.2.1 Physical constraints

The first constraint is given by physics. The amount of matter, in the active area of detection, must be as small as possible. For this reason, we decided to give a maximum limit of $\sim 0.3\% X_o$ of matter in the physics area. Therefore, only few materials could fill this requirement : carbon fiber (X_o = 188 mm), kevlar fiber (X_o = 407 mm) and eventually Glass fiber (X_o = 123 mm). The amount of matter depends

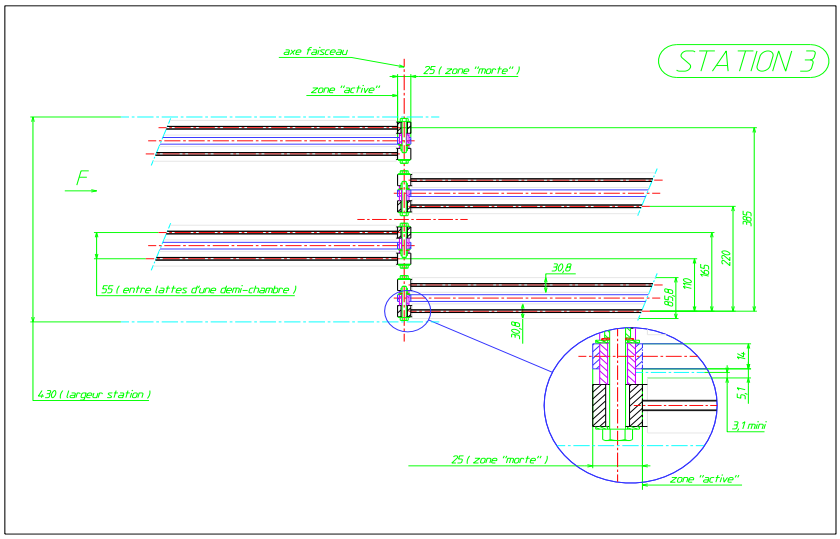

Figure 3.1: Top view of Station 3 : detailed parameters on slats and supports thickness are shown ; the dead zone is 25 mm. The total thickness of Station 3 is 430 mm.

on the number of layers needed for the sandwich. Glue has to be considered too in the sandwich panel : epoxy-araldite (X_o = 456 mm).

Moreover in order to minimize the hit losses due to the vertical part of the supports, the two half chambers must overlap in the middle, by a distance corresponding to the width of the slats spacers (25 mm for Station 3, and 35 mm for Stations 4 and 5, due to the readout cables passage in the central part). The Stations thickness is illustrated by figure 3.1 for Station 3 and figure 3.2 for Stations 4 and 5.

3.1.2.2 Mechanical constraints

The structure must be able to support the weight of all slats with electronics and cables, with the smallest deformation as possible. Slats must not be affected by the deformations of the support in time. The specification on the maximum tolerated deformation in that case is $\delta_{maxi} < 1\,mm$. Of course, this constraints is solved by the type of raw material used for the structure. For this reason, several calculations have been performed in order to determine what are the appropriate materials.

Mechanical deformations of panels are simulated with NASTRAN code for Station 5, for several raw materials, number of layers and layer thicknesses. All these results are presented in Table 3.2. Station 5 represents the most unfavourable case with the biggest dimensions, loadings and risks of deformations. The applied strengths in simulation are : the weight of the sandwich panel ($\sim$ 18 kg), the weight of slats (78 kg for 13 slats) and the weight of cables ($\sim$ 130 kg : $\sim$ 10 kg per slat).

Results of simulations show that carbon fibers give very satisfactory results, whatever the composite type is (HR, HM1, HM2, HM3). Carbon sandwich panels offer a better rigidity for the slats, compared to the other materials, with not an excessive value of X/X_o ($X/X_o < 0.3\%$ for 2 skins composed with 2 layers of 0.15 mm). The maximum mechanical deformation observed is 0.4 mm in the round-shaped part of the panel, with high resistance of carbon fibers with 2 layers of 0.15 mm each.

In addition of a good stiffness, a stability in time is required for the composite materials. They must have a good behaviour in fatigue, no corrosion, and they will age under heat and a certain humidity rate.

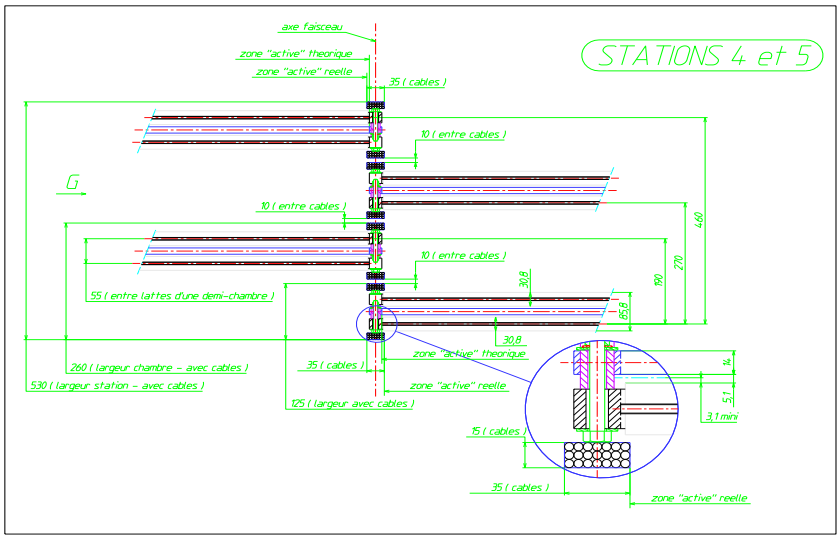

Figure 3.2: Top view of Stations 4-5 : detailed parameters on slats and supports thickness are shown ; the dead zone is 35 mm, due to the readout cables passage. The total thickness of Stations 4 and 5 is 530 mm.

3.1.2.3 Thermal constraints

Deformations of the support, due to thermal expansions, must be limited. Indeed, each deformation leads to a deterioration of the expected resolution, because of the errors made then in the slats positionning. Thermal calculations, presented in the cooling subsection, shows a hot zone, with a maximum temperature value of 37°C on the panel. The initial temperature in the cavern is 20°C. This indicates the maximum gradient of temperature expected on the support. We suggest a raw material with correct thermal behaviour, i.e, with a very small thermal expansion coefficient : order of magnitude should not exceed $5 \times 10^{-6}/°\mathrm{C}$.

Once again, carbon fibers offer a good thermal control. Its thermal expansion coefficient is $\alpha_l = 1.2 \times 10^{-6}/°\mathrm{C}$; consequently, the maximum displacement of the structure with a $\delta T = 20°\mathrm{C}$, for Station 5, with 6 m long, is $144\,\mu m$. The maximum displacement of one slat (with 400 mm in height, in Y direction) is $9.6\,\mu m$ in that case. This last value represents a very low deformation, compared to the resolution expected in the Y Bending Plane ($100\,\mu m$).

3.1.2.4 Other constraints : environment, interface with other sub-systems

In the present situation, some other subsystems as Dipole Magnet and Absorber, are soon going to have a complete design frozen. Several meetings were organised in 2001, in order to get a compromise about the room for Station 3, inside the Dipole, and the room left in the Absober for all Stations 3-4-5 (axial and radial clearance for the recess).

During the year 2001, external envelopes for all Tracking Stations must have been fixed very quickly, as for the other subsystems of the Dimuon Arm, in order to have a better coordination of the whole Dimuon Forward Spectrometer. Envelopes of Stations 3-4-5 are considered as almost frozen, with total thickness of 450 mm for Station 3, 562 mm for Station 4 and 563 mm for Station 5, taking into account the axial clearance of the extended recess in Absorber [3]. These envelopes brings a new constraint on the thickness of the supports itself, due to the environment. For this reason, thin sandwich panels, with severe tolerance, must be required, in order to keep the Stations in their envelopes.

Table 3.2: Mechanical deformations results for panels of Station 5, for different raw materials, number of layers, layer thickness and orientation of fibers.

Composite Type	**layers number**	**layer thickness (mm)**	**Orientation**	**Total deformations (mm)**
Kevlar	2	0.10	0°, 90°	1.07
Kevlar	2	0.15	0°, 90°	0.74
Kevlar	3	0.10	0°, 45°, 90°	0.47
Glass	2	0.10	0°, 90°	1.03
Glass	2	0.15	0°, 90°	0.70
Glass	3	0.10	0°, 45°, 90°	0.64
Carbon HR (E=220 GPa)	2	0.10	0°, 90°	0.58
Carbon HR	2	0.15	0°, 90°	0.40
Carbon HR	3	0.10	0°, 45°, 90°	0.30
Carbon HM1 (E=380 GPa)	2	0.10	0°, 90°	0.41
Carbon HM1	2	0.15	0°, 90°	0.29
Carbon HM1	3	0.10	0°, 45°, 90°	0.18
Carbon HM2 (E=540 GPa)	2	0.10	0°, 90°	0.41
Carbon HM2	2	0.15	0°, 90°	0.29
Carbon HM2	3	0.10	0°, 45°, 90°	0.15
Carbon HM3 (E=880 GPa)	2	0.10	0°, 90°	0.32
Carbon HM3	2	0.15	0°, 90°	0.22
Carbon HM3	3	0.10	0°, 45°, 90°	0.09

3.1.3 Slats supports proposition from Saclay

Taking into account all the previous constraints, Saclay has developed a complete design of sandwich panels, which answers to all the requirements, cited above.

The sandwich panels can be composed of 2 skins of 0.3 mm thick carbon fibers, at maximum $\sim 0.3\% X_o$, and the core can be made with Nomex honeycomb of 15 mm thick. The raw material carbon fiber is not mandatory, but it reveals to be the best choice for mechanical and thermal reasons (slats must not be affected by the deformations of the support and deformations due to thermal expansions must be very limited).

The external dimensions of the supports are given in Table 3.1. Figure 3.3 shows the dimension of support for Station 5 with the active zone for physics. The thickness of the structure, $14^{\pm 1}$ mm with a flatness of 2 mm, fit the fixed external envelopes. This figure presents the location of several kinds of holes with inserts too : inserts to centre and to support the slats, drillings for targets used in photogrammetric technique, drillings for laser beams (Geometry Monitoring System) and drillings for tooling.

Our specifications for the 3 stations are :

- In the vertical plane of the support structure (figure 3.3) : a flatness of 2 mm (± 1 mm) is required. This tolerance is hard to achieve in industry and leads to an expensive cost.

- Inserts for the slats centring : length > 1 mm in comparison with the thickness of the support structure.

- Slats supports inserts determine the precision of the x, y, z positions of slats for physics (figure 3.5). These inserts are of great importance. The flatness for 4 inserts of one slat is 0.5 mm. The length of all these inserts is $9^{\pm 2}$ mm. Each group of 4 inserts, equivalent to one slat, have to be placed in a virtual common vertical plane with a total flatness of 2 mm.
- Drillings for slats adjustment tooling (figure 3.4) in the different parts of the support structure (on the side of panel and on the central circular part).
- Drillings for target used in photogrammetric process.
- Drillings for laser beams of the Geometry Monitoring System are illustrated in figure 3.6. For Station 5, 2 holes are foreseen with the actual laser beams design. Ellipse holes dimensions are 180 mm$\times$ 100 mm for small and large axis. The laser tube section is not frozen at the moment.
- Drillings for supports hanging are illustrated in figure 3.6. For Station 5, 3 holes are foreseen at the top and the bottom of the half chamber.
- Due to the fixed external envelopes, the distance, between inserts extremities of 2 successive support structures, must not exceed 31.5 mm.

To conclude, our actual proposition fill the 4 constraints detailed above : physical constraints, small mechanical deformations, very small thermal expansions and fitting the fixed external envelopes. On the other hand, all these specifications have a high cost, explained in the following section.

3.1.4 Preliminary investigations in companies

The goals of these investigations is to know if there were companies technically capable of manufacturing slats supports as we want, and to evaluate the price of the sandwich panels as well as the time necessary for their realization.

10 french compagnies have been consulted. Saclay encounters a lot of difficulties to obtain answers from these companies :

- Hesitations, because it was not a legal invitation to tender, and moreover they had no time to waste to evaluate the feasability and the prices of our supports structures. Some other companies, not cited above, have declined immediately.
- Composite materials are used essentially in aeronautics. Usually, companies are in charge of big contracts with aeronautics companies (EADS, Boeing). In consequence, they are not interested in the manufacturing of only a few pieces.
- Specificity of the supports with very large dimensions (3 m to 6 m). Companies have rarely the equipment suited to these large dimensions (autoclave, press and table).
- Required tolerances (flatness of ± 1 mm over 6 m $\times$ 2.6 m) demands precise equipment and accurate machining. Also, severe tolerances induce high prices, because of specific tooling.

In spite of all these difficulties, their propositions for 12 supports are : an average cost around 2 to 3 millions FF, i.e., much more than expected in the Core Cost : 0.96 millions FF, and the average facturing time for the 12 supports is T0 + 12 to 15 months (with T0, the date of order).

These investigations learn us that, for the required flatnes, the raw material is not of great importance in the total price (contribution of $\sim$ 10% to 20%). For example, we will not divide the cost by two, replacing carbon fiber, which is the best material, by glass fiber or aluminium for the same flatness and same tooling. What makes the price so high is clearly the non standard tooling needed for the realization of the large dimensions of panels (especially for Station 5).

On the four constraints detailed above, one constraint can allow us to decrease a little the price : increase a little the flatness of the panels, but this induces immediately to increase the axial recess of the Absorber. On the other hand, another solution is to find a company able to realize our supports with less specific tooling as possible. From that point of view, we found a company, which seems to be able to produce a carbon sandwich panel, with the flatness of 2 mm (± 1 mm) on 6 m $\times$ 2.6 m, with only few simple toolings not very expensive. We will investigate this solution in the coming months.

3.1.5 Next phases : prototyping and redaction of the terms of the contract

A prototype would be useful to check the capability of the company to do a carbon sandwich panel with the required tolerance. For this prototype, our requirements could be : production of a carbon sandwich panel with the dimension of Station 3 (3800 m $\times$ 1700 m), with a thickness of 15.6 mm. 2 carbon skins of 0.3 mm thick, with a flatness of 1 mm (or ± 0.5 mm).

This prototype would allow the company to test their tooling, and would allow us to check different technical points of our design before we freeze the redaction of the terms of the contract for tender procedure.

In the mean time, a draft of the terms of the contract is in progress, with a functional definition of slats supports structures. All specifications will be given in terms of our proposition, described above.

From the planning point of view, it takes around 2 years for the panels delivery : around 8 months for administrative procedure for order in CEA, and then around 16 months at maximum for the total production of the 12 sandwich panels. If we start the administrative procedure in January 2002, the last panels will arrive around January 2004 in agreement with the general planing.

[1] "ALICE: Addendum to the Technical Design Report of the Dimuon Forward Spectrometer", Addendum 1 to ALICE TDR 5, CERN/LHCC 2000-046, Dec.2000.

[2] "Status report on frames design", F. Orsini, presentation at the Dimuon Meeting 2001 in Cagliari, May 2001.

[3] "ALICE Dimuon parameters and Geometry", A. Tournaire, file dimuonparameters44.xls, transmitted to all subsystems of the Dimuon Arm, updated on 25/09/2001.

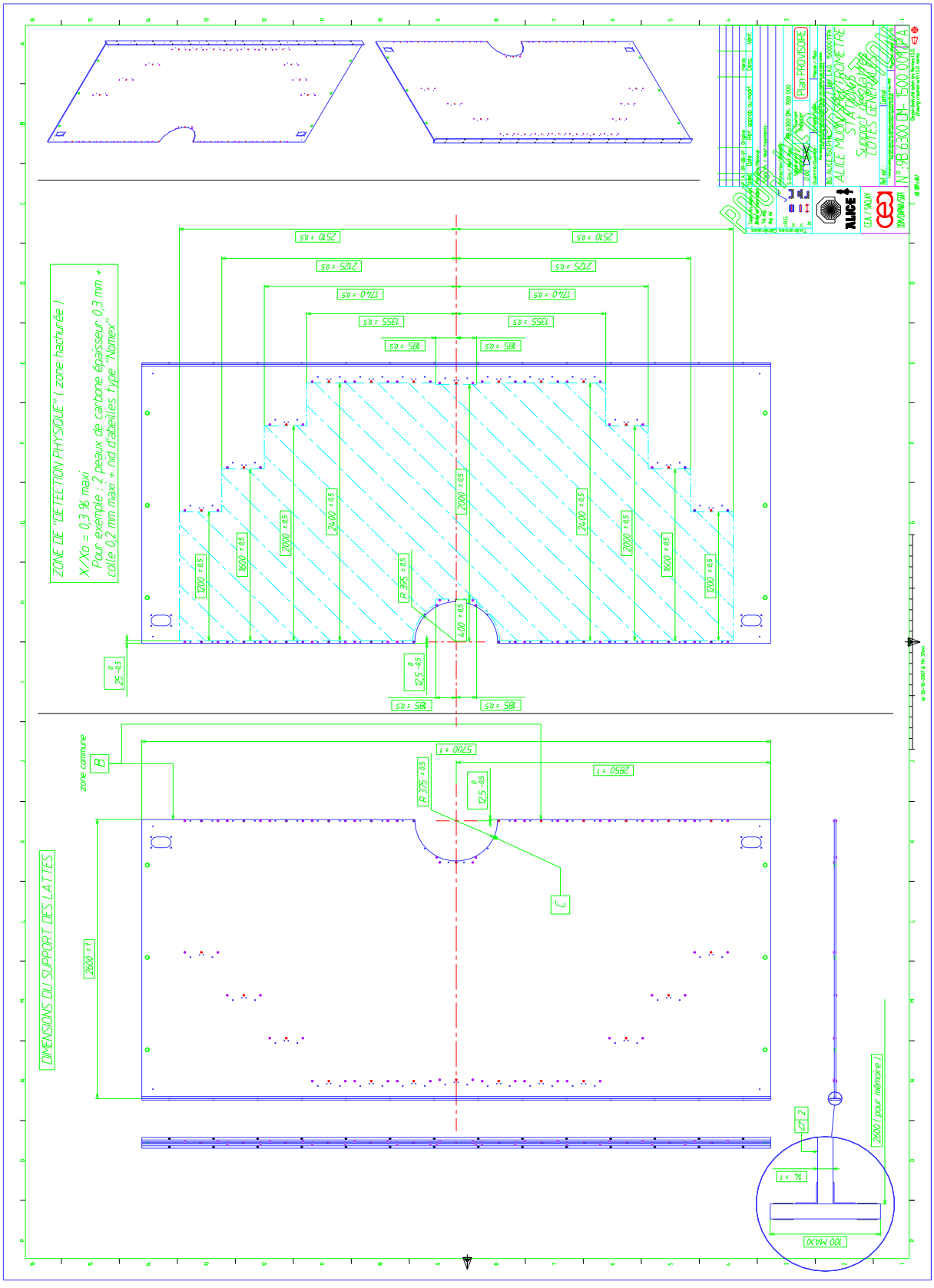

Figure 3.3: Station 5 : external dimensions of the support and active zone for detection.

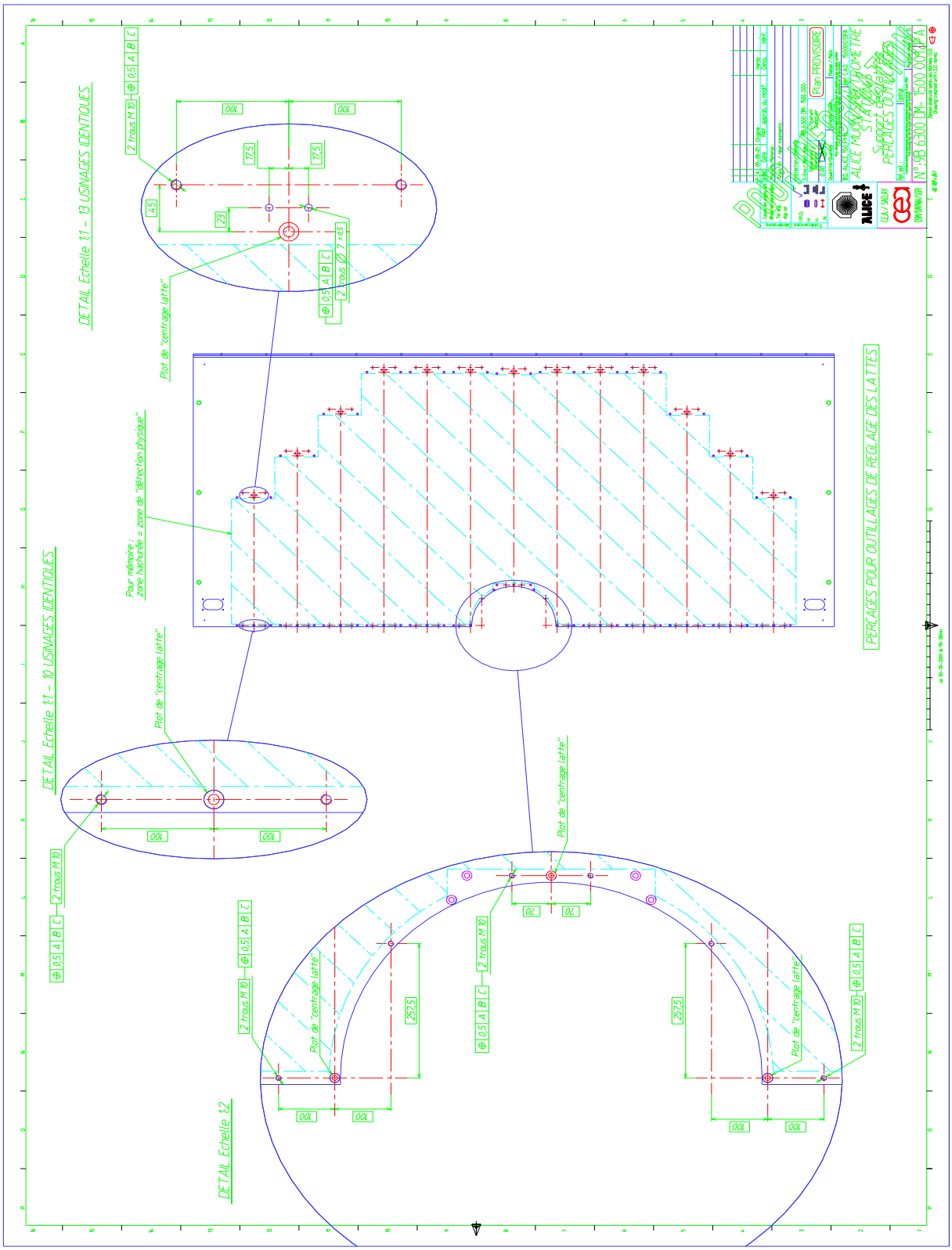

Figure 3.4: Station 5 : locations of several drillings for slats adjustment tooling are shown.

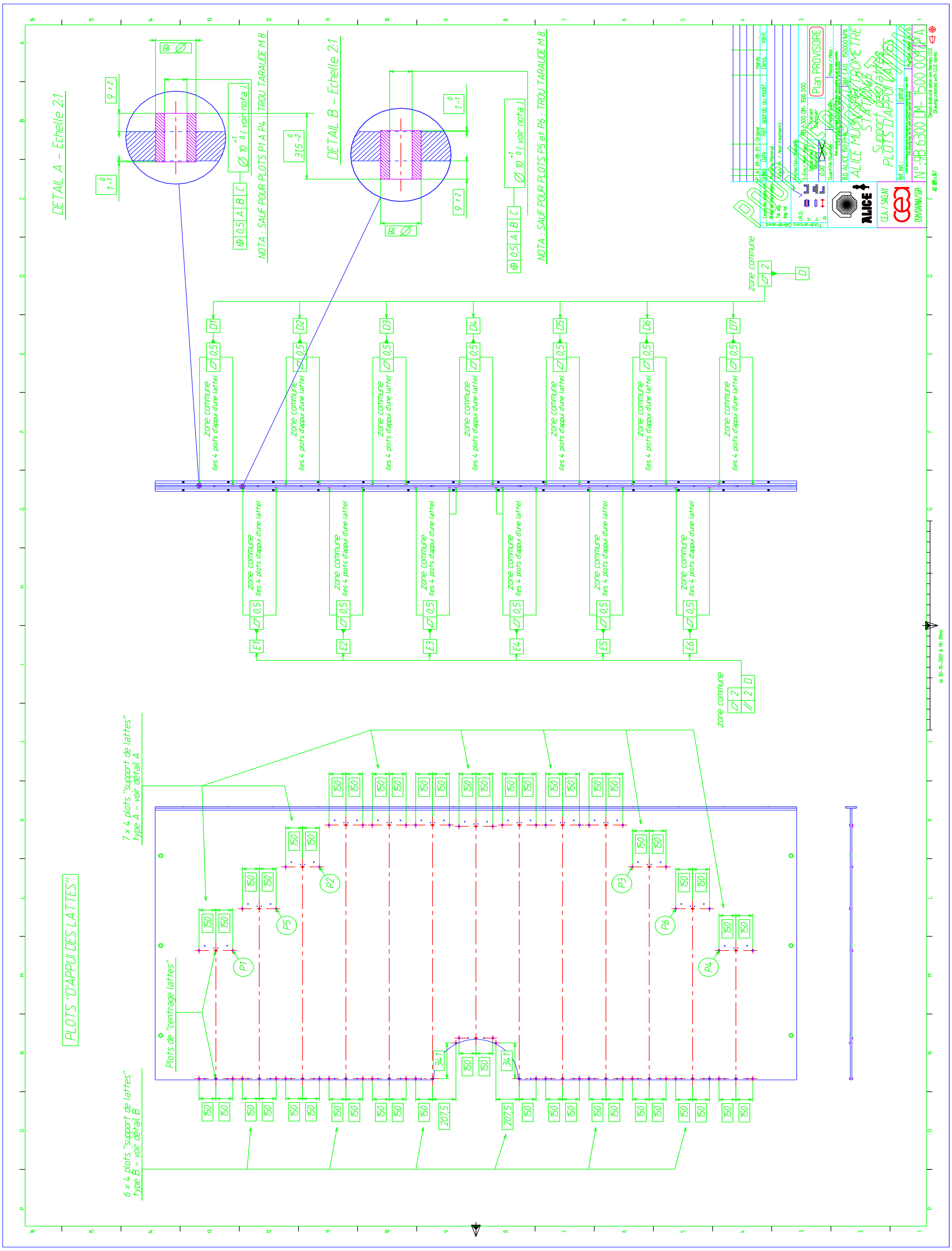

Figure 3.5: Stations 5 : location of slats inserts for support. The flatness of these inserts will determine x, y, z positions of slats for physics.

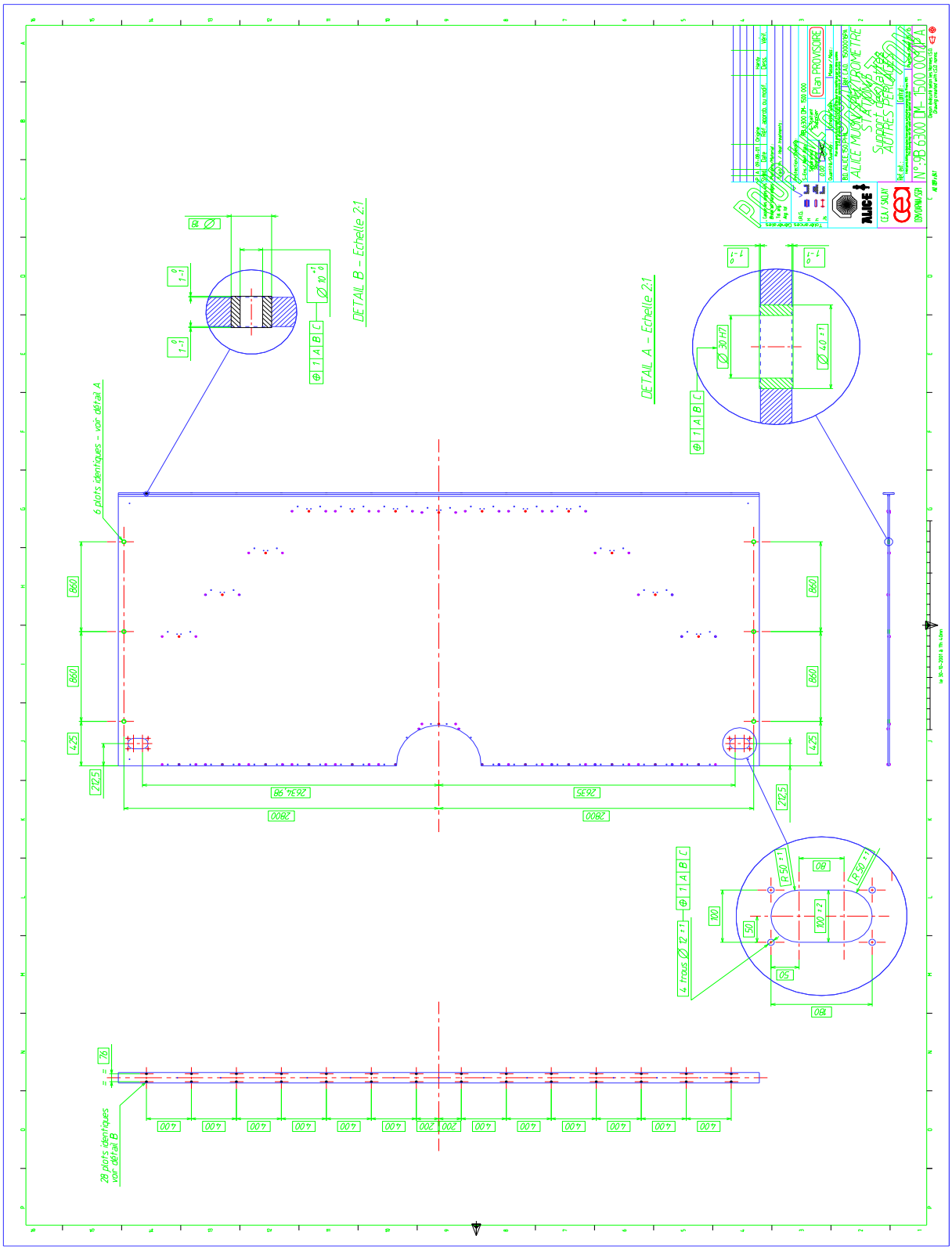

Figure 3.6: Stations 5 : drillings for supports hanging at the top and the bottom of the half chamber, and drillings for the laser beam of the Geometry Monitoring System are shown.

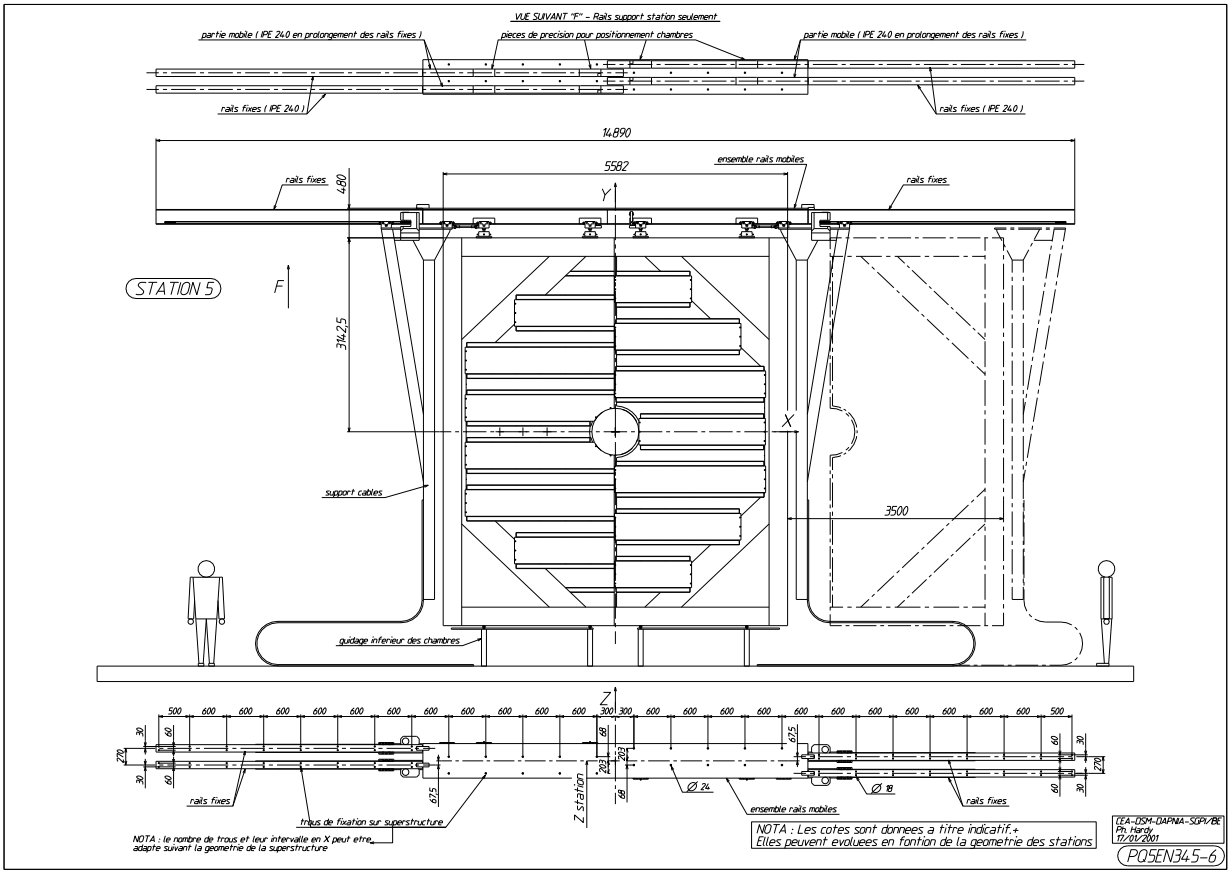

Figure 3.7: View of one chamber of the Station 5. Dash lines show the open position.

3.2 Chamber integration

3.2.1 Slat mounting and positioning

Each chamber is composed by two half chamber that are mechanically independent with its own frame. Each one is composed by several slats of different sizes (see for instance fig. 3.7) in order to cover the geometrical acceptance ($2^\circ < \theta < 9^\circ$). The slats are fixed to the frame with 2 screws ($\oslash$12) in each side.

The assembly will be done vertically in the SXL2 hall at the surface of Point 2. Due to the lack of place, each half-chamber will be transported down to the working position horizontally. A set of supporting tools will be designed to reinforce the frame structure of each half-chamber during the transportation from the surface down to the pit.

Each slat has two survey marks at each side, placed in a $\oslash$18 hole, that will be used to the precise positioning of each slat with respect to the frame. A positioning device will be used for the fine tuning (fig. 3.8). The photogrammetry technique will be used to measure the position of each slat with a precision in the range of 50-100 μm in the 3 directions (x, y and z). The position measurement will be done for each half-chamber separately in the *open position* (see fig. 3.7), where each half chamber is accessible to take the photogrammetry pictures. For the station 3, the pictures will be taken before the final installation inside the magnet.

The frame itself will also be equipped with survey marks in order to monitor the displacements during the experiment and to position the chamber with respect to the dimuon arm coordinates. Since the frames and the slats structure are made of carbon fibers (~10^{-6} K^{-1}) the thermal expansion is expected to be negligible. The final alignment will be done with particles.

The slats active area have a 15mm (3 pads, equal to the typical cluster size) recovering in the vertical direction to avoid losses and to have some redundancy. In the Z direction, along the beam, the half

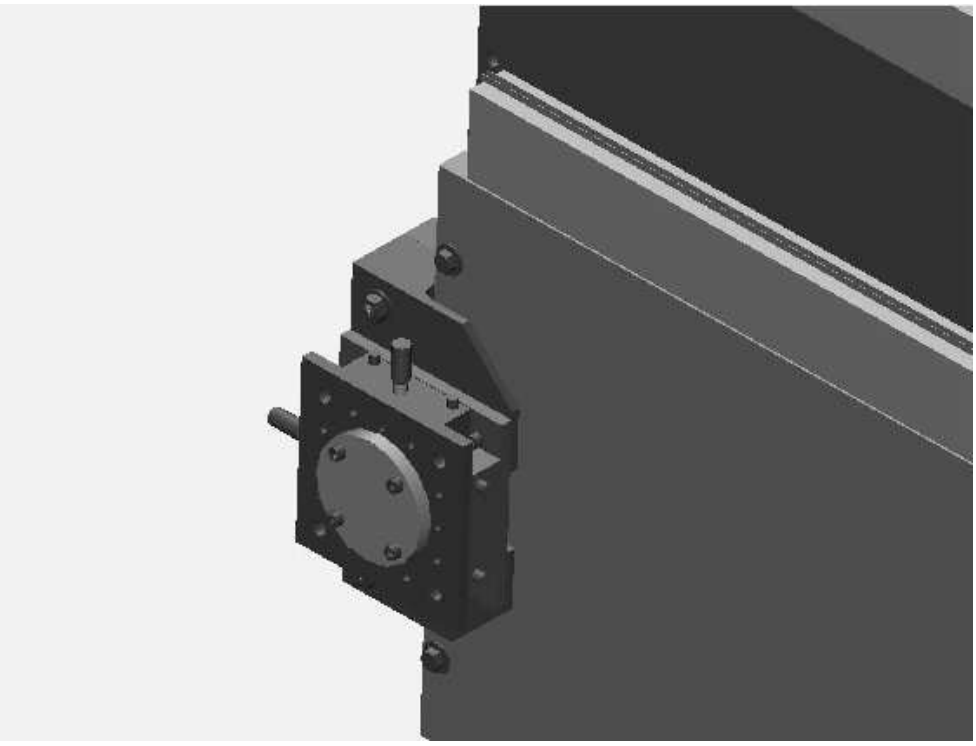

Figure 3.8: Device for the slat position fine tuning

chambers are arranged as shown in the fig. 3.9. For the station 3 the cables are removed from the central part and all the services come from the outer part, while in the stations 4 and 5 this is not possible because the readout can not be done only from one side due to the readout dead time.

3.2.2 Chamber hanging : interface with the superstructure

The interfaces of the stations 4 and 5 are different from the station 3 which is inside the magnet. We will briefly describe both.

3.2.2.1 Stations 4 and 5

The frame of each half-chamber is fixed in a separate rail along the X direction (fig. 3.10). A position ajustement in X, Y and Z is foreseen for each half-chamber which allows a fine tuning during the final positioning. In the running position (chamber close) the two half frames overlap in the middle. This solution has been chosen to reduce the loss in the central part (~1% of hits loss per cm of frame). Each rail is fixed to the superstructure using “I” structures. Fig. 3.11 shows a general view of the integration of stations 4 and 5. The displacement along the X direction of a half-chamber is motorized and there is a system to lock the two half chambers in the middle.

3.2.2.2 Station 3

The integration of the station 3 inside the magnet is under study. The fig. 3.12 shows 3 steps of the installation inside the magnet. First, each half chamber is hanged to an external removable rail parallel to the beam axis in order to introduce it inside the magnet. At this point the chamber is also parallel to the beam axis. Second, the chamber is rotated when at the level of the recess. Finally, the chamber is pushed to the final location.

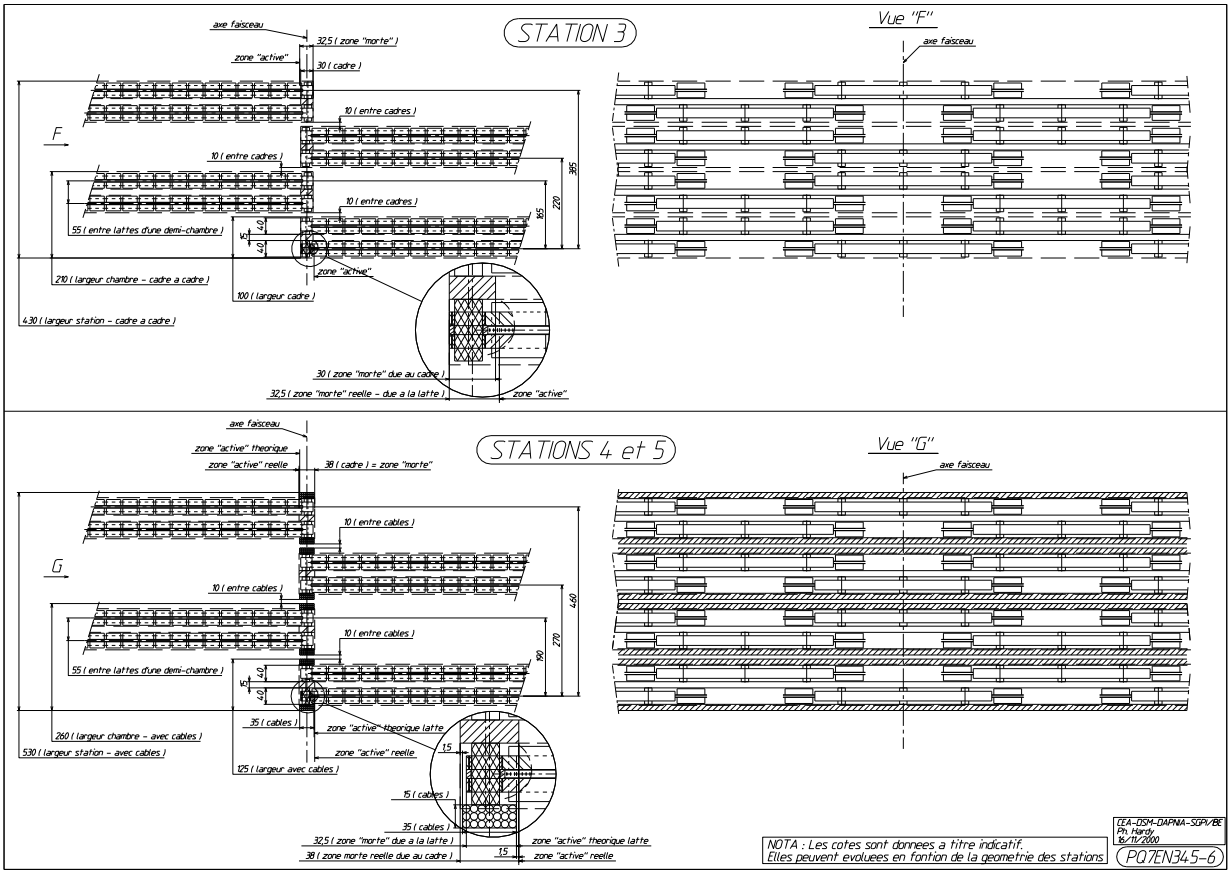

Figure 3.9: Chamber positioning along the Z direction

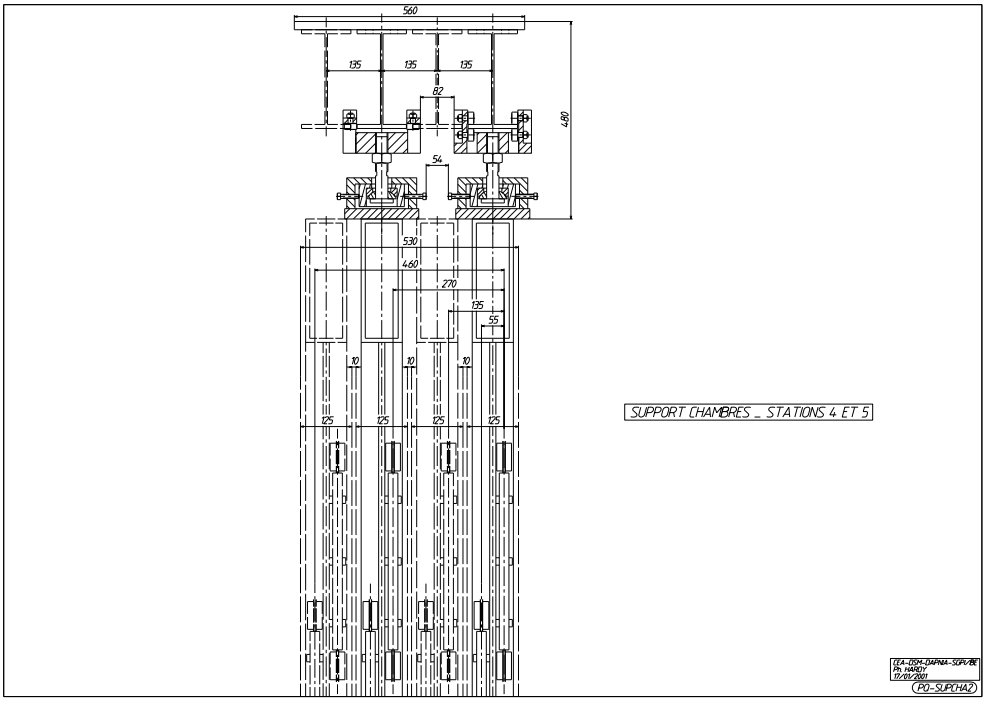

Figure 3.10: Chambers hanging. The rails and the fine position tuning are shown.

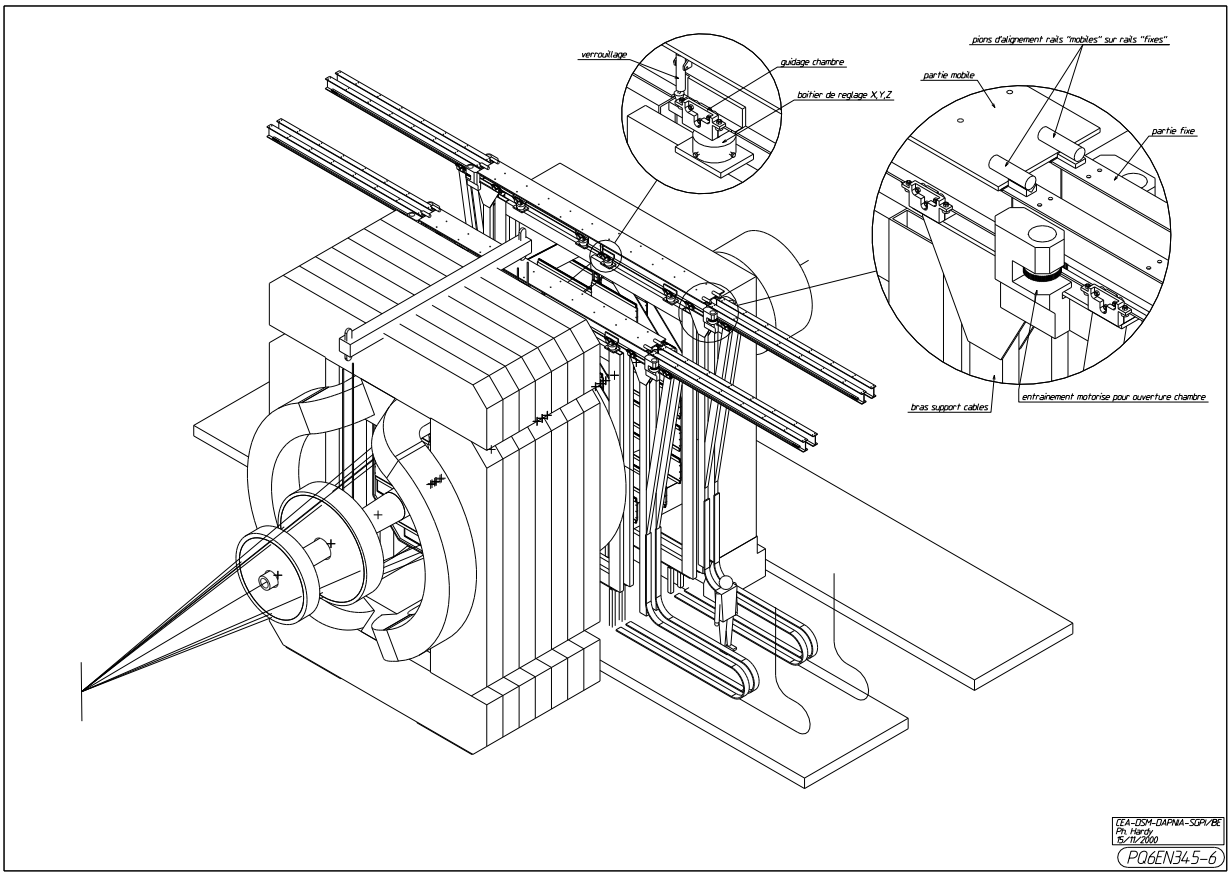

Figure 3.11: General view of the integration of the stations 4 and 5.

The same system of fine tuning in X, Y and Z is also integrated in the station 3. We are in close contact with the magnet team to define the interface between the rails of the station 3 and the magnet.

3.2.3 Chamber interfaces : Muon filter, beam shield

3.2.3.1 Beam shield

The inner part of all the chambers are close to the beam shield (stations 4 and 5) or the beam pipe (station 3). In order to cover the geometrical acceptance down to 2°, an appropiate recess is needed. A radial margin of 5mm is taken.

3.2.3.2 Muon filter

The last chamber of the station 5 is close to muon filter. A 10 cm distance has been kept to insure an easy installation and cooling.

3.2.4 Slat mounting/dismounting during operation

The access to each chamber is quite different from station 3 and stations 4 and 5. A slat from station 4 or 5 is easily accessible by opening the corresponding half-chamber and can be dismounted in a rather short time (~1 day). The situation is far more complex for the Station 3. In order to dismount a slat the corresponding half-chamber has to be extracted from the magnet. In that case, the Station 4 has to be also opened. The overall operation could take a week. In the case of a slat is replaced, the re-alignement will be done with particles.

3.3 Status report on Cooling

3.3.1 Introduction

The cooling system aims of dissipating the heat produced by electronics and keeping all the stations in a stable environment with temperature around 20°C. No dissipation is allowed in the L3 cavern. Considering the present version of GASSIPLEX, the heat dissipation of the electronics amounts to 2.1 kW in Station 3, 2.8 kW in Station 4 and 3.3 kW in Station 5.

Direct cooling by conductive exchange between components and water circulating in tubes is efficient, but inadequate because of the amount of matter in the active area of tracking stations. A cooling, based on forced circulation of air is therefore investigated since 2000 (natural convection of air leads to a maximum temperature of 83.5°C).

The principle of air cooling for the tracking system has been approved by the ALICE Integration Team since the Cagliari Meeting in May 2001. Installation of a common cooling unit for the five stations of Tracking System is under study at CERN. Stations 1-2, with their specific closed environment and quadrant design, are the object of studies lead by IPN Orsay. The present status report concerns only Stations 3-4-5, which are build with modular slats design and placed in an open environment (except for Station 3 into the Dipole magnet). The cooling of Stations 3-4-5 is under the responsability of CEA Saclay.

Thermal studies of the Stations 3-4-5, presented here, have been made with StarCD code, which computes thermal heat transfer in fluids and dynamical flows. The heat dissipated by electronics is simulated by heat flows on strips, located on the top and the bottom edges of PCBs. Air flows are

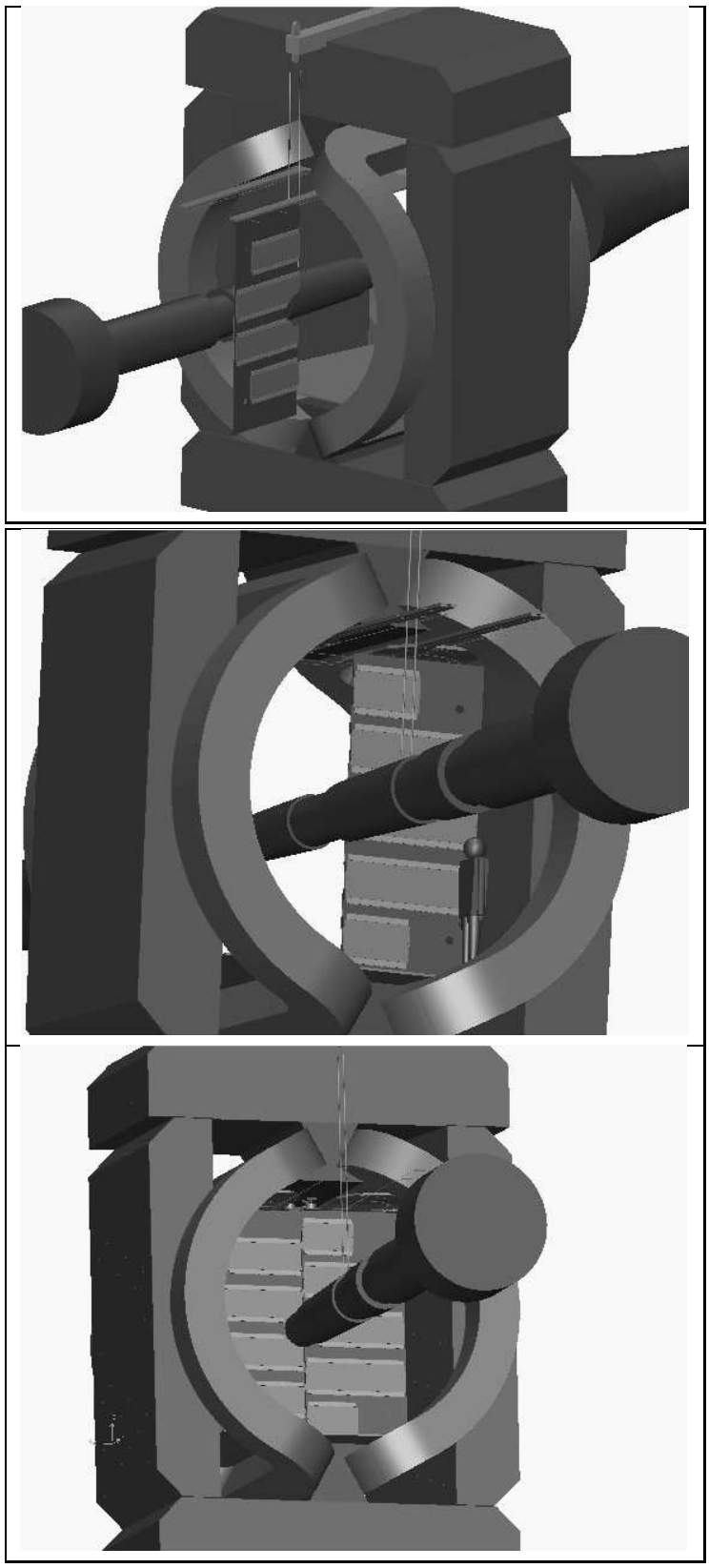

Figure 3.12: Integration of the station 3 inside the magnet.

considered as laminar (air speed remains inferior to 1 m/s), and ambient temperature of air in the cavern is 20°C. Temperature in the magnet is 30°C, according to the calculations of the Dipole group.

3.3.2 Cooling with Panels geometry

In present time, cooling calculations with panels geometry have been performed only for Station 5, which represents the most unfavourable case : Station 5 is the most loaded station with slats and electronics components. The power dissipated by electronics is 3.3 kW.

For Station 5, in our present simulations, air extraction was made on the both side of the station. In the future, air extraction will be placed at the top of this station. Two air flow values for extraction have been tested : 600 m^3/h and 1200 m^3/h. Results are summarized in Table 3.3, where $<\Delta T>_{simu}$ is the temperature difference, obtained by simulation, between the inlet temperature at 20°C and the mean value of the outlet temperature, corresponding to a given air flow. This last value can be compared to $<\Delta T>_{calc}$, which is the temperature difference, obtained by a simple calculation, coming from the basic heat transfer equation, between the inlet temperature and the outlet temperature, corresponding to a given air flow :

$$<\Delta T>_{calc} = \frac{P}{\rho \times G \times C_p}$$

where P is the power dissipated (W), G the volumic flow rate m^3/s, ρ the density of air = 1.20 kg/m^3 (air at 20°C, 50% HR) and C_p the specific heat for air = 1000 J/(kg.K). In Table 3.3, a good agreement is observed between the values $<\Delta T>_{simu}$ and $<\Delta T>_{calc}$, which reinforces our model taken for the simulations. Moreover $<\Delta T>$ gives the information about the temperature of the air, which has to be removed by the future cooling unit for Station 5.

Figures 3.13, 3.14 and figures 3.15, 3.16 illustrate the results obtained by simulation, about temperatures and velocities of air on the slats plane, for an air flow equal to 600 m^3/h and 1200 m^3/h respectively. In both case, air velocities remain laminar and do not exceed 0.67 ms^{-1}.

Air flow is well canalized and circulates vertically along the slats plane. Nevertheless, a extended hot zone at 42°C is still remaining with an air flow of 600 m^3/h. This might induce permanent heating for electronics in this area on long term. For this reason, it is better to employ an air flow more important such as 1200 m^3/h ; then the hot zone surface decreases and its temperature is lower : 37.5°C.

Table 3.3: Results on the cooling by air for the Station 5 (forced convection).

Description of Cooling	**Air flows (m^3/h)**	**T_{max}(°C)**	**$<\Delta T>_{simu}$(°C)**	**$<\Delta T>_{calc}$(°C)**	**comments**
extraction	600	42.1	14.2	16.5	extended hot zone at 42.1°C
extraction	1200	37.5	8.1	8.2	hot zone at 37.5°C

Conclusion :

For Station 5, air extraction on the top of the station is good enough to cool electronics on slat, with an air flow equal to 1200 m^3/h. A hot zone is still remaining at 37.5°C and this point has to be optimized and will be studied more closely in next simulations. Cooling by air is therefore sufficient for the 3 Tracking Stations with such an air flow and this solution has been approved since the Cagliari Meeting

in Villasiamus, in May 2001. Saclay group requires then 1200 m^3/h per station to the CERN EST/LEA group.

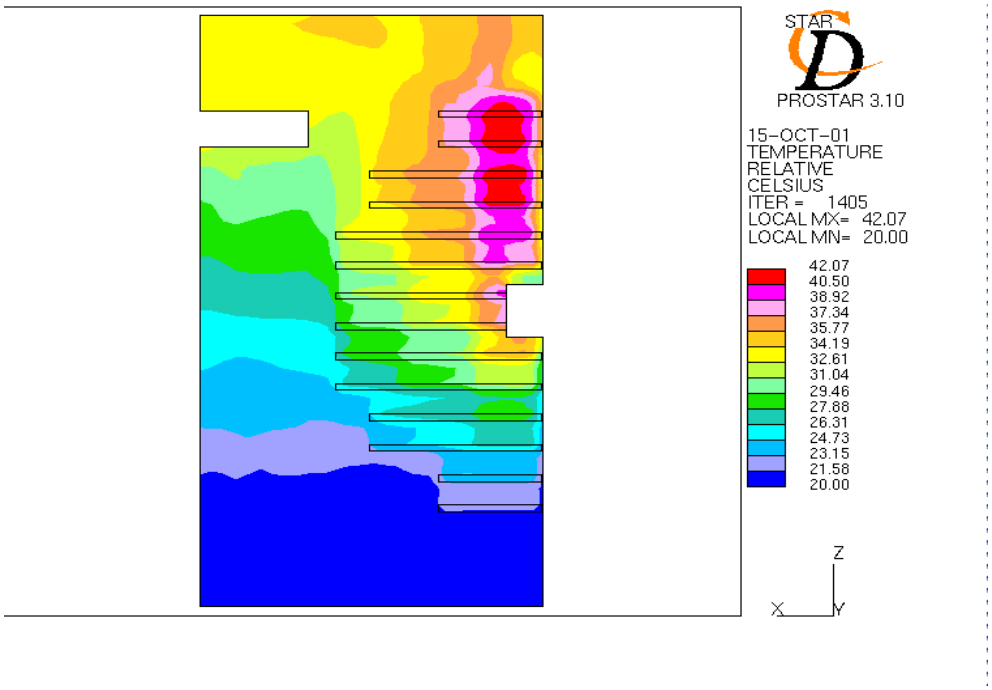

Figure 3.13: Station 5 : forced convection with air extraction flow = 600 m^3/h. Longitudinal cut of temperatures in the slats plane, where temperatures are maximum.

3.3.3 Proposition from CERN EST/LEA : one common cooling unit for the five stations of the tracking system

Several cooling meetings have taken place in 2001, with R.C. Gregory and S. Evrard from CERN EST/LEA group, who are in touch with CERN ST/CV group. Then CEA Saclay's request is approved :

- Station 3 : air injection at the bottom of the station (air flow=1200 m^3/h, with $T_{input} = 20^\circ C$), and air extraction at the top of the station (air flow=1200 m^3/h).
- Station 4 : air extraction at the top of the station (air flow=1200 m^3/h).
- Station 5 : air extraction at the top of the station (air flow=1200 m^3/h).

The proposal from EST/LEA group is a common cooling unit for the five stations of the Tracking System (presentation made by S. Evrard [3]) ; Table 3.4 resumes the main cooling parameters for all stations. The cooling unit will be placed in the UX25 cavern, and its characterics are the following :

- The ideal dimensions for the common unit are planed to take into account some spare : total flow is 5000 m^3/h, with a total power to dissipate of 20 kW.
- $T_{inlet} = 20^\circ C$, $T_{outlet} = 30^\circ C$, $T_{max}(chamber) = 40^\circ C$.
- Recycling for Stations 1-2-3 is provided ; recycling for Stations 4-5 can also be provided very easily, if necessary. This last solution is under study.

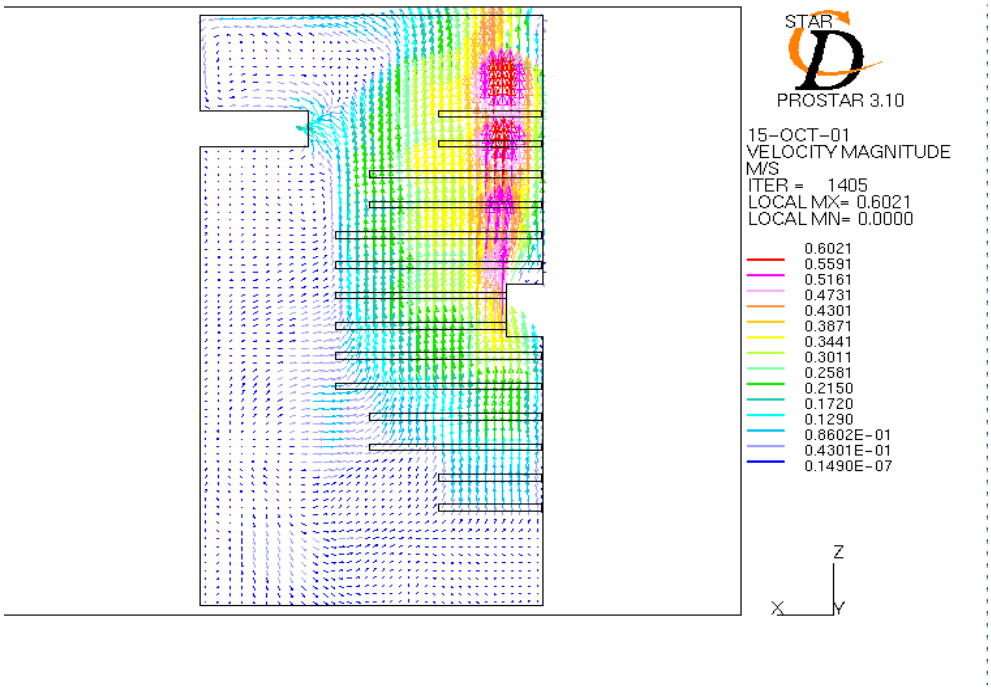

Figure 3.14: Station 5 : forced convection with air extraction flow = 600 m^3/h. Air velocity vectors in the slats plane, where temperatures are maximum.

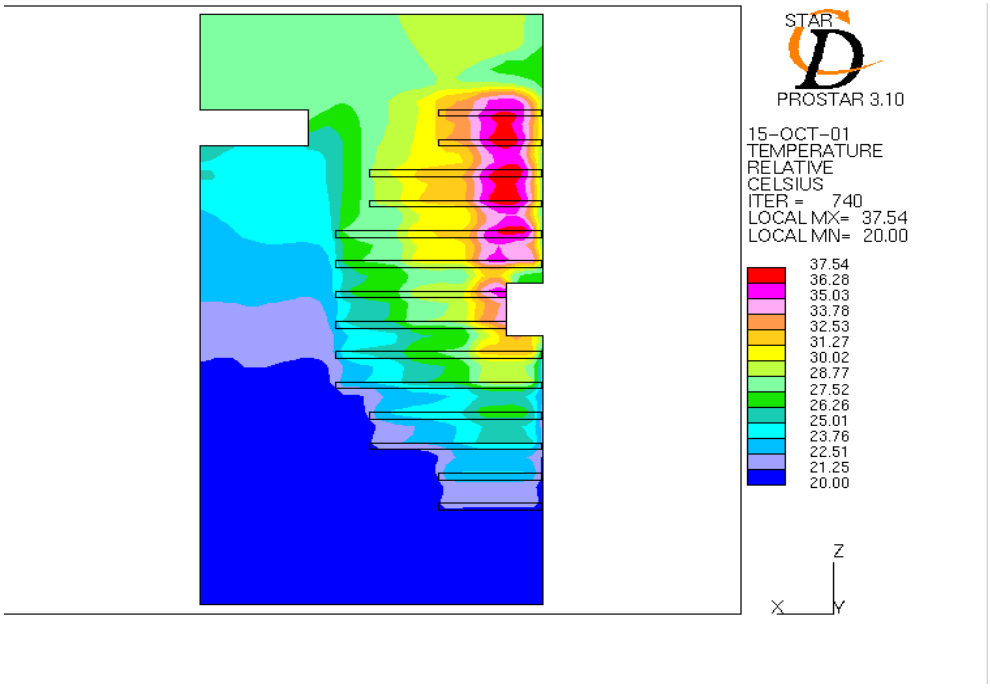

Figure 3.15: Station 5 : forced convection with air extraction flow = 1200 m^3/h. Longitudinal cut of temperatures in the slats plane, where temperatures are maximum.

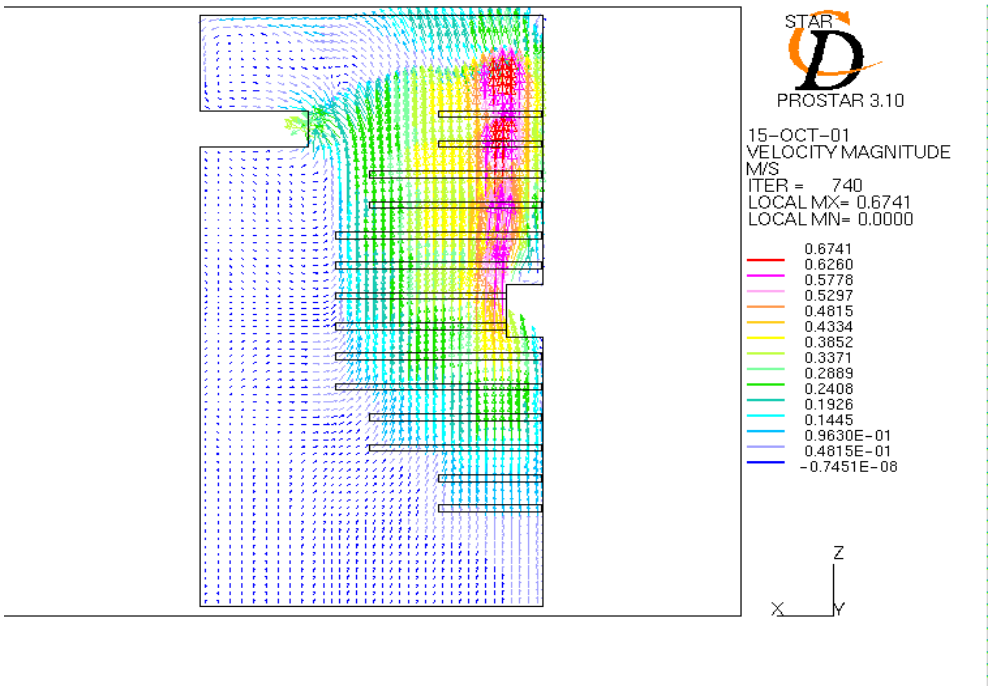

Figure 3.16: Station 5 : forced convection with air extraction flow = 1200 m^3/h. Air velocity vectors in the slats plane, where temperatures are maximum.

Table 3.4: summary of the cooling parameters for all Tracking Stations

	P (kW)	**Qv** (m^3/h)	$<\Delta$**T**$>$ (°**C**)
Station 1-2	5.8	1000	17.4
with water cooling	2.3 (40%)	1000	6.9
Station 3	2.1	1200	5.3
Station 4	2.8	1200	7.0
Station 5	3.3	1200	8.2
TOTAL	**14**	**4600**	**9.1**

- High reliability (due to the access difficulties in the L3 cavern during run period) : two engines are foreseen.
- Fans with variable velocities. Mind the magnetic field in the cavern.
- Dimensions of the unit : $1m \times 0.5m \times 1.5m$.
- Cost : 30 to 40 kCHF.

3.3.3.1 Share of the tasks

EST/LEA group provides the cooling unit and air ducts up to the bottom of the five stations. The conception and integration of suitable diffusers is under the responsability of IPN Orsay group for Stations 1-2 and CEA Saclay group for Stations 3-4-5.

Some characteristics about air ducts for cooling are given in the following Table 3.5 : for each air duct diameter, the air flow, the corresponding velocity (considered as uniform on the pipe section) and

loss of pressure are given. This table gives an idea of the different type of air ducts that can be used. No definitive solution is decided at that time ; the best solution depends mainly on the integration possibility for each station.

Table 3.5: Pipes parameters

Diameter of air ducts (mm)	Qv (m^3/h)	v (m/s)	dPi (Pa/m)
200	1000	8.8	4.5
200	1200	10.6	6.5
250	1200	6.7	2.0
400	4600	10.2	2.5

3.3.4 Planning : next phases

Cooling activities at CEA Saclay will continue for the 3 stations at the beginning of 2002 :

- Simulations : new calculations for the three stations will continue with a new software CFDesign at the beginning of 2002. Air flow will be optimized for the three stations, in order to remove or decrease as much as possible hot zones. But in any case, all flow values will remain in the same order of magnitude than the current values given above. Calculations will be performed in the same time for Stations 1-2.

- Experimental validation ? : due to the lack of manpower and time, Saclay is not able to produce some experimental validation for Stations 3-4-5 in 2002. But as Orsay have validated their simulation code (IDEAS) with a thermal mock up of Station 1 (scale 1) in 2001, it is now possible for Saclay to compare our simulation results with experience from Orsay.

- Diffusers have to be studied and integrated for the Stations 3-4-5.

- Integration of air ducts and cooling units have to be checked in agreement between CERN and CEA Saclay.

- Collaboration is reinforced in 2001 and will be increased in 2002 between CEA Saclay (Stations 3-4-5), IPN Orsay (Stations 1-2) and CERN (EST/LEA & ST/CV).

- Collaboration with other sub systems have to be reinforced, because of the interfaces between Stations 3-4-5 and Muon Filter (Gatchina) and Dipole Magnet (CERN & Sarov). Temperatures cartography has been sent by CEA Saclay group to Muon Filter group in June 2001, for thermal calculations for the Muon Filter [4].

The planning for the cooling, from the CERN EST/LEA point of view, which is in agreement with the planning of CEA Saclay, is the following :

- Finalisation of requirements : January 2002 up to May 2002.

- Purchase equipment : March 2003 up to the end of October 2003.

- Installation equipment : January 2005 up to May 2005.

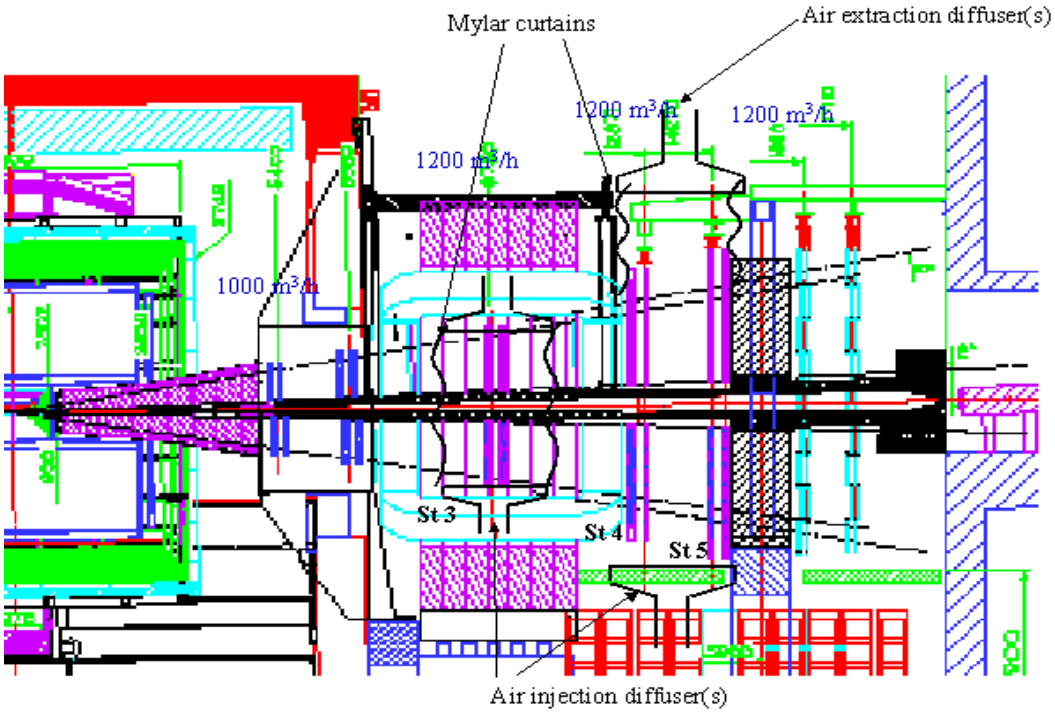

Figure 3.17: Principle of practical integration of cooling diffusers for the Stations 3-4-5 : diffusers for air extraction, diffusers for air injection and mylar curtains are represented schematically.

To conclude, the difficulties of the cooling integration can be presented schematically in Figure 3.17. For Stations 4-5, diffusers for extraction of air must be installed above the rails and above the Superstructure, because of the lack of room just at the top of the stations. Mylar curtains are foreseen to canalize air flow as best as possible. Air injection diffusers are now foreseen.

The cooling for Station 3 could be improved with mylar curtains, which supply a protection against the heat dissipated by the Dipole coils. On the other hand, the integration of diffusers of Station 3 will be more difficult than for Stations 4-5, because of the lack of place inside the dipole at the top and bottom of the station. This last point can be seen on figure 3.18.

Finally, the cooling group of Stations 1-2-3-4-5 (IPN Orsay & CEA Saclay) is worried about the heat dissipated by the coils of the Dipole magnet. In present time, the magnet dissipates up to 10 kW, i.e. practically the heat dissipated by all the five tracking stations. Moreover, the average temperature inside the magnet is around 35°C (last information given by A. Tournaire, Technical Coordinator of the Dimuon Arm). A message has been sent in September 2001 to inform the ALICE collaboration and the Dipole magnet group of our worry. Since, the Dipole group is studying some isolation of the coils with thermal screens.

[1] "ALICE: Addendum to the Technical Design Report of the Dimuon Forward Spectrometer", Addendum 1 to ALICE TDR 5, CERN/LHCC 2000-046, Dec.2000.

[2] "Calculs sur le refroidissement des Stations 3, 4 et 5 (calculs effectues en 2000)", S. Salasca, Note interne Alice Bras Dimuon, CEA Saclay, Ref.6S3221C012DA01, Janv.2001.

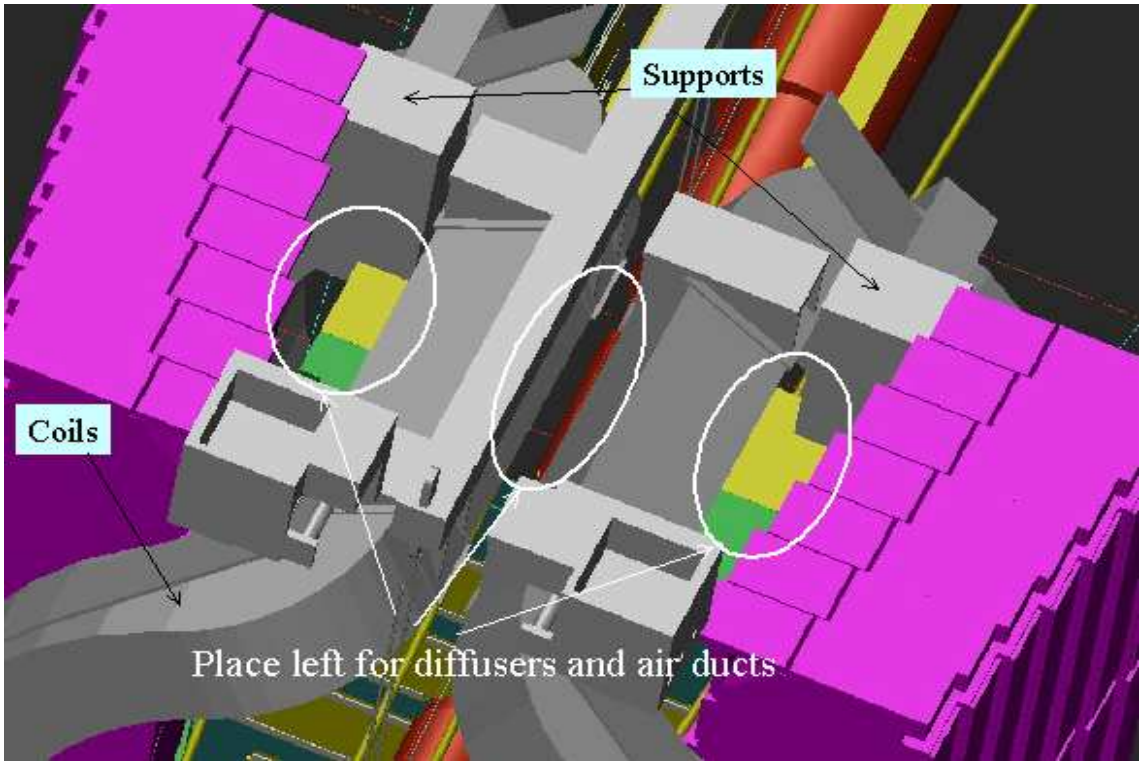

Figure 3.18: Top view of the Dipole : place left for the integration of cooling diffusers for Station 3 is small. Diffusers for air extraction will be probably divided into three parts ; dipole coils and supports are in the way of the air ducts.

[3] "Cooling of Tracking Chambers by air", presentation by S. Evrard, Alice Week Forum, on 12th September 2001 at CERN.

[4] "Report on the Engineering Design of the Muon Filter", Note CERN-PNPI Gatchina 2001, transmitted on 20/08/01.

4 Slat Electronics

The PRR for the electronics part is foreseen by the end of May 2002, so in what follows, just a brief summary of the electronics will be given together with the performances obtained with a full size slat prototype. A much more detailed description of the electronics equipment has been reported in the Addendum to the TDR published less than one year ago.

4.1 General principle

- Although the Dimuon System is composed of two types of chambers (quadrants for Stations 1 and 2 and slats for Stations 3,4 and 5), it has been decided to use the same electronics for both types.
- It is well known that the spatial resolution obtained with pad chambers depends mainly of the signal over electronical noise ratio . In order to minimize the electromagnetic pick-up on the lines it is preferable to preamplify the measured signal close to the source, i.e. the pad.
- Given the large number of pads on a slat, it has been decided to avoid a huge number of lines or wires for transmitting the preamplified signals towards the edges of the chambers. The consequence is that all what concern the coding, the pedestal subtractions and the zero suppressions will be performed directly on board. It is then possible to reduce the number of lines down to a few number for the read-out of the non-zero values.

4.2 Present status description

4.2.1 the signal treatment:

All the operations described above will be ensured by small boards called MANU (for MAnas NUmerical) plugged directly on the pad planes. These MANUs (see photo 4.1) are essentially composed of:

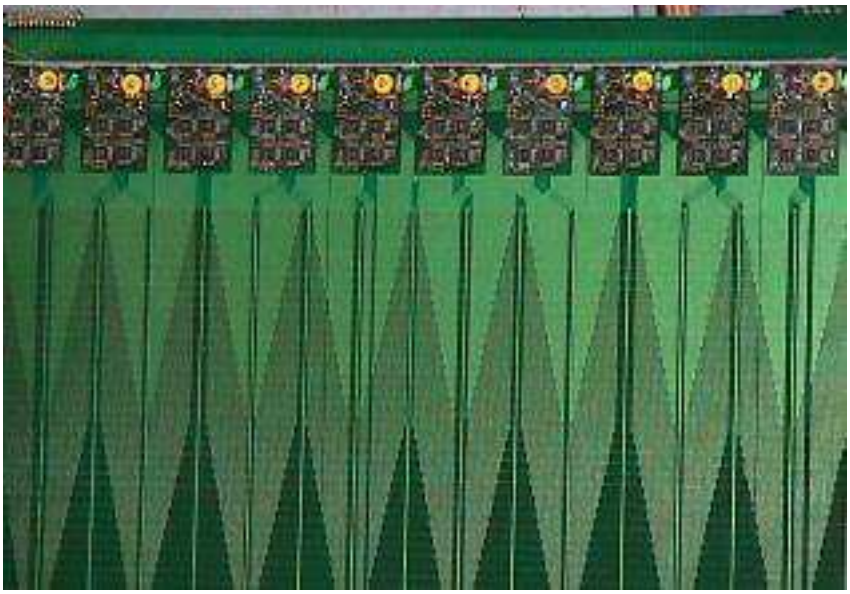

Figure 4.1: View of a part of a slat with 10 MANU345 plugged

1. 4 preamplifiers, filters and shapers with 16 channels each. In the present version of MANU, a new version of the CERN chip (GASSIPLEX 0.7 microns) has been used. The previous version (1.5 microns) had been studied for the HMPID characteristics with a very small number of primary electrons compared to our case. To avoid a lot of saturated information due to a too high gain, a new version has been asked by the team in charge of the electronics at J.C. SANTIARD with a gain three times lower. Moreover it has been asked to modify the low voltage values.

2. two 12 bits ADC with a conversion range of 0 to +3V. The use of two ADC instead of one permits, for the same coding time, to choose chips with a lower consumption. These chips have a nap mode.

3. one MARC chip studied and realized by INFN Cagliari. The role of MARC is to sequence the GASSIPLEX read-out, the coding, to perform the pedestal subtractions, the zero suppression and to push the data on the numerical buses towards the front-end DSPs.

4.2.2 the read-out:

The data are transmitted at 40 MHz by nibbles (4 bits) towards the DSPs link ports located outside the slats via numerical buses. With a so high frequency, these buses encounter two limitations:

- the number of MANUs plugged on the same bus must not exceed about 20 boards. The main reason is the signal adaptation along the line.

- the length of the buses makes level adaptators necessary to translate the signals from LVTTL to LVDS standards.

4.2.3 DAQ:

For the 2001 October tests, a bench-test has been constructed in which, the front-end DSP sends towards an other DSP located in a VME crate in which are also present the Si tracker CRAMS (Caen Read-out Analog Multiplexed System). This bench test structure will be reproduced for testing the slats in the different labs during the slats mass production. An industrial bench test will also be made for the MANU tests during the manufacturing

4.2.4 Accessories:

The MANUs are fed by busbars carrying 3 low voltages (+2.5 V, -2.5V and +3.3 V). For an average consumption of 13 mW/channel, the voltage drop along a line in the worst case is estimated to beabout 40 mV

4.3 Measured performances:

This electronics set-up has been tested during the last in-beam tests at PS in October. The main results are:

- the measured overall electronics noise with everything taken into account (pad, line, connector capacitances, ADC noise and LSB, GASSIPLEX noise) is around 1150 electrons. The same measurements in which the lines were cut just after the connector gave 900 electrons

- This value obtained in the experimental hall has been obtained after insulating all the grounds of the slat and of the electronics from the general ground available in the hall. We have been obliged to proceed in such a way because the ground of the hall was really noisy and this fact having already been remarked by our colleagues of the HMPID. It is completly opposite to the scheme we wish to

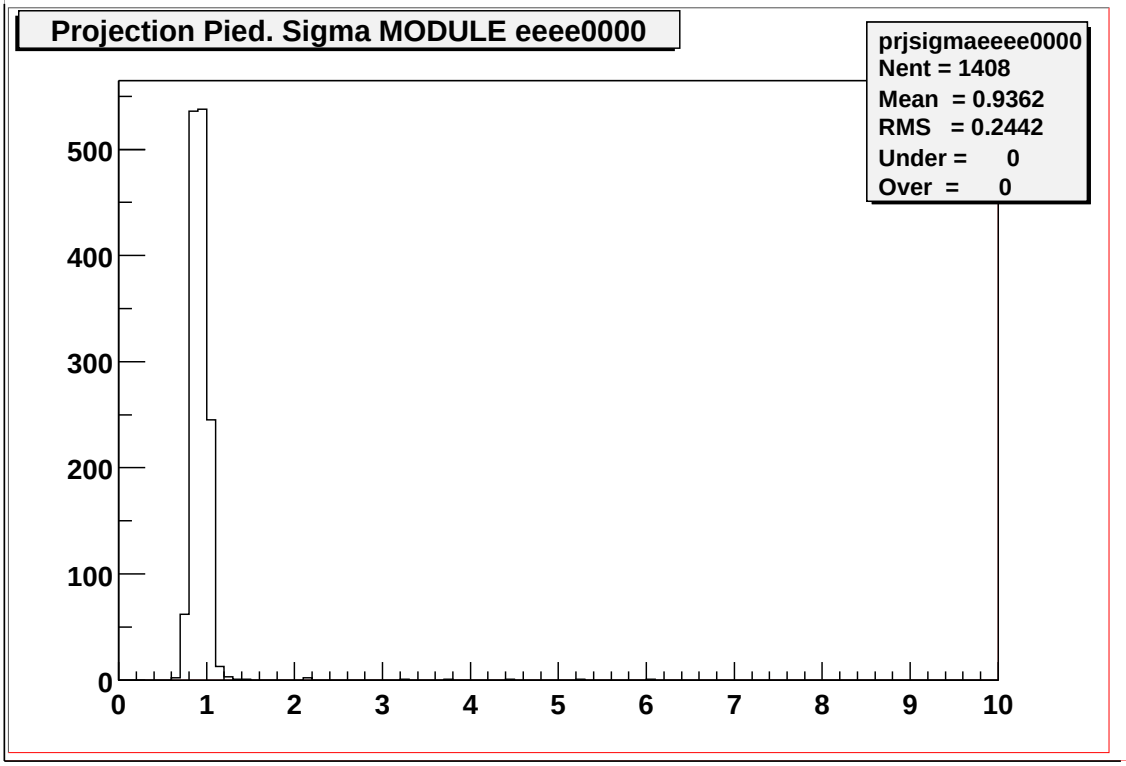

Figure 4.2: Histogram of the electronics noise measured on more than 1400 channels

follow in the final stage, i.e. to connect (the most often possible) all the grounds of the detectors, of the electronics with the general ground of ALICE. WE ARE STRONGLY DEMANDING, IN A SHORT DELAY, A COMMON POLICY FOR ALL THE ALICE DETECTORS CONCERNING THE GROUNDING QUESTIO

4.4 Next future

4.4.1 Manas:

In a next future, the preamplifiers GASSIPLEX will be replaced by the MANAS which have been studied by our indian colleagues of SINP Calcutta, in collaboration with J.C. SANTIARD. This preamplifier is a clone of GASSIPLEX and the first iteration has given good results excepted a drooping which occured during the 10 first μs.

A comparison between the two chips is reported in table 4.1

A few chips, with this drooping suppressed, of the second iteration should be ready by November 2001 and if the tests are satisfactory, about 1 000 chips should be provided by March 2002. There remains a concern with the size of these chips and with the compatibility with the chosen GASSIPLEX packaging because the manufacturer accepts to package this small number but has still not given an answer for the mass production.

4.4.2 MARC2:

In the first iteration the READ/WRITE operations were performed on the same bus and it has been remarked that during the read-out some misinterpretations were done by the MARC which interpreted data as instructions. To avoid such problems it has been decided to separate the buses for the two functions (READ/WRITE) which has for consequences to simplify the chip but to need two lines more.

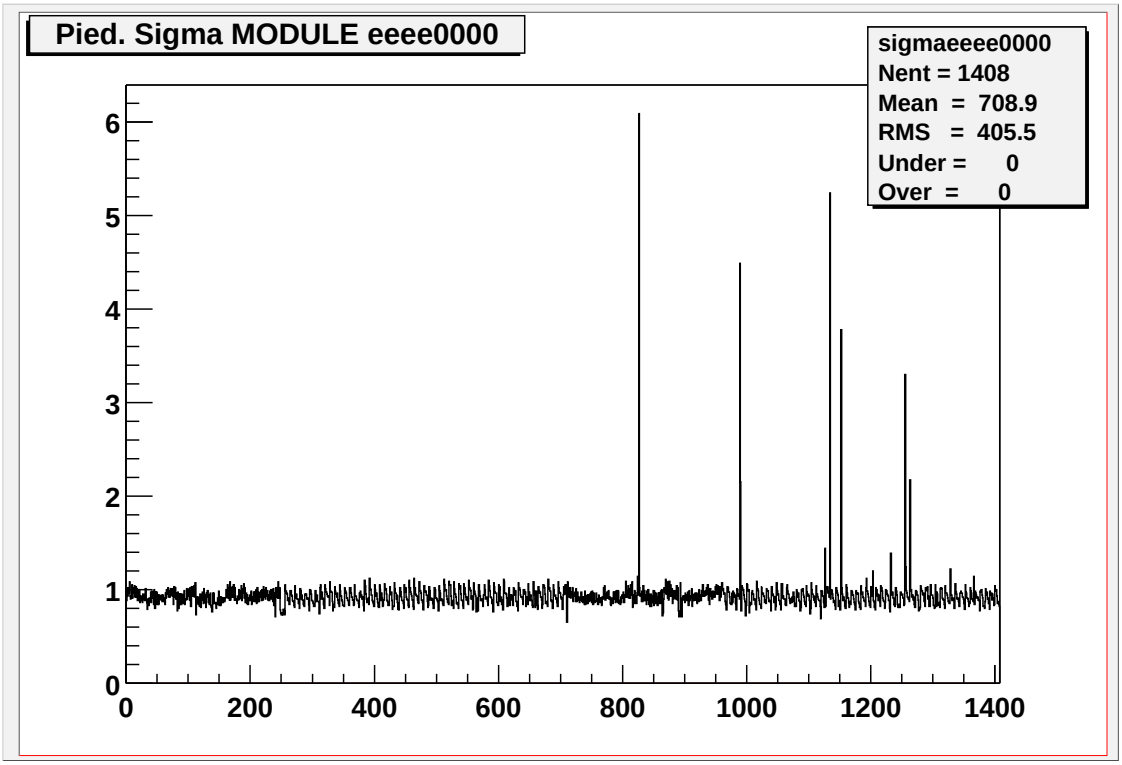

Figure 4.3: Noise vs. channel number

This solution has been successfully tested during the last in-beam tests by using an artefact. Now the second iteration of MARC will be launched and should be ready by the end of February 2002.

4.5 Status Report on Low Voltage

4.5.1 Introduction

The readout electronics for the tracking chambers of the Dimuon Forward Spectrometer require three types of low voltage supplies:

- for the analog part : Vdd = +2.5 V, with a total power of 3755 W and Vss = -2.5 V, with 4587 W;
- for the digital part : Vnum = +3.3 V, with 3577 W.

The overall power is estimated to 12 kW. These requested powers imply high intensity currents with low voltages and, consequently, the energy efficiency of the electrical connections has to be carefully considered.

In order to make easier the energy distribution (cost, diameters, rigidity and weight of cables), each alimentation current is limited to 25 A. From this constraint, Stations 3-4-5 are segmented in order to limit the consequences of local breakdown and to not create a breaking of the readout bus chain.

Low voltage supply responsability is divided into three parts : low voltage power system, low voltage cables & connectors (under IPN Orsayresponsability) and busbars, which are soldered on slats (under CEA Saclay responsability). CERN EST/LEA group is in charge of the racks for low voltage power supply and integration of cables up to the bottom of the stations. CEA Saclay is in charge of the remaining integration up to the busbars connections on slats. This report presents only the status about busbars and

	MANAS	GASSIPLEX 0.7 μm
Technology	SCL 1.2 μm	Alcatel-Mietec-0.7μm
Peaking time	1.2 μs	1.2 μs
Noise at 0 pF	640 e$^-$rms	530 e$^-$rms
Noise slope	11.58 e$^-$rms/pF	11.2 e$^-$rms/pF
Dynamic range (+)	500 fC	560 fC (0 to 2 V)
Dynamic range (-)	275 fC	500 fC (0 to -1.1 V)
Gain (+)	3.5 mV/fC	3.6 mV/fC
Analog readout speed	10 MHz (max)	10 MHz (50 pF load)
power consumption	7 mW/channel	8 mW/channel at 10 MHz
output temp. coefficient	0.03 mV /^{o}C	0.05 mV /^{o}C

Table 4.1: Comparison of MANAS and GASSIPLEX 0.7 μm characteristics

cables, which are in the slats environment ; the LV supplies description will be one of the next subject of the electronic PRR, organised in May 2002.

4.5.2 Busbars

4.5.2.1 Busbars material

Busbars are made of three tinplated copper bars (high conductivity copper), which are assembled together to form the bus. Each bar is isolated from the other one by a thin isolant sheet (ex :kapton sheet), in order to avoid short-circuits between the three low voltages. Moreover, isolant material and glue should fill the Fire Safetyinstructions of CERN (TIS IS 41). Busbars must provide low voltages to the electronic components and they are soldered directly, standing up on the PCBs. Their location can be seen on Figure 4.4, under the MANU 345 board.

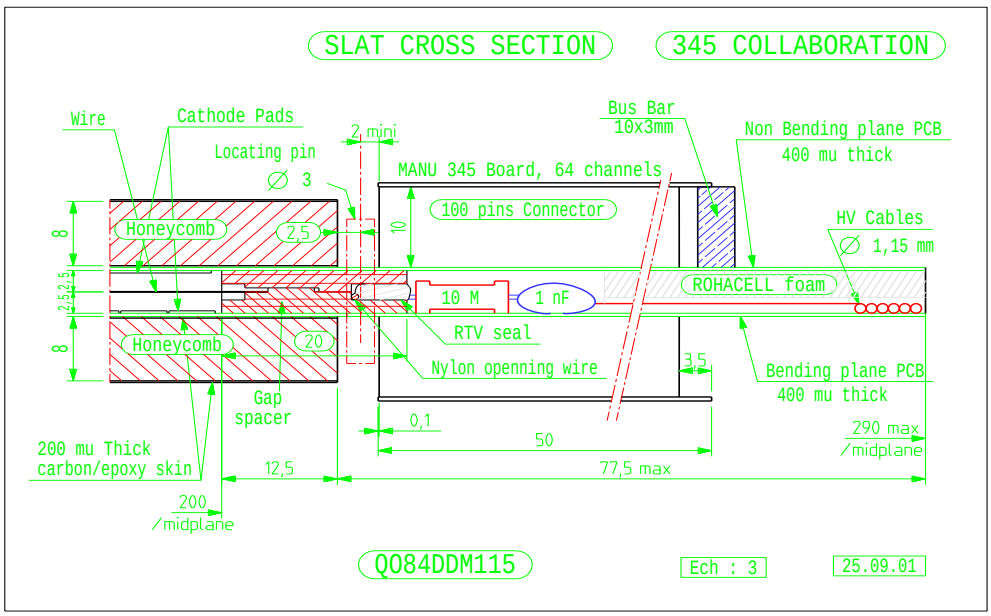

Figure 4.4: Busbars location on the slat, under the MANU 345 board.

4.5.2.2 Busbars dimensions and conception

Each bar of the bus has a section of 0.8 mm width by 6 mm height. This section is sufficient to provide correctly the voltages along the slat, even for the longer slat of 2400 mm long. The maximum loss of voltage is estimated to be 40 mV in a complete loaded line of 2400 mm long.

Both ends of the bar are bent in two plies and the total length of the core is 396.5 mm. Both extremities plies are not identical : one is shorter than the other one, in order to facilitate the busbars recessed fitting. The three busbars bring low voltages to electronics through 3 lugs. The thickness of one lug is 2 mm, in order to offer a good surface for the weld on PCBs. These 3 lugs are bent so as to be placed, all three, of the same level on the PCB. All these details are illustrated with the photographs below.

Isolant thickness is about 0.1 mm and its height must not exceed the height of the copper bars. Details on busbars dimensions can be found on the drawings figures 4.5 for the Bending Plane and 4.6 for the Non-Bending Plane.

In total, only four conceptions of busbars are foreseen for standards PCBs, whatever the pads density is. In other words, the other PCBs, with density 2 or 3 of pads, will receive the same busbars as PCBs with density 1. All the PCBs chips will be arranged as a multiple of 10 for the Bending Plane or 7 for the Non-Bending Plane. There will be also some specific busbars conception (special busbars with adapted lengths) for the non standars PCBs (round-shaped PCBs of Stations 3-4-5 and half-moon PCBs of Station 3), but this conception is not ready at the moment.

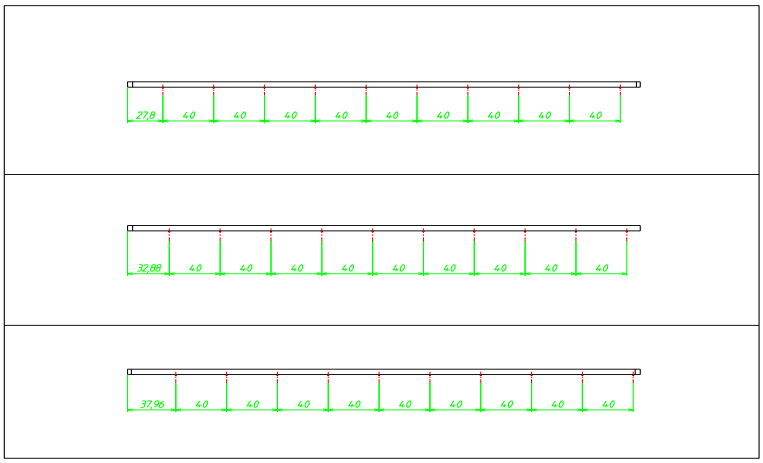

Figure 4.5: Busbars drawings for the Bending Plane

The four types of busbars for standars PCBs, with the maximum density of pads (density 1), are distinguished by the part of the slat where they are soldered :

- Bending Plane Top (10 MANUs 345) : 10 groups of 3 lugs, bent to the right. The pitch inter group is 40 mm and the pitch between lugs is 5.08 mm.
- Bending Plane Bottom (10 MANUs 345) : 10 groups of 3 lugs, bent to the left. The pitch inter group is 40 mm and the pitch between lugs is 5.08 mm.
- Non-Bending Plane Top (7 MANUs 345) : 7 groups of 3 lugs, bent to the right. The pitch inter group is 57.15 mm and the pitch between lugs is 5.08 mm.
- Non-Bending Plane Bottom (7 MANUs 345) : 7 groups of 3 lugs, bent to the left. The pitch inter group is 57.15 mm and the pitch between lugs is 5.08 mm.

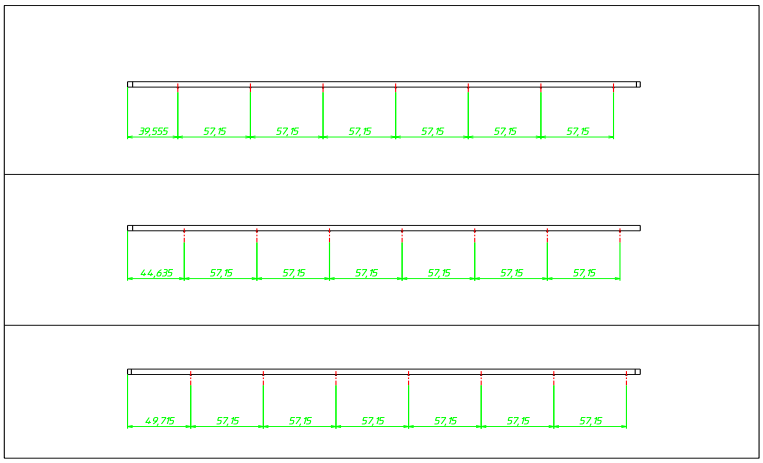

Figure 4.6: Busbars drawings for the Non Bending Plane

4.5.2.3 Busbars realization and planning

- First prototypes, made in April 2001 : some pieces have been produced in a french company, in order to validate the mechanical conception. Mechanical cutting is employed for the copper bars. Some defects have been found in the design and improvements are thenintroduced for the next design. The company validates some tooling and produces an assembling template.
- First pre-production made for the biggest slat of 2400 mm, in July 2001 : 24 busbars are produced by the same french company (12 for the Bending plane and 12 for the Non Bending plane). The cutting of this serie was made with laser. This cutting prove to be very bad, as we discover a visible arrow on all the busbars. This point make us understood that the best way for cutting is bymechanical technique. Since the last test beam in October 2001, moreover, there was problem with lugs height, which were of different level. During assembly on slat, these defects lead to soldering problems, which must be improved for the following.
- Future production in India ? For financial reason, it seems that the busbars have to be produced in India. First contact is established with an indian physicist of ALICE. We think that we shall start again some prototypes with the future indian company, and then produces a small set of busbars before the completeproduction. In other words, we start from the beginning our procedure of fabrication with an unknown indian company.

From the planning point of view, the final design must be achieved in March 2002 and the order procedure is foreseen between September 2002 and middle October 2002. Realization have to start in November 2002. We hope to finish the design before March 2002, in order to spend more time with indian company to prepare the tooling and to be sure of the way to proceed.

4.5.3 Low voltage cables

4.5.3.1 General points

Cables provide low voltages to the different slats busbars. The following photograph (on the left) shows the connections with LVcables, using“cosse faston”. The drawing (on the right) shows the principle of LV cables distribution on the slat busbars. The LV cables passage is done only on the external side of the chambers, due to the important amount of matter brought by the large section of these cables.

On this drawing, the separation of cables is shown : one rigid cable(S=$5 \times 16 mm^2$), placed on the external service support structure (SSS), is divided inthiner and more supple cables, via a distribution

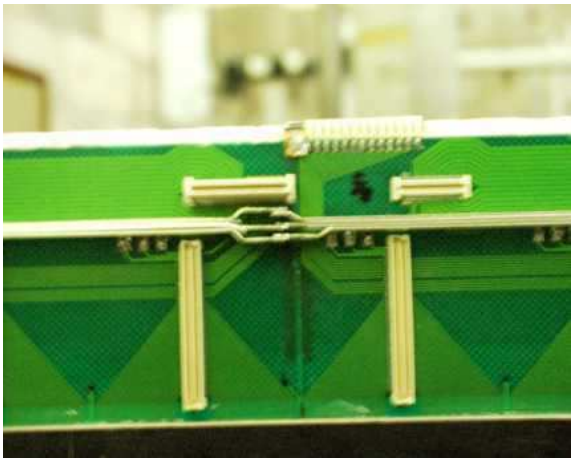

Busbars junction in Top Non Bending Plane

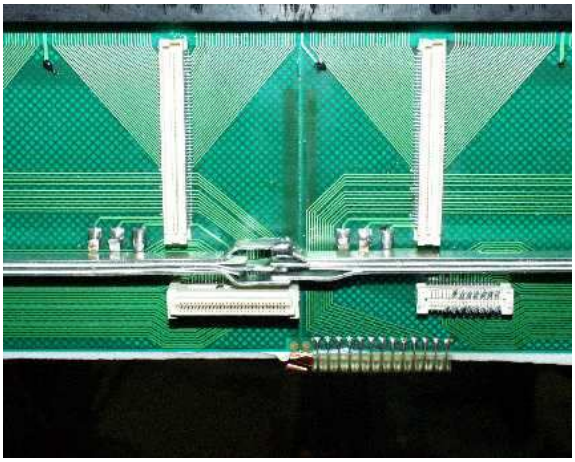

Busbars junction in Bottom Non Bending Plane

Busbars in Top Bending Plane

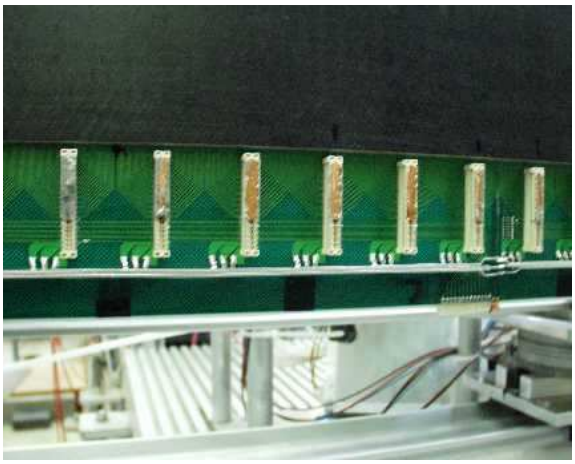

Busbars in Bottom Bending Plane

Figure 4.7: Four types of busbars.

box. The distribution is then made on four points for each slat, corresponding to the four extremities of busbars : Non Bending Top, Non Bending Bottom, Bending Top and Bending Bottom.

4.5.3.2 Description of LV cables

Cables should fill the CERN safety standards, with respect to the firesafety and radiation resistance. One cable coming from LV supplies is composed of five conductors of$16 mm^2$ section each. The following drawing, figure 4.8, details the composition of LV cables. Moreover, there are three senses : 3 pairs of twisted cables, which have to be connected on the distribution box, in order to decrease the loss of voltage not regulated.

Section, amount of cables, weight, loss voltage in lines and powerdissipated in lines for Stations 3-4-5, were estimated in [1] and are resumed, with the most recent design of slats and electronicchannels, in Table 4.2 :

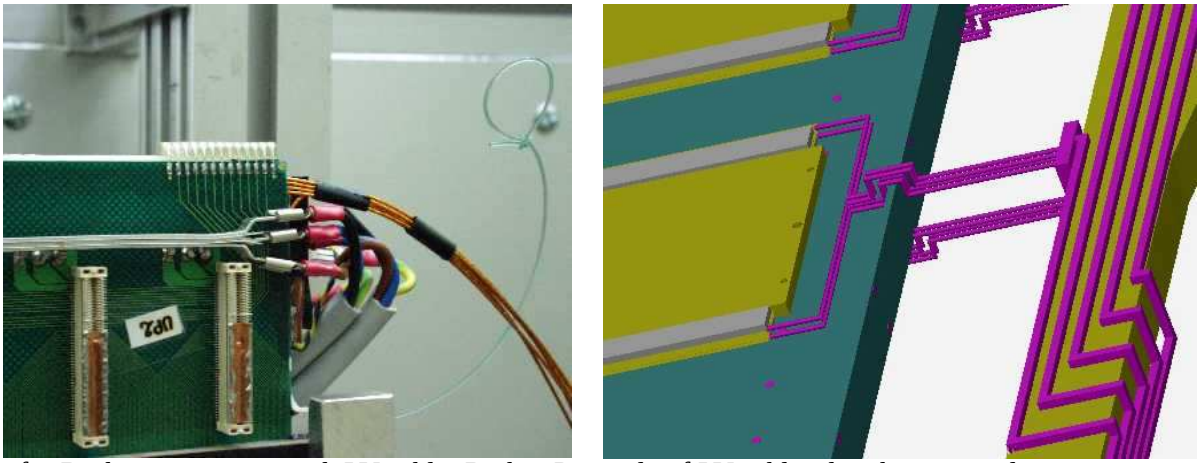

Left : Busbar connection with LV cable. Right : Principle of LV cables distribution on slat.

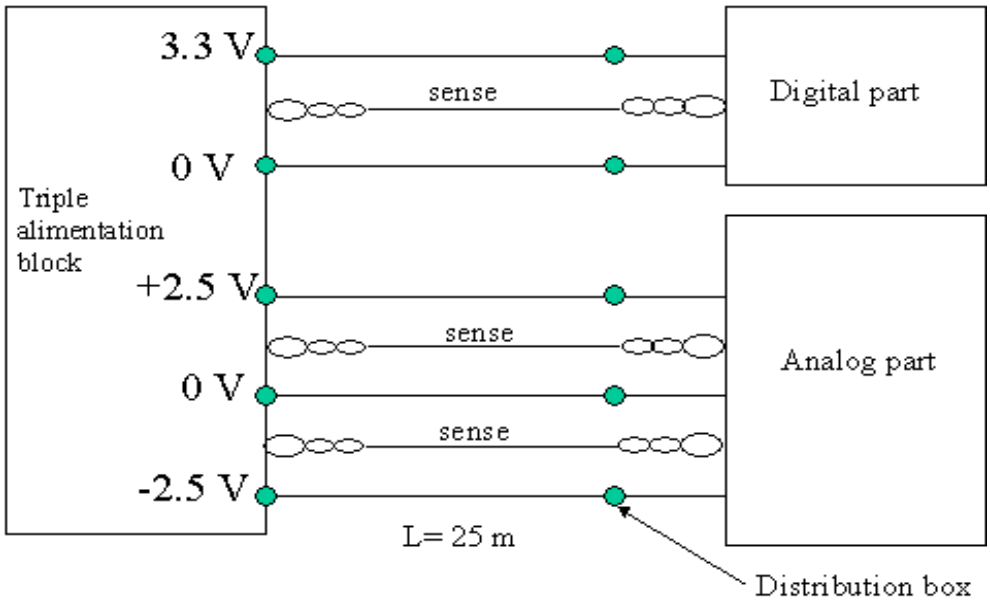

Figure 4.8: LV cables composition : 5 conductors with section of16mm^2 each and 3 twisted pairs of senses.

4.5.3.3 Chambers segmentation with LV cables

The main constraint for the segmentation is to respect the maximum current value of 25 A, supported in LV cables, coming from the supplies. In that case, taking into account the number of electronic channels per slat, and the strongest current value, given by the negative voltageVss=-2.5 V (Iss=1.69 mA/channel), the segmentation and sections of LV cables are the following [2]:

Station 3 (figure 4.9) : 16 triple LV supplies for the whole station. 4 supplies for 9 slats of one half chamber ; segmentation from the top to the bottom of one halfchamber :

- 3 slats arranged together : separation of 1 big cable in3×4=12 thiner lines of 5 conductors$\longrightarrow$ each conductor section is 1.33 mm^2.
- 2 slats arranged together : separation of 1 big cable in8 thiner lines of 5 conductors$\longrightarrow$ each conductor section is 2.0 mm^2.
- 1 slat : separation of 1 big cable in4 thiner lines of 5 conductors$\longrightarrow$ each conductor section is 4.0

Table 4.2: LV cables parameters

length per cable (m)	**section (mm^2)**	**total number of cables**	**weight per cable (kg)**	**total length (m)**	**total weight (kg)**
25 /cable	5×16	96	24	2400	2300

cables	**R_{line} (Ω)**	I_{max}line (A)	**ΔV (V)**	**$P_{dissipated}$/line (W)**	**total P (W) in all lines**
V_{num}	0.053	13	0.7	8.96	573
V_{dd}	0.027	18	0.5	8.75	560
V_{ss}	0.027	22	0.6	13.07	837

Total Power dissipated in all3×64 **lines of ST3-4-5 is 1970 W**

mm^2.

- 3 slats arranged together : separation of 1 big cable in3×4=12 thiner lines of 5 conductors$\longrightarrow$ each conductor section is 1.33 mm^2.

Station 4 (figure 4.10) : 24 triple LV supplies for the whole station. 6 supplies for 11 slats of one half chamber ; segmentation from the top to the bottom of one half chamber :

- 3 slats arranged together : separation of 1 big cable in3×4=12 thiner lines of 5 conductors$\longrightarrow$ each conductor section is 1.33 mm^2.
- 1 slat : separation of 1 big cable in4 thiner lines of 5 conductors$\longrightarrow$ each conductor section is 4.0 mm^2.
- 2 slats arranged together : separation of 1 big cable in8 thiner lines of 5 conductors$\longrightarrow$ each conductor section is 2.0 mm^2.
- 1 slat : separation of 1 big cable in4 thiner lines of 5 conductors$\longrightarrow$ each conductor section is 4.0 mm^2.
- 1 slat : separation of 1 big cable in4 thiner lines of 5 conductors$\longrightarrow$ each conductor section is 4.0 mm^2.
- 3 slats arranged together : separation of 1 big cable in3×4=12 thiner lines of 5 conductors$\longrightarrow$ each conductor section is 1.33 mm^2.

Station 5 (figure 4.11) : 24 triple LV supplies for the whole station. 6 supplies for 13 slats of one chamber ; segmentation from the top to the bottom of one chamber :

- 3 slats arranged together : separation of 1 big cable in3×4=12 thiner lines of 5 conductors$\longrightarrow$ each conductor section is 1.33 mm^2.
- 2 slats arranged together : separation of 1 big cable in8 thiner lines of 5 conductors$\longrightarrow$ each conductor section is 2.0 mm^2.
- 2 slats arranged together : separation of 1 big cable in8 thiner lines of 5 conductors$\longrightarrow$ each conductor section is 2.0 mm^2.

- 1 slat : separation of 1 big cable in4 thiner lines of 5 conductors $\longrightarrow$ each conductor section is 4.0 mm^2.
- 2 slats arranged together : separation of 1 big cable in8 thiner lines of 5 conductors $\longrightarrow$ each conductor section is 2.0 mm^2.
- 3 slats arranged together : separation of 1 big cable in3×4=12 thiner lines of 5 conductors $\longrightarrow$ each conductor section is 1.33 mm^2.

4.5.3.4 Practical integration of LV cables

Figures 4.9, 4.10 and 4.11 illustrate the principle of LV cables segmentation, function of the chamber segmentation for Stations 3-4-5. For Stations 4 and 5, a service support structure (SSS) is immovably-attached to the half plane, in order to support the weight of cables. Its dimensions are 180 mm by 90 mm, and it is placed at 400 mm from the panels support. Thus, all LV cables are fixed on one side of the SSS and the other side is keeping free for HV cables and other services for example.For Station 3, there is no room left to place such a SSS inside the magnet ; LV cables will be attached directly on the slats support and drivenoutside the magnet along the platform.Finally, for each half plane of Stations 4 and 5, an extension cable can be added in order to provide LV to stations in open or closed position.

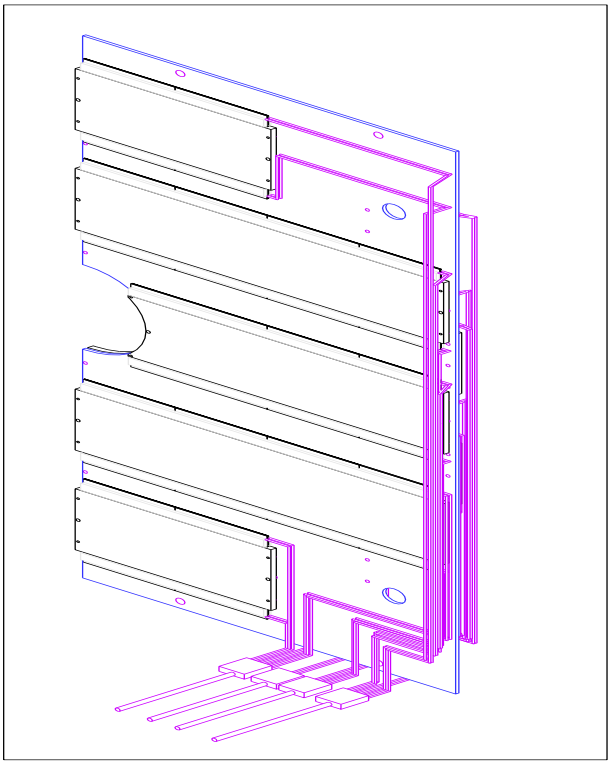

Figure 4.9: Station 3 (1/2 chamber 5 or 6) : principle of LV cables on slats : 4 cables of$5 \times 16 mm^2$ are divided in cables of smaller sections.

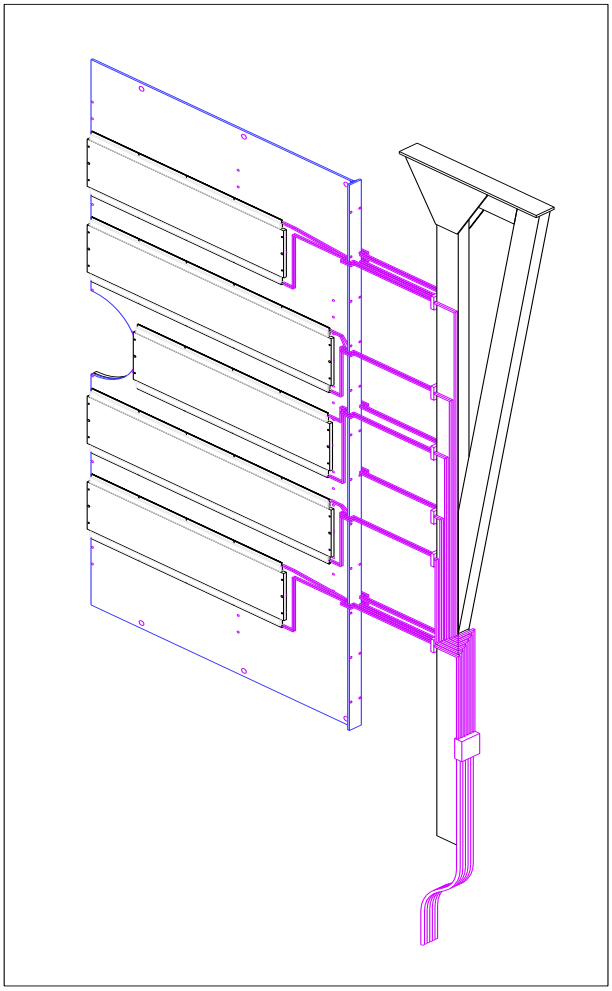

Figure 4.10: Station 4 (1/2 chamber 7 or 8) : principle of LV cables on slats : 6 cables of$5 \times 16\,mm^2$ are divided in cables of smaller sections.

4.5.4 Low Voltage Supplies

All concerning the LV supplies have already been presented in theDimuon Meeting in 2001 [3],and there are no changes since May 2001. The LV supplies description will be one of the subject of theelectronic PRR, organised in May 2002.

We recall that for all tracking stations, 288 supplies are needed, i.e. 24 chassis for LV supply in 3 racks under the Dimuon Arm platform.

[1] "Alimentation Basse Tension Bras Di-muon", P. Courtat, Internal IPN SEP Note Ref : 01 29, 30 Janvier 2001.

[2] "Cablage des stations 3, 4 et 5", F. Orsini, JC Lugol, Internal CEA DAPNIA/SED Note Ref : 6C3221T002DA01, 09 Janvier 2001.

[3] "Dimuon Electronics", P. Edelbruck and P. Courtat, presentation at the Dimuon Meeting 2001 in Cagliari, May 2001.

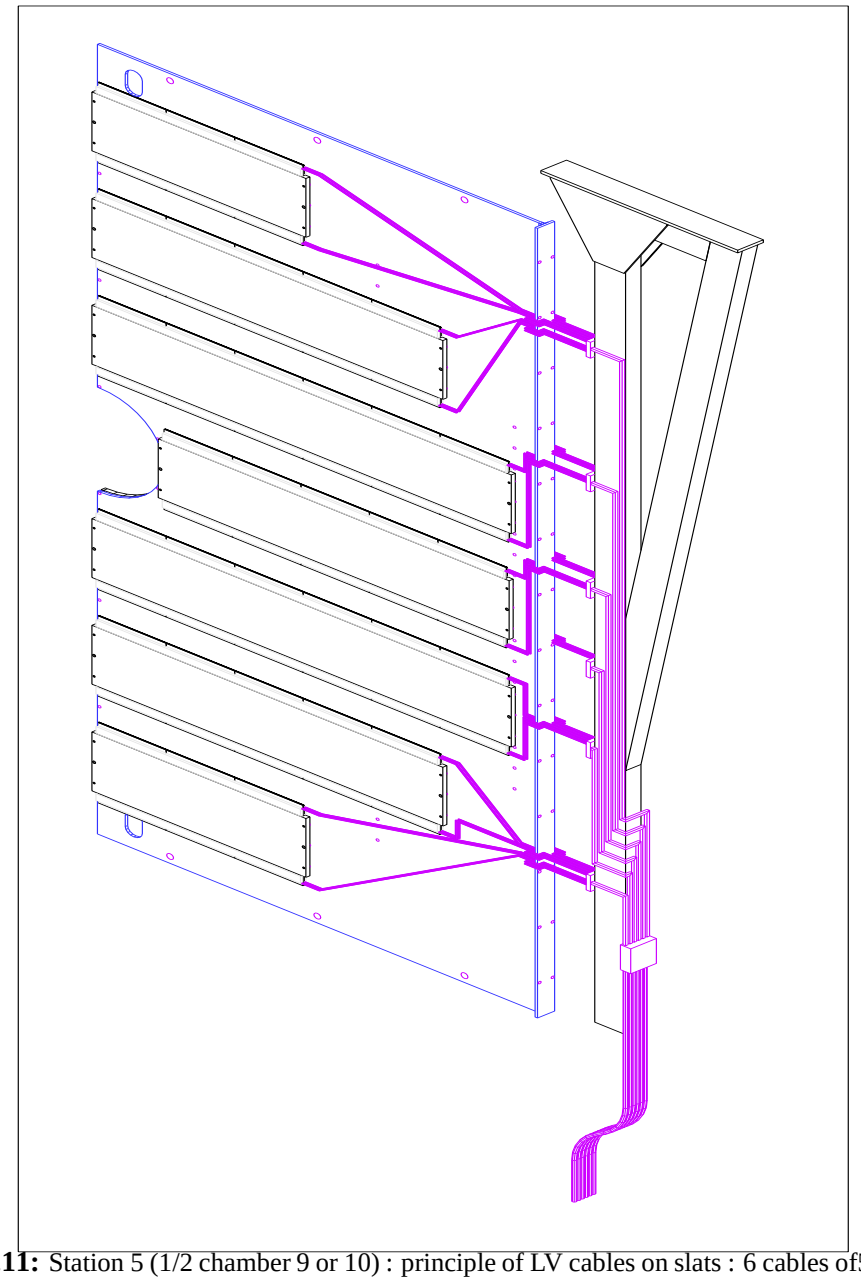

Figure 4.11: Station 5 (1/2 chamber 9 or 10) : principle of LV cables on slats : 6 cables of$5 \times 16\,mm^2$ are divided in cables of smaller sections.

5 Test beam results

5.1 Introduction

Several cathode pad chamber (CPC) prototypes have been developed and tested in-beam at CERN PS by different groups. The main goal was to determine the basic characteristics of the chamber (noise, gain, resolution, efficiency...), in order to validate the choice of the pad segmentation. The mechanical aspects were subject to an R&D program in laboratories, concerning the structure and sealing of the chamber, the machining and gluing of the PCB's. The CERN tests have also validated parts of these aspects.

Three main periods of test have been realized, in May 2000, July 2001 and October 2001, each one with a different electronics, the one available at the time of the test: first, with Gassiplex 1.5 μm and separated 10 bits ADC CRAMS, second, with Gassiplex 0.7 μm and separated 12 bits ADC CRAMS and the last with an electronics close to the final foreseen one, Gassiplex 0.7 μm, with on board 12 bits ADC.

The final electronics is expected to run with MANAS instead of Gassiplex 0.7.

5.1.1 Experimental set-up

Tests were performed with negative pions of 7 GeV/c at the PS even if an "ultimate" resolution cannot be achieved at the PS, due to non-negligible multiple scattering.

As described in the TDR (section 2.3.1), prototypes were mounted on a test bench which allowed vertical and horizontal displacements, by hand. The prototype was located between a set of ten silicon strip detectors, located along the beam axis, that defined the telescope for the tracking system. Five planes were used to measure the x coordinate (2 upstream and 3 downstream of the prototype) while other five measure the y coordinate (again 2 upstream and 3 downstream). Each silicon detector was 300 μm thick with 384 strips of 50 μm pitch ($\simeq$ 15 μm resolution). The trigger system was defined by the coincidence between two pairs of crossed plastic scintillator blades, located upstream (overlapping surface = 2×2 cm^2) and downstream (overlapping surface = 1×1 cm^2) of the prototype.

5.1.2 General mechanical description of a prototype

The prototype is very similar to a slat module described in the TDR (section 2.4.5.3) and TDR Addendum (section 2.4.3).

- the rigid structure on which are glued the PCB is a sandwich panel made of carbon-Nomex honeycomb-carbon,

- a Nomex foil (high permittivity) is glued between the carbon skin and the PCB in order to reduce the capacitive noise.

The anode wires (W-Rh: 20 μm gold plated) are soldered or glued depending of the prototype. The gas sealing is obtained by a silicon joint allowing a quite easy opening of the chamber.

5.1.3 General description of data analysis

To define a track from the silicon detectors, a 4σ pedestal subtraction has been applied on-line and only one hit per y plane has been required. A simple linear extrapolation to CPC is done without multiple scattering correction.

Two cluster finding algorithms have been used for the CPC: one searches the pad with the maximum charge and add to the cluster the two adjacent pads in the y direction, the other is a more general algorithm

which connects all the adjacent hit pads in y and x directions. The position of the cluster is obtained by a center of gravity method (COG).

The spatial resolution of the chamber is defined as the standard deviation of a Gaussian fit to the residual distribution of the expected track position on the CPC and the CPC impact point determined from a COG evaluation. Due to the COG method, the residual must be corrected of well-known geometrical effects (see TDR section 2.3.5.2).

5.2 Prototype 2000

Prototype characteristics and test results are detailed in the TDR Addendum (section 2.4.1). We only summarize here the important features and conclusions.

5.2.1 Goals and characteristics

The main goal was to measure the noise, resolution and efficiency on a small pad (5×25 mm^2) prototype. This segmentation corresponds to the highest density in the bending plane.

A 250 μm Nomex foil (high permittivity) was glued between the carbon skin and the PCB in order to reduce the capacitive noise.

The read-out for the tracking system and prototype used the same method of multiplexed charge measurements. The prototype used the 1.5 μm GASSIPLEX chips whose main characteristics are a noise level at 0 pF of 650 e^-r.m.s, a noise slope of 15 e^-r.m.s and a gain of 12mV/fC. The dynamic range of the 10 bits ADC is 1.5 V i.e 1.46 mV per ADC channel.

The gas mixture was the standard 80% Ar + 20% CO_2.

5.2.2 Results

We obtained a good gain linearity and a plateau for the resolution and efficiency as a function of the high voltage.

The resolution was 80 μm, including multiple scattering for a 1.5 ADC channel of noise, the best level of noise we had. This corresponds to 1150 electrons. The multiple scattering was estimated around 50 μm leading to a real resolution of the CPC around 60 μm.

The corresponding efficiency was 97 % at ±1 mm and 93 % at 3 σ on the residual.

5.3 Prototype 2001

5.3.1 Goal

The goal was to measure the characteristic parameters of the CPC with large pads (5×100 mm^2 in the bending plane) where the noise is expected larger. This has been the opportunity to study in more detail the different components of the noise and to try to reduce them. The resolution is linearly related to the noise and the efficiency dependent of the resolution.

We have seen, for example on the 2000 prototype, a dependence of the noise with the read-out strip length (fig. 5.1). This was the starting point of an attempt to simulate the capacitive noise of the chamber.

5.3.2 Noise studies

5.3.2.1 Capacitive noise

The noise seen by a GASSIPLEX 0.7 μm is:

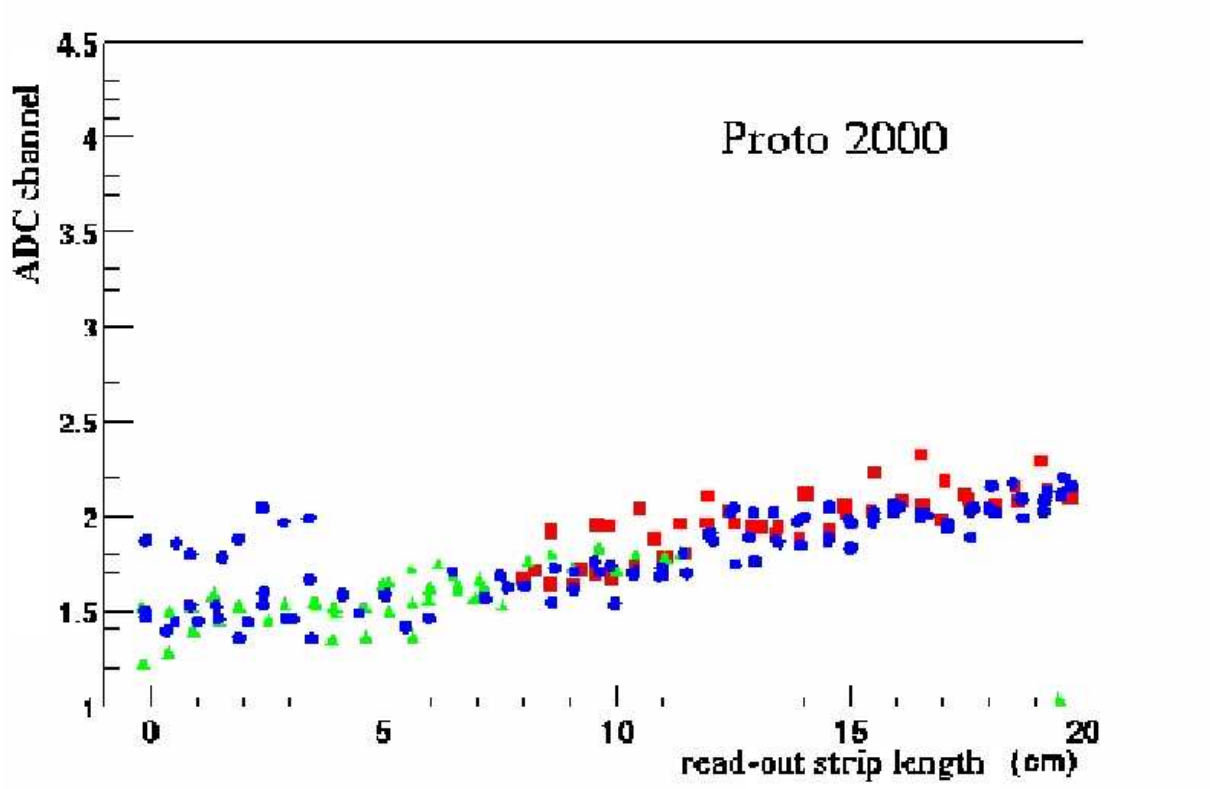

Figure 5.1: Noise (expressed in ADC channels) in the bending plane as a function of the read-out strip length

$$noise\,(e^-) = 530 + 11.2 \times C\,(pF)$$

Figure 5.2 (left) is a cut view of the detector while figure 5.2 (right) represents the corresponding capacitive modelisation.

From an electrical point of view, the pads are grounded through the electronics and the carbon skins are grounded too: the internal, the external or both depending on the prototype.

We distinguish three terms in the model:

- a first term, involving PCB, glue and Nomex capacitance between one pad and the grounded carbon skin,
- a second, involving the glue and Nomex capacitance between the read-out strips and carbon,
- a third, involving PCB capacitance between read-out strip and other pads.

The total capacitance can be written as:

$$C_{total} = \frac{\varepsilon_0 S_{pad}}{\frac{e_{PCB}}{\varepsilon_r(PCB)} + \frac{e_{glue}}{\varepsilon_r(glue)} + \frac{e_{Nomex}}{\varepsilon_r(Nomex)}} + \frac{\varepsilon_0 l_{strip} L_{strip}}{\frac{e_{glue}}{\varepsilon_r(glue)} + \frac{e_{Nomex}}{\varepsilon_r(Nomex)}} + \frac{\varepsilon_0 l_{strip}(L_{strip} + L'_{strip})}{\frac{e_{PCB}}{\varepsilon_r(PCB)}}$$

with ε_0 = 8.85 pF.m^{-1}, ε_r(PCB) = 4.9, ε_r(Nomex) = 1.2.

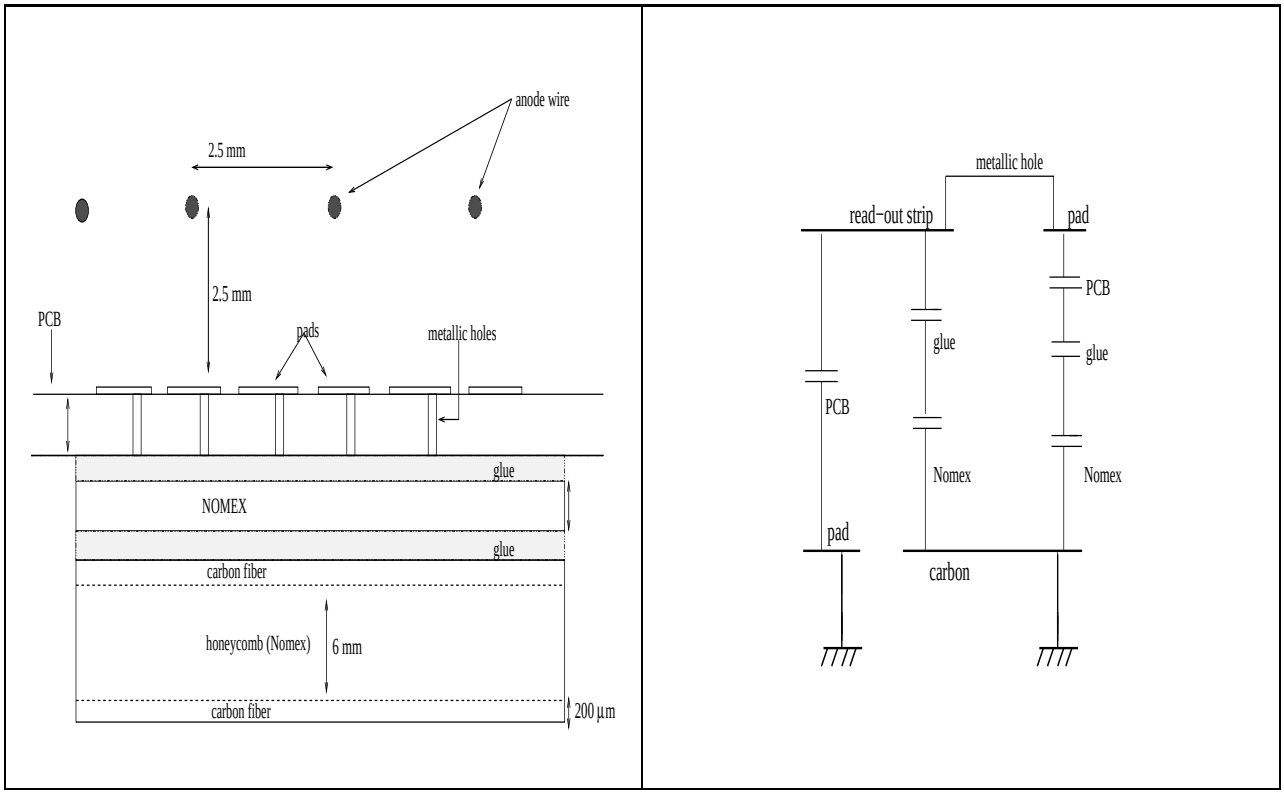

Figure 5.2: Left: Cut view of a slat. Right: Capacitive modelisation of a slat

In our case, terms involving glue parameters (glue thickness $e_{glue} \approx 80$ μm, glue relative permittivity $\varepsilon_r(glue) \approx 3.9$) are negligeable, and the second term is small compared to the two others.

The third term shows the dependence of the capacitance and therefore the noise to the read-out strip lengths (L_{strip}, L'_{strip}) and width (l_{strip}). To reduce this dependence, l_{strip} changed from 180 to 150 μm and the PCB thickness e_{PCB} doubled from 200 to 400 μm.

To cut on the global noise depending on the pad area (first term), we increased, in addition, the thickness of the dielectric foil.

5.3.2.2 Prototypes and characteristics

Two small prototypes (40×40 cm^{2}active area) have been constructed.

- The bending plane had large pads (5×100 mm^2) with a small area of small pads (5×25 mm^2) used as reference.
- The pad dimensions in the non-bending plane were 8.333×100 mm^2 and 8.333×25 mm^2.
- The thickness of the PCB was 400 μm.
- The difference between the two prototypes came mainly from the different thicknesses and materials of the dielectric foil. One prototype had the standard Nomex thickness of 250 μm, the other a 2 mm thick Nomex-air honeycomb foil. The other difference was the way to ground the carbon fibers: one prototype had the two carbon skins grounded while the other had only the external skin.
- The prototype used the 0.7 μm GASSIPLEX chips whose main characteristics are a noise level at 0 pF of 530 e$^-$r.m.s, a noise slope of 11.2 e$^-$r.m.s and a gain of 3.6 mV/fC. The dynamic range of the 12 bits ADC was 1.5 V i.e 0.36 mV per ADC channel.

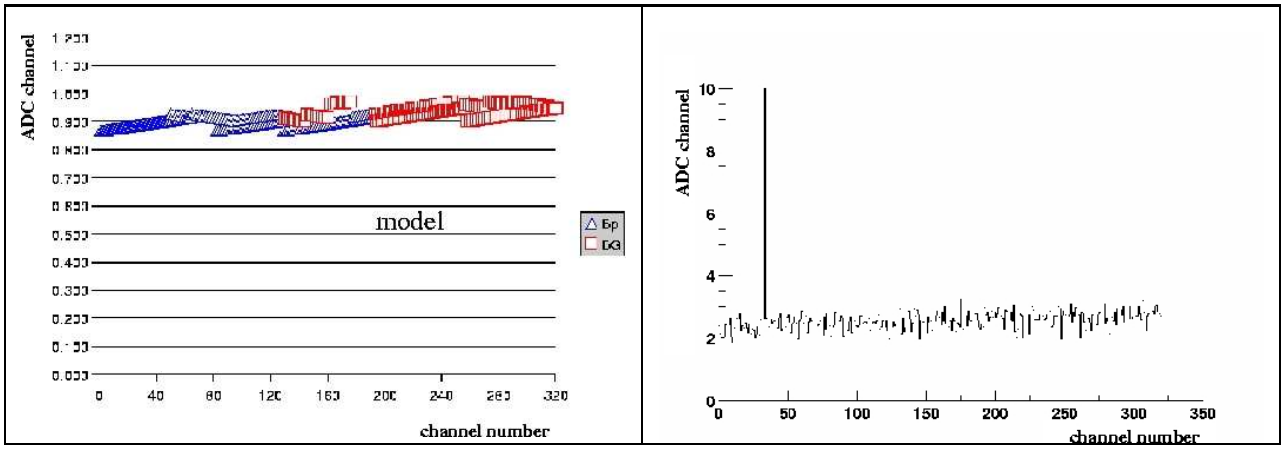

Figure 5.3: left: Noise obtained from modelisation as a function of the electronic channels . right: Measured noise in laboratory

5.3.2.3 Modelisation results

The results of the modelisation show a flat behavior with the read-out strip length as well as the pad area. We display this behavior on figure 5.3 (left) as a function of the electronic channels.

The corresponding measured noise in laboratory exhibits also a flat behavior (figure 5.3 (right)).

The absolute value of the noise is nethertheless much higher than the modelled one. One part of the explanation is that the ADC noise itself has not been taken into account in the simulation.

5.3.3 Test beam results

5.3.3.1 Noise

The noise measured in July 2001 test beam is displayed on figure 5.4 for the two prototypes.

The first prototype does not show any structure (figure 5.4 left) while the other does (figure 5.4 right). The difference of dielectric foil thicknesses does not explain such a level of structure which seems indicate a poorer shielding of the second prototype. Indeed, a pick-up noise enhanced the structure behavior. For example, a non filtered high voltage causes such a behavior, as we observed.

In both cases, the value of the noise is much too high and not explained. To obtain the same kind of resolution than in 2000, i.e 80 μm, the noise should be at the level of 1.8 ADC channel, instead of 3.5. As a new large prototype is expected to be tested in october with a new and almost final electronics including ADC on board, we decide to wait for this test to conclude on the noise.

5.3.3.2 Gain and gas

The gain has been measured for different gas mixtures (figure 5.5). Going from Ar(70%)CO_2(30%) to Ar(80%)CO_2(20%) represents a 50 volts gap while 200 volts and a steeper slope differ between Ar(90%)CO_2(10%) and Ar(80%)CO_2(20%). Considering stability on one hand and not too large voltages on the other favors the Ar(80%)CO_2(20%) mixture. Between 1700 and 1750 volts the proportion of more than two pads hit is high leading to a better resolution.

5.3.3.3 Resolution and efficiency

The resolution and efficiencies are presented on figure 5.6 as a function of the high voltage. The plateau ranges from 1700 to 1750 volts for Ar(80%)CO_2(20%) gas mixture. The poor resolution around 150 μm is due to the large noise, leading to a poor efficiency of 90 % for a ± 1 mm cut on the residual.

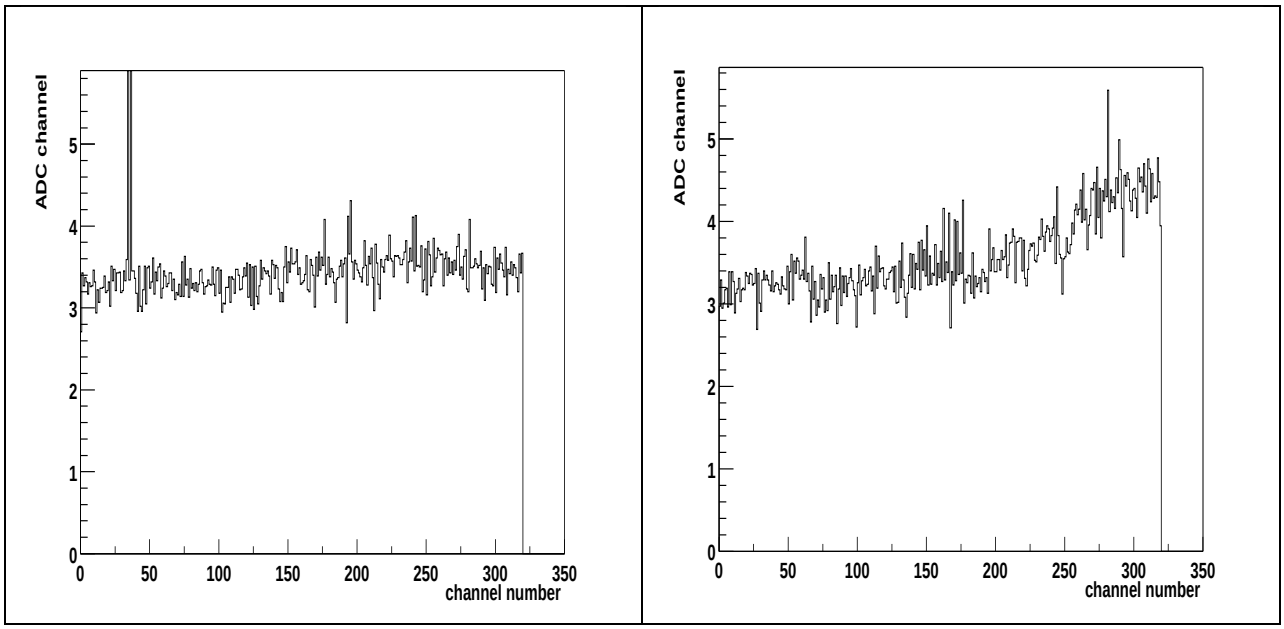

Figure 5.4: Measured Noise in test beam: left: prototype with two grounded carbon skins and 2 mm honeycomb-Nomex dielectric foil ; right :prototype with external carbon skin grounded and 250 μm Nomex foil.

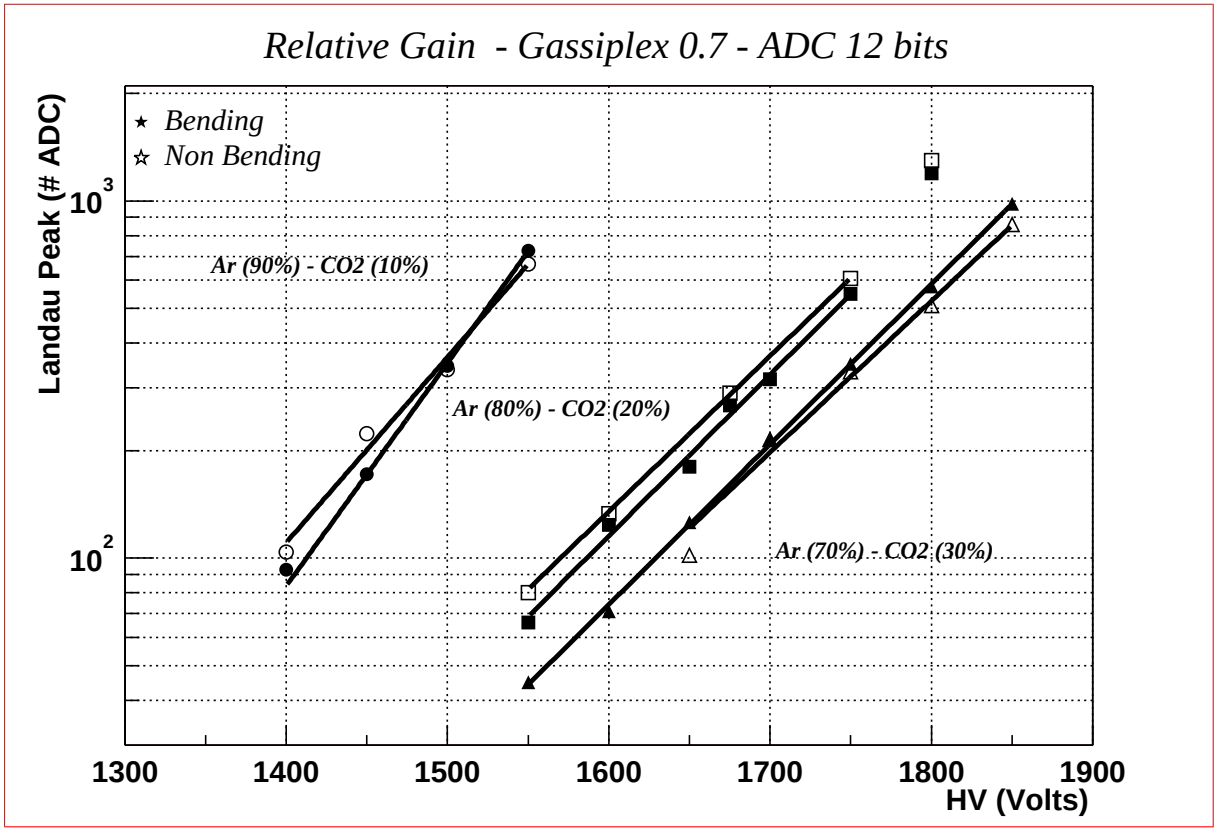

Figure 5.5: Measured gain for three gas mixtures.

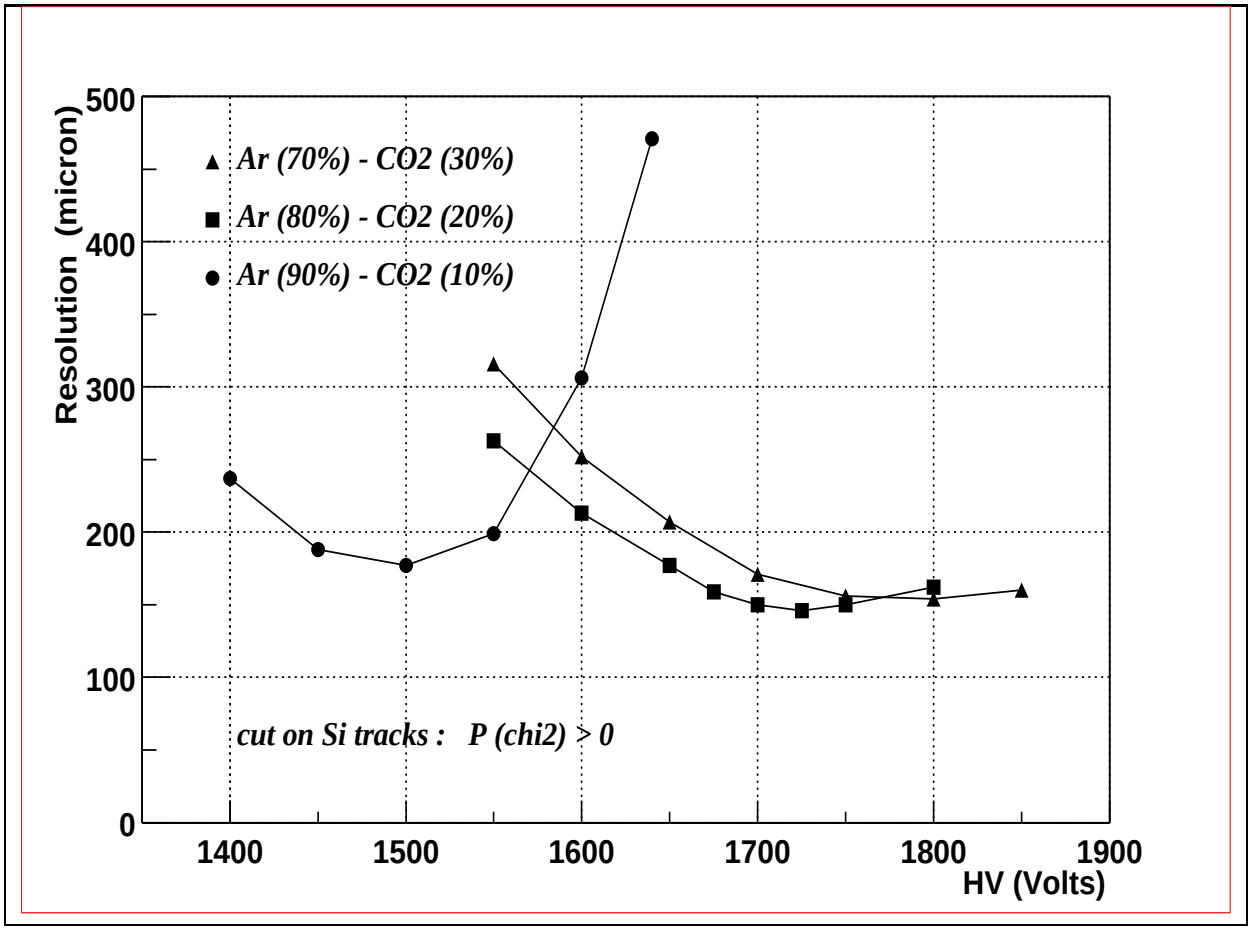

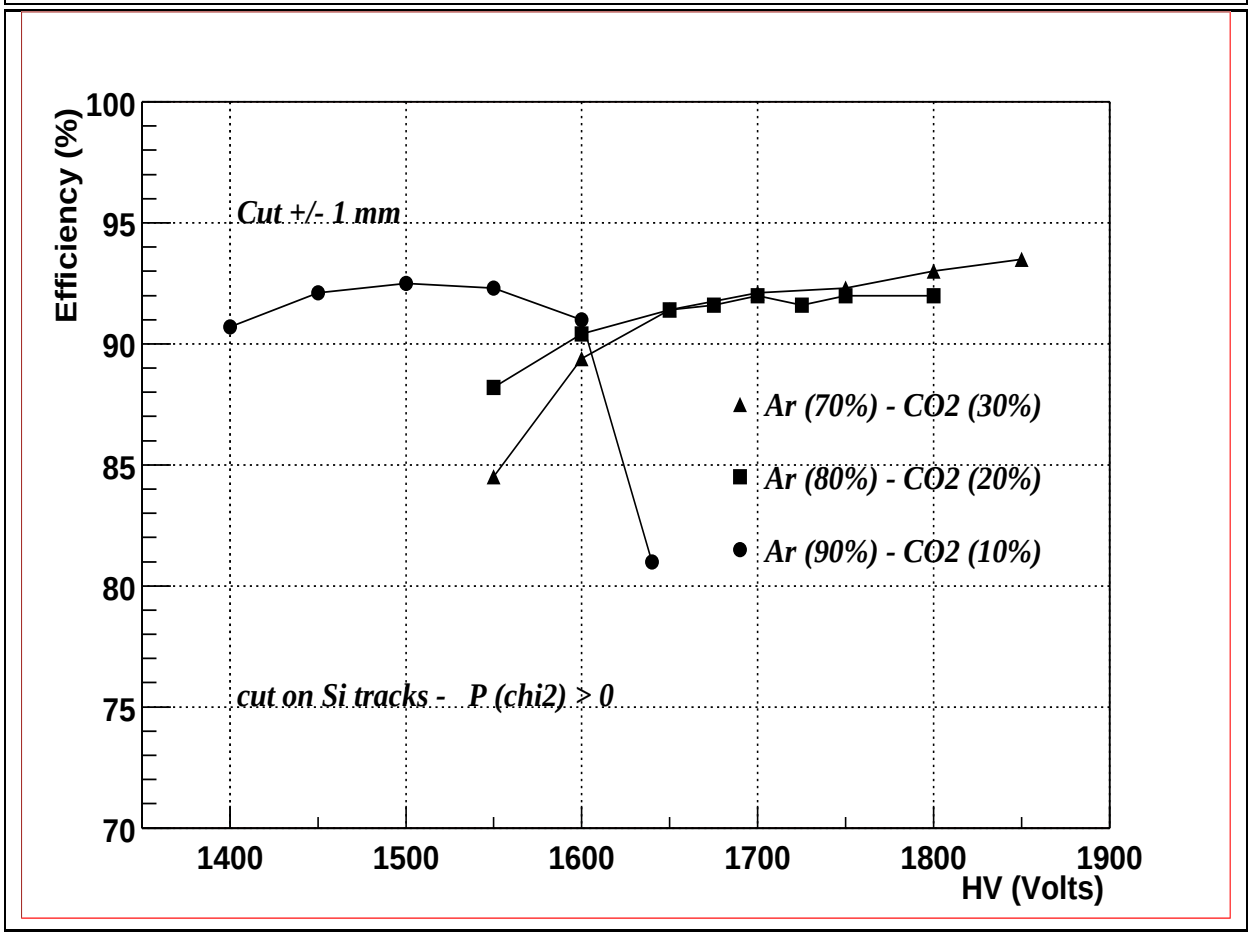

Figure 5.6: Resolutions and efficiencies as a function of high voltage.

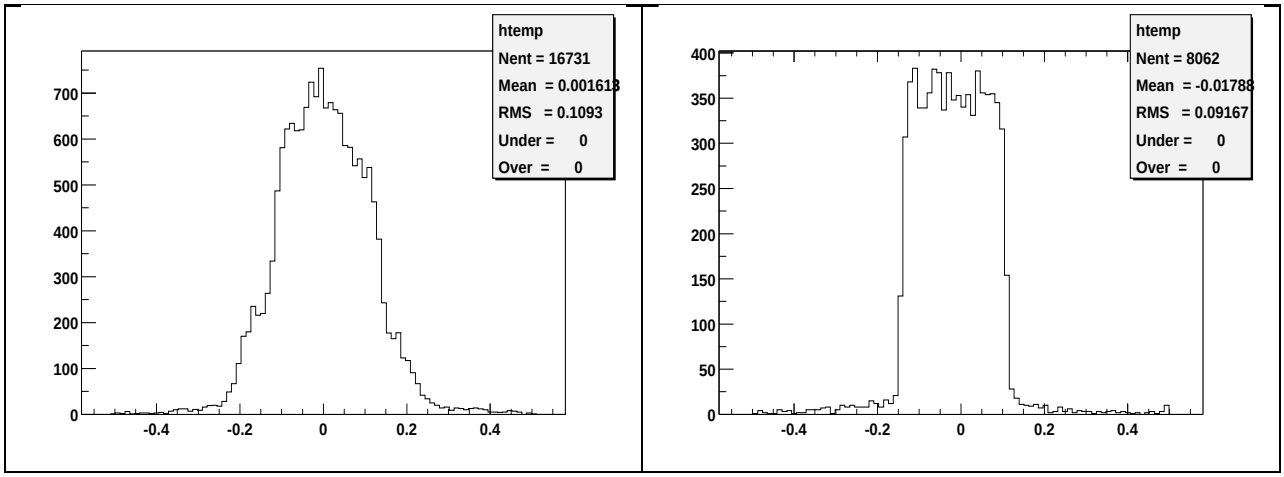

Figure 5.7: Residual in the non-bending plane for a pad width of 8.333 mm (left) and 7.143 mm (right).

5.3.3.4 Non-bending plane

In the non-bending plane the hit position is given by the position of the wire on which the avalanche takes place. Knowing the pitch of the anode wires and trusting the positionning of the wires and the PCBs', the wire position is reconstructed from the cluster position in the non-bending cathode plane. Figure 5.7 shows the residual between the reconstructed wire position and the track position in the plane for a 7.143 mm and a 8.333 mm pad width. These numbers come from PCB dimensions and electronic channels numbers considerations.

The hit wire position is well reconstructed in only 75 % for a 8.333 mm width and 88 % in the 7.143 mm case. The corresponding resolutions are 1 mm and 917 μm.

5.3.4 Conclusions

- **Noise:** the measured noise is high but with a flat behavior with pad sizes and read-out strip lengths. An improvement is expected with the next and almost final electronics which will be tested in october. A better shielding must be studied with this electronics.
- **Gas :** the gas mixture will be close to Ar(80%)CO_2(20%).
- **Non-bending pad sizes :** the pad width kept is 7.143 mm.

5.4 Large slat prototype 2001 - october tests

In this section, the aim of a large slat test and some preliminary results are presented shortly after data taking period of 17-24 October. Detailed analysis will deepen our understanding in the next future.

5.4.1 Goal

The goal was to build, for the first time, the largest slat foreseen of 2400 mm long, in its almost final design, to equip it with the almost final electronics and test it in beam to determine its characteristics.

From a mechanical point of view, the building of this slat allowed to refine the mounting procedure. The assembly was made with the same kind of tooling foreseen for the production. No critical problems arose during this assembly.

On the electronics side, problems uncountered on connectors, buses, read-out and data transmission have been overcome.

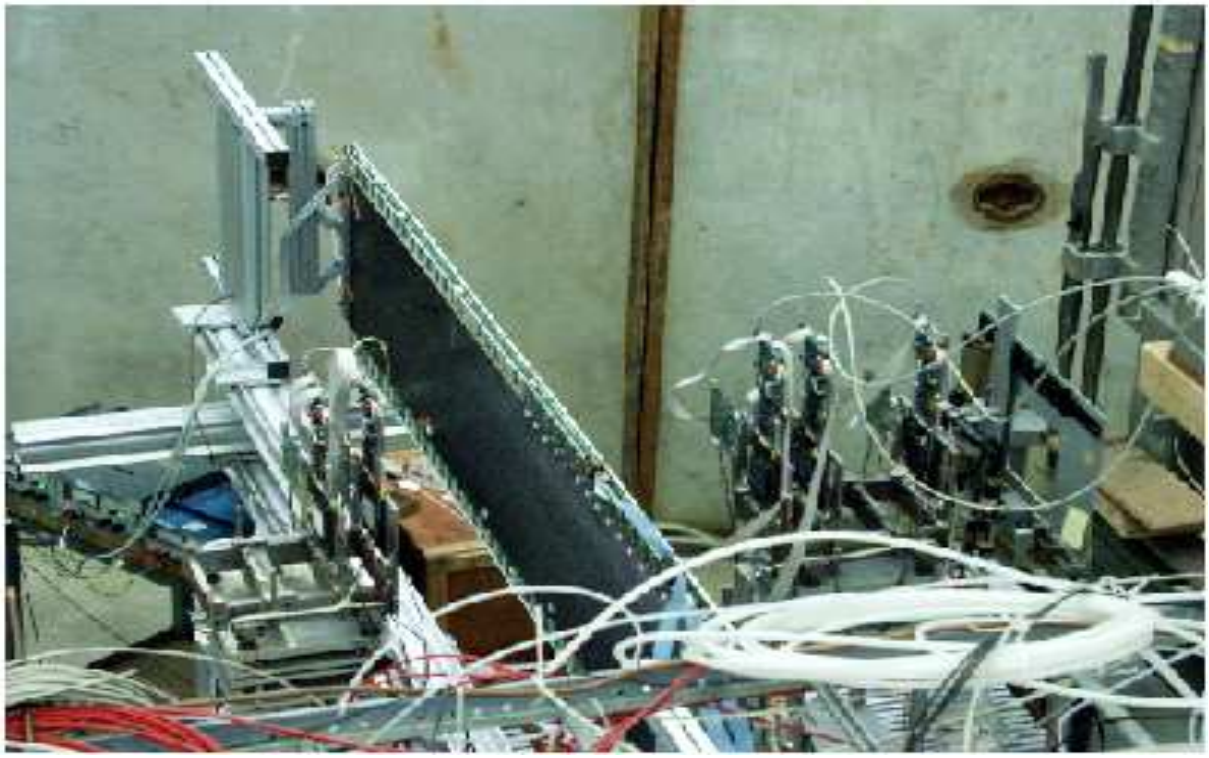

Figure 5.8: Global view of set-up with the large slat prototype located between the silicon tracker.

The physical properties (gain, resolution, efficiency...) have been determined. Nethertheless, a real and complete cartography of the chamber has not been realized: first, the relatively small number of electronic circuits allowed to equip at the same time the equivalent of one of the six PCBs' on each cathode plane, second, some areas were not able to be read. Moreover, electronics calibration was not yet implemented. Taking into account these considerations, we have nethertheless made few different positions by moving some circuits.

5.4.2 Characteristics

- the 2.4 meter long slat contained 6 standard high density PCBs' on each cathode plane.
- the pad size in the bending plane was 25 $\times$5 mm^2.
- the pad size in the non-bending plane was 7.143 $\times$25 mm^2.
- the signal treatment was ensured by the MANU boards described in section 4.2.1: Gassiplex 0.7 μm chips were used as preamplifier, filter and shaper, with a gain of 3.6 mV/fC. The analog signal was digitally converted in a 12 bits ADC, also on board, with a conversion range up to 3 V, i.e 0.732 mV per ADC channel.
- the gas mixture was Ar(80)-CO_2(20).

Figures 5.8, 5.9, 5.10show some picture of the large slat taken during the test.

5.4.3 Results

5.4.3.1 Gain

- a good gain linearity is obtained.

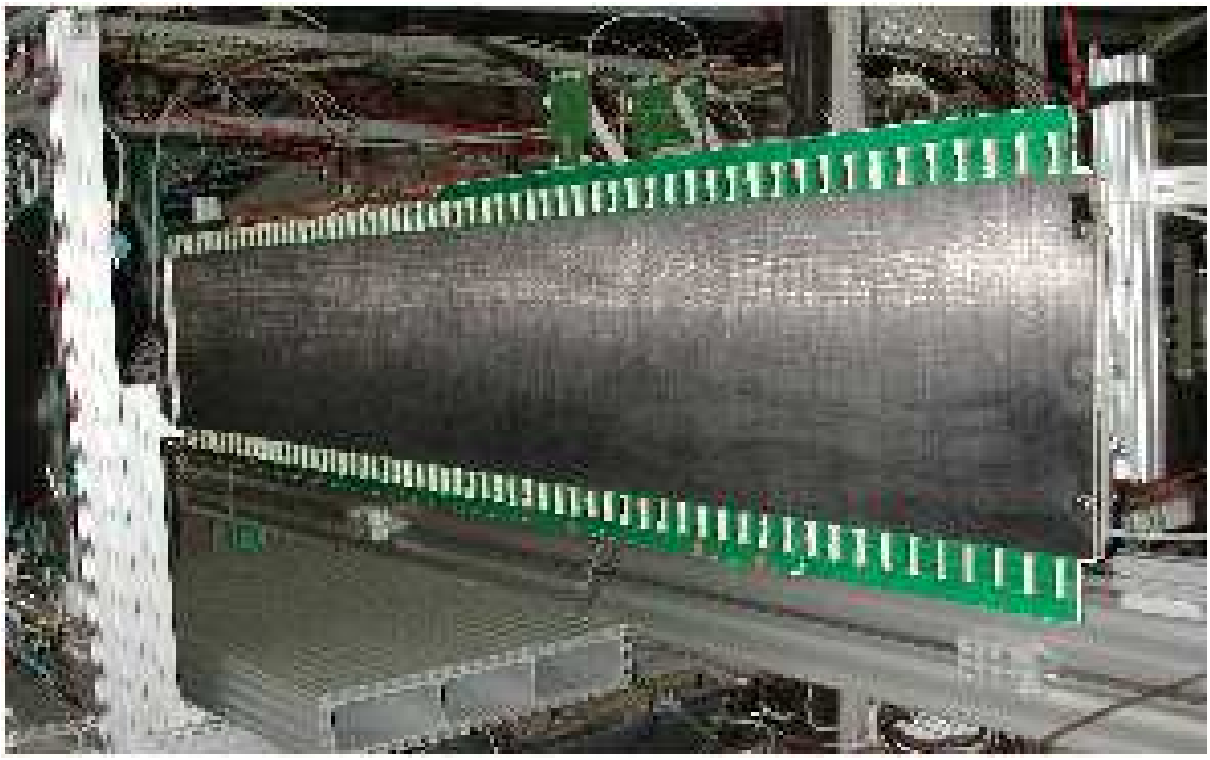

Figure 5.9: View of the large slat with all the bending plane connectors visible.

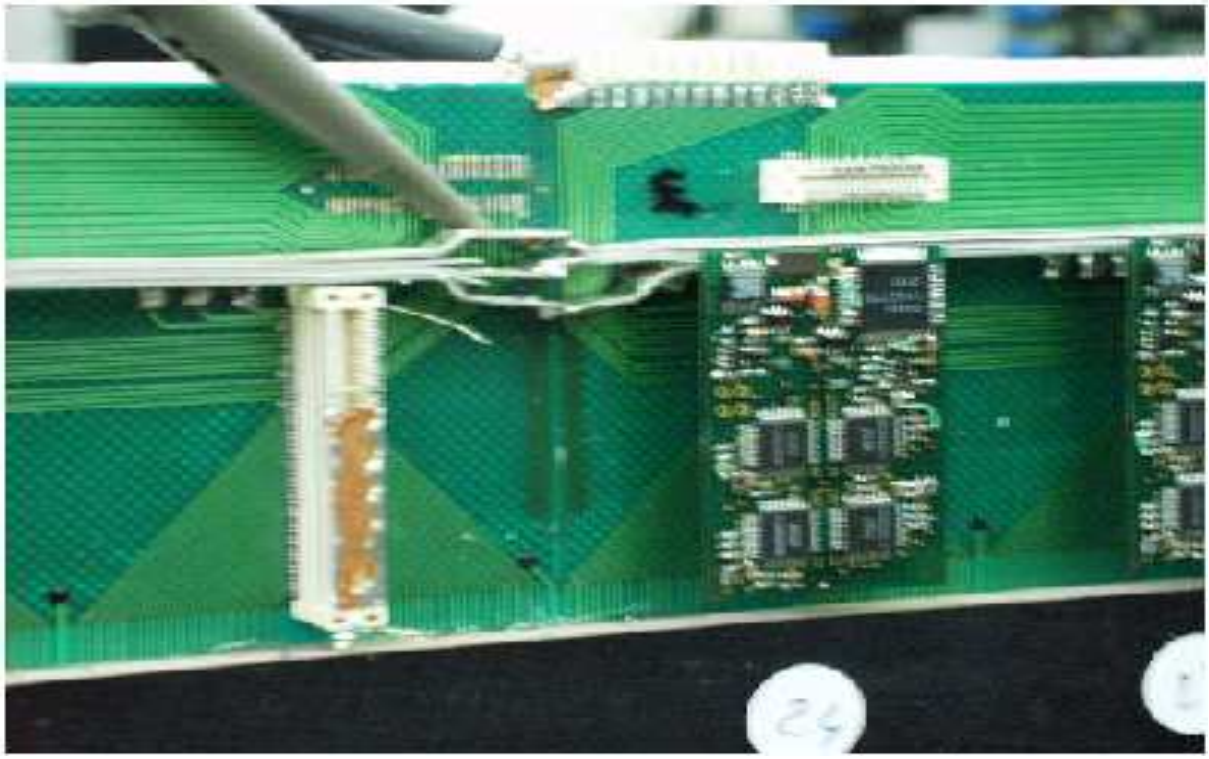

Figure 5.10: View of the MANU boards with its 4 16 channels Gassiplex chips, the connectors and the busbars.

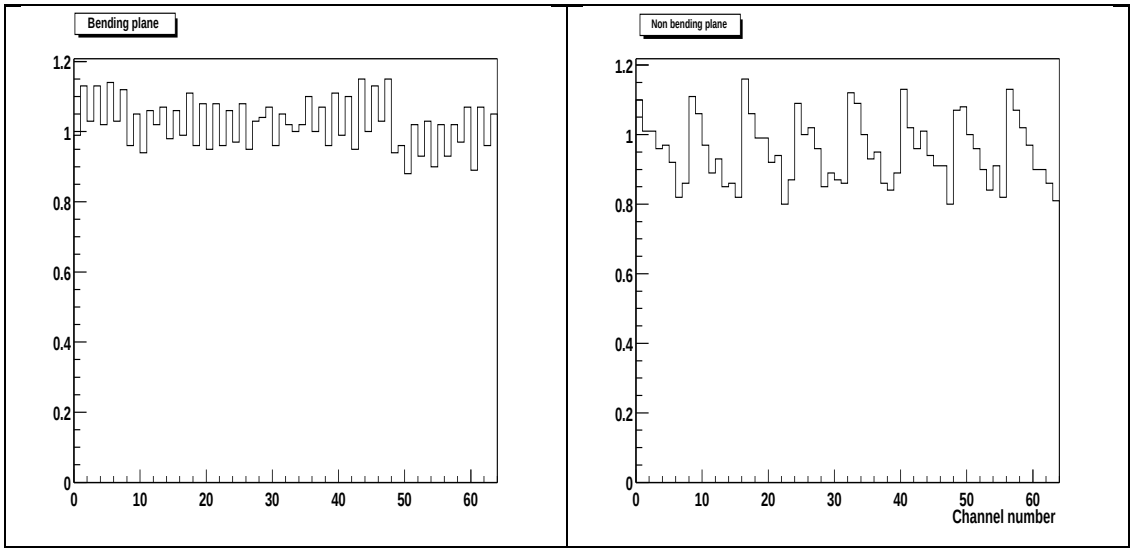

Figure 5.11: Sigma of the pedestals (in ADC channels) for bending and non-bending planes.

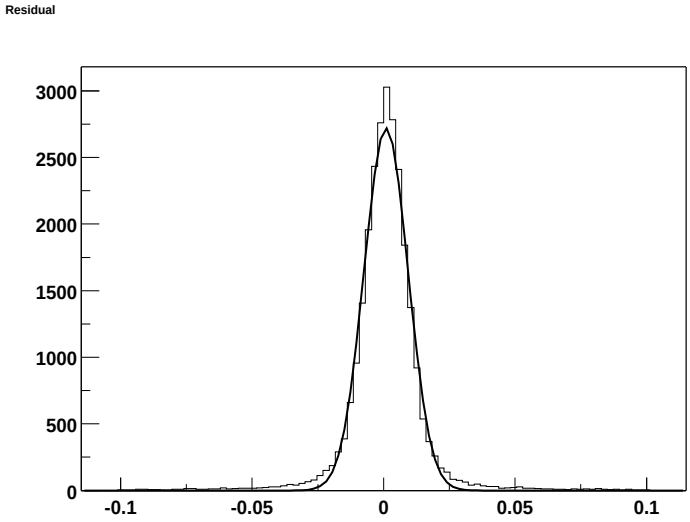

Figure 5.12: Resolution in the bending plane : σ = 84 μm.

- the absolute gain is 2.5 10^4 at 1700 V and 5 10^4 at 1750 V.

5.4.3.2 Noise

We measured a noise level between 1150 and 1400 electrons (0.9 to 1.1 ADC channel), with a reasonably flat behaviour with the read-out strip length, as shown on fig 5.11.

Such a noise has been achieved, first by linking all the planes (carbon skins and pads) to a same ground, second, as explained in section 4.3, by insulating this ground of the slat from the general ground of the hall.

5.4.3.3 Resolution and efficiency in the bending plane

A typical resolution plot is shown on fig 5.12, while the dependence of the resolution and the efficiency with high voltage is displayed on fig 5.13.

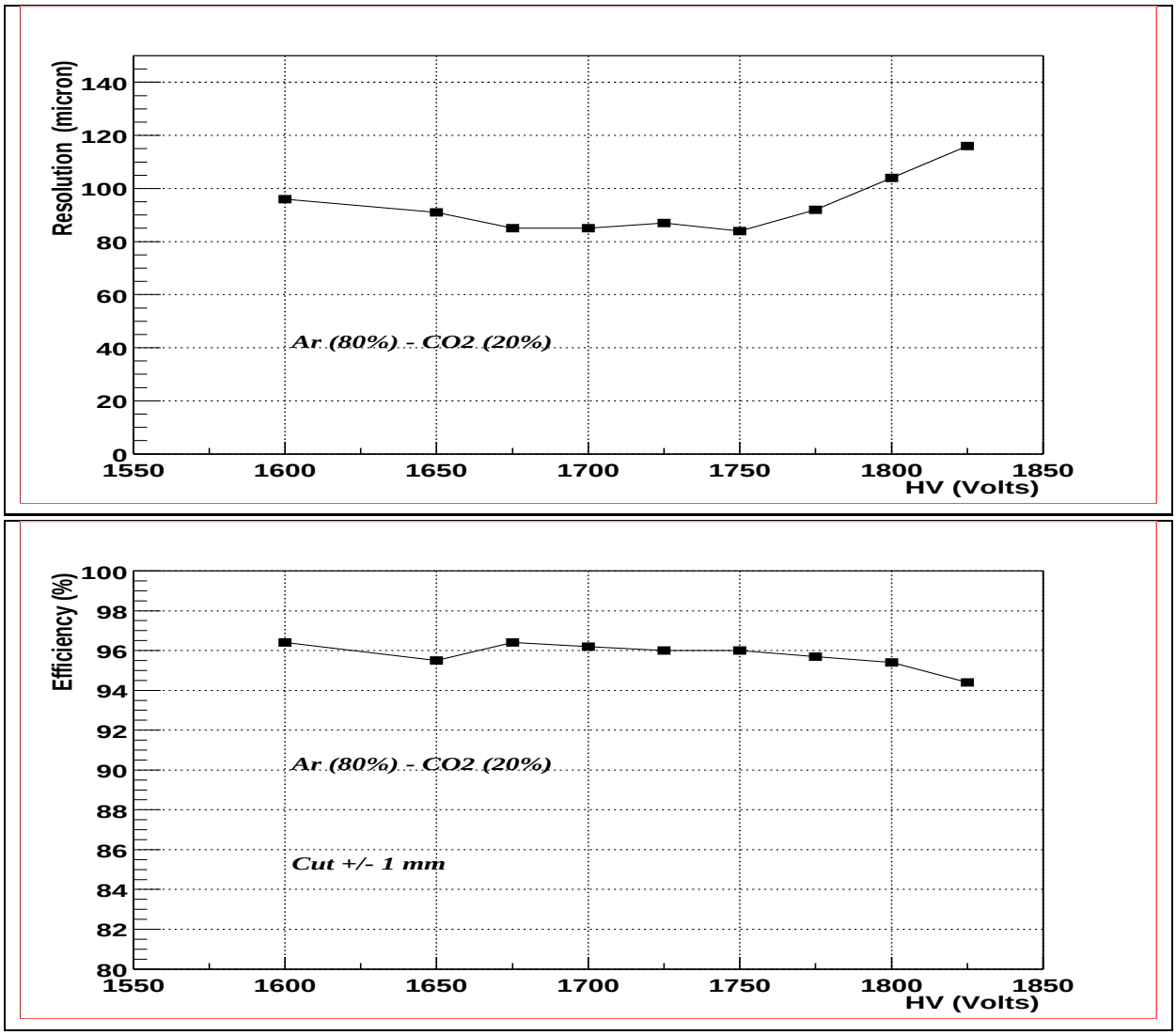

Figure 5.13: Resolutions (top) and efficiencies (bottom) as a function of the high voltage (bending plane).

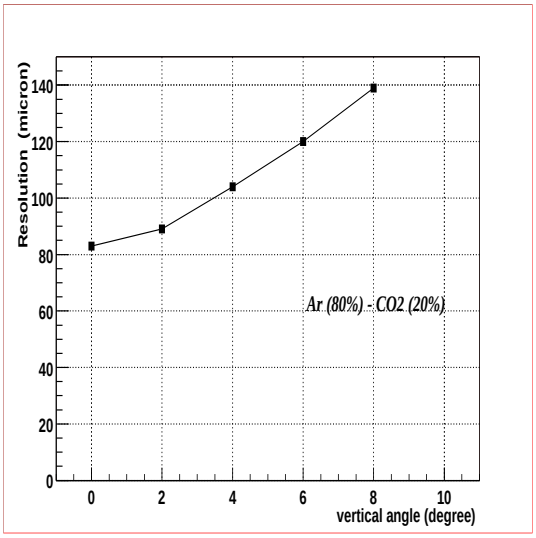

Figure 5.14: Dependence of the resolution with the vertical angle of the track.

A plateau is reached between 1675 and 1750 volts with a resolution of 85 μm and an efficiency of 96 % for $\pm$1 mm cut on the residual or 92 % for a 3σ cut.

Below 1675 volts, the degradation of the resolution is visible, while the raise above 1750 volts reflects the saturation of the Gassiplex (range up to 560 fC or 2 V, according to the specifications).

The resolution and efficiency are not spoiled at the border of two PCBs'.

All the resolutions shown include multiple scattering.

5.4.3.4 Vertical Angle studies

Figure 5.14 displays the dependence of the resolution with the vertical angle of a track.

5.4.3.5 Non bending plane

The hit wire position is well reconstructed in 91 % of the case, i.e for a residual cut at $\pm$1.25 mm (half a wire pitch) for an RMS of 845 μm. This number becomes 96 % for a $\pm$2.5 mm cut.

This reconstruction is little affected by an horizontal angle of the track: angles of 0, 5 and 10 deg give a reconstruction efficiency and a resolution of 91 % and 845 μm, 88 % and 870 μm and 87 % and 884 μm respectively.

6 Planning, task sharing and cost

In what follow, will be presented the different aspects of the organisation with the task sharing, the planning till the on-site installation and finally the cost as we know it today before the tenderings.

6.1 General Planning

The planning is given in Annex A and some comments can be done:

- after several prototypes construction, the time for the mounting of a slat is estimated at 2 weeks

6.2 Tasks sharing

After the TDR (Technical Design Report), it has been decided that the tracking chambers of the Dimuon Arm will be constructed with the same internal geometry but two different technologies following two different requirements:

- Stations 1 and 2 have moderate sizes (radii smaller than 1.25 m) but a very high pad densities due to the neighboring of the front absorber. These stations will be made of quarters with the electronics plugged on the whole surface of these detectors

- Stations 3,4 and 5 have large radii (up to 2.6 m) but with moderate hit densities. To solve the difficulties due to the large sizes (wire length, gas pressure, manufacturing...), it has been decided to construct these stations by assemblying of modules of moderate sizes (the slats) which individual useful sizes are typically 40 cm high (in the the bending plane) and between 80 and 240 cm long in the other plane. Every slat, itself, will be composed by assembling PCBs of small sizes (58 cm high and 40 cm wide) of a few number types (~ 8 types per plane). The details of construction have been described in chapter 2.

This choice has three main advantages:

- to reduce the R&D program, the validation of a structure being valuable whatever will be the location of the elementary PCB

- to reduce the manpower for the design of the different elements of the slats and the cost of the tooling of the PCBs

- to allow an “industrial” organisation for the construction

The 3 stations with their support structures and their cooling will be constructed by 4 laboratories:

- INFN Cagliari
- PNPI Gatchina
- SUBATECH Nantes
- DAPNIA Saclay

IPN Orsay participates at this collaboration for all the aspects in connection with the electronical equipment: PCB design, connectors, level translators...

Some principles have been applied for the task sharing between these labs:

- every labs will provide pieces of the slats or equipments to the other labs. The laboratory supplier of each element will be unique to optimize the cost, the manpower and to ensure the homogeneity of all the materials. The laboratories will also be responsible for testing and validation of what they deliver.

- every labs will construct slats and test them. This choice has been done to ensure interest for the work and visibility for each institute in front of the ALICE collaboration. Moreover, it would permit a backup solution in case of a laboratory failure.

- exactly the same protocole will be applied for the slat mounting whatever the laboratory is

With these rules of the game, the following task sharing has been adopted, independently of the financing repartition:

- **INFN Cagliari** (group leader Corrado CICALO, E-mail: corrado.cicalo@ca.infn.it), independantly of its tasks on the MARC chip, will be in charge of:

1. responsability for the design of all the types of PCBs for the two planes
2. purchasing of all the PCBs (around 1400 pieces) and electrical tests
3. cutting the PCBs to the required sizes
4. purchasing and soldering of the connectors on the PCBs then electrical controls will be performed before sharing and shipping towards the other labs.
5. construction and test of a wiring machine with the required precision on the wire strengths
6. construction, tests and shipping of about one quarter of the total number of slats.

- **PNPI Gatchina** (group leader Vladimir SAMSONOV, E-mail: samsonov@hep486.pnpi.spb.ru)will be in charge of:

1. construction and test of the cutting machine for the PCBs, delivery to INFN Cagliari, installation and teaching on the manner to use it
2. construction and test of 4 HV check stands, delivery to the three external labs.
3. construction and test of a wiring machine with the required precision on the wire strengths
4. construction, tests and shipping of about one quarter of the total number of slats.

- **SUBATECH Nantes** (group leader Lionel LUQUIN, E-mail: luquin@subatech.in2p3.fr) will be in charge of:

1. Design of the slat chambers
2. Design, engineering of the assembly tooling
3. Design, engineering, delivery to the others labs of the carbon sandwiches panels
4. the NOMEX purchase and delivery to the others labs
5. Design, engineering, delivery to the others labs of the spacers
6. the study and the construction of the level translators LVDS-LVTTL and the bridge boards between the PCBs
7. construction, checks and shipping of about one quarter of the total number of slats.
8. Technical coordination for engineering of Stations 3, 4 and 5 chambers and the associated equipments (mainly the frames and the cooling). The technical coordinator is Manoël DIALINAS till the end of December 2001 (E-mail dialinas@subatech.in2p3.fr)

- **DAPNIA Saclay** (group leader Alberto BALDISSERI, E-mail: a.baldisseri@cea.fr associated with the technical project leader Fabienne ORSINI, E-mail: forsini@cea.fr) will be in charge of:

1. modification of a wiring machine and delivery of wire planes to SUBATECH

2. purchase, control and delivery of the bus bars for the low voltages supplies
3. construction, control and delivery at CERN of the frames for the three stations
4. fabrication and installation of the cooling setup for the three stations
5. Responsibility for the integration of the 3 stations (cables and services)
6. construction, tests and shipping of about one quarter of the total number of slats.

6.3 Available manpower in labs

- INFN Cagliari:

1. 2 technicians equivalent full time for the assembly
2. 1 electronics engineer at 50%
3. 1 electronics engineer full time starting on beginning of 2002

- PNPI Gatchina

1. 3 technicians for the assembly full time
2. 2 engineers

- SUBATECH Nantes

1. during the R&D phase, 4 persons are involved
2. during the construction phase, one technician and teporary manpower are foreseen

- DAPNIA Saclay

1. 2 technicians starting on middle 2002
2. an engineer at 50%

6.4 Cost CORE update

As, by principle, PRR must be held before launching the tendering procedures, it is clear that it is impossible to have a precise view of what will be the overall cost of the system. The numbers which are known today are just coming from evaluations after discussions with several manufacturers and are too much imprecise to be published. The WBS (Working Breakdown Structure) and the PBS (Product Breakdown Structure) have been done and are included below. It has to be remarked that some items were missing as, for example: busbars, bridges between PCBs, NOMEX, mechanical pieces for frames hanging...